Corrosion of copper in ultrapure water

Mats Boman, Mikael Ottosson, Rolf Berger, Yvonne Andersson,
Maria Hahlin, Fredrik Björefors, Torbjörn Gustafsson

Uppsala University, Department of Chemistry
– Ångström Laboratory

April 2014

SKB

Corrosion of copper in
ultrapure water

Mats Boman, Mikael Ottosson, Rolf Berger, Yvonne Andersson,
Maria Hahlin, Fredrik Björefors, Torbjörn Gustafsson

Uppsala University, Department of Chemistry
– Ångström Laboratory

April 2014

Summary

Claims that copper metal may corrode substantially even by dioxygen-free water, yielding hydrogen, could, if proven correct, have detrimental consequences for the nuclear waste management by SKB (Swedish Nuclear Waste Management Co.). In order to cast new light on the subject, we have performed an independent scientific investigation of the Cu-H_2O system at 50°C, using ultrapure components, namely 99.9999% copper and ppt quality water. The experiments were based on two types of setup, one where gas evolution was monitored, and one where copper oxidation products were investigated at discrete time intervals, possible only after dismantling the equipment. In both cases, the reaction chamber was a stainless steel container, gas tight except for a lid made of palladium foil acting as a selective membrane, since only hydrogen can pass. The reaction chamber contained a Duran glass beaker with a holder of silica glass for pieces of copper. Three setups were individually connected for measuring the pressure of hydrogen, their data being continuously logged. Two of these were used as reference systems (not loaded with copper pieces) but differing in choice of material for the backing that makes the main parts gas tight (except for the palladium membrane).

Before the start of the experiments the copper metal was purified in three steps: electropolishing for making the surface smooth and freed from scratches, hydrogen reduction to remove a remaining thin layer of oxide, and eventually heat treatment to remove excess hydrogen and relieve strain. The quality was checked by various analysis techniques (XPS, ERDA), showing that the metal was oxide free and that the hydrogen content had not increased in the process. The effect of purifying the water from dissolved oxygen was checked by a special optical probe. All reaction experiments were executed in a glove box filled with dry nitrogen to avoid any contamination from oxygen during the experimental handling, be it on starting or breaking experiments. Crucial for keeping the purity was special gas tight equipment for transporting material in and out, quite essential for ascertaining the quality of the materials and their analyses.

We have monitored the gas pressure evolution by time in three setups (including two reference systems) and have by mass spectrometry shown that it is due only to hydrogen gas. However, the initial pressure increase at the start of the experiments seems rather similar, irrespective of whether there is copper immersed in the water or not. Some differences do occur as to the attained maximum pressure but these cannot be correlated with the fact that also the reference systems yield almost the same hydrogen evolution characteristics. One source of hydrogen gas production, except that from possible corrosion by copper, is probably the stainless-steel components of the equipment.

We have dismantled the setups without pressure monitoring after 1, 3 and 6 months, while assuming that hydrogen gas has evolved there as well. In these cases only hydrogen would pass the palladium membrane, the experiments starting with the nitrogen gas environment of the glove box within the reaction chamber. Thus, no external contamination could occur, and the continuous removal of hydrogen from the reaction chamber would drive any copper corrosion process to proceed beyond equilibrium. We have analysed the copper pieces, the water and the glass in contact with the water, all for establishing how far the copper metal has reacted. There is an increased dissolution of various species into the water by time, including the copper content. However, part of that increase must emanate from the glass: It contains copper that is probably leached out progressively by time, in fact the increase in copper and iron content follow the same trend, still at very low concentrations as analysed by ICP-MS.

The most crucial analysis result concerns the formation of corrosion products onto the copper metal surface where the most sensitive analysis technique, that of Auger spectroscopy, does not reveal the presence of the expected Cu_2O. Only the signal of pure copper metal is shown in the Auger Cu *LMM* spectrum. Minute oxygen signals were detected that, however, could not be attributed to any copper oxide but rather to adsorbed oxygen-containing species, since there was an increase in signal within 30 minutes even in the UHV (ultra-high vacuum) environment of the spectrometer. This fact illustrates the surface detection limit: Even parts of monolayers give measurable signals.

We strongly suspect that the copper contents obtained from the analyses of the water by ICP-MS are partly due to corrosion of the glass, since it has been shown to contain copper by XRF, and the copper and iron concentrations in the water increase with approximately the same rate. Therefore, these copper contents as solely emanating from copper metal get overestimated. Again, from Auger spectroscopy on copper from the 6 months' sample, the amount of copper oxide must be considerably less than 1 nm, considering the extreme surface sensitivity together with the fact that only pure copper metal was detected.

Putting our analysis data together with these remarks taken into consideration, we conclude that the corrosion rate of pure copper in pure water is very small, probably less than 1 nm/year.

This report constitutes an evaluation of experiments performed during a period of six months, concerning pressure measurements and analyses of corrosion products. Further work is in progress with extended analyses of long-term experiments of copper corrosion, as well as new pressure measurements made after a reconstruction of the equipment in order to eliminate leakage and to minimize the hydrogen background. The results from all these efforts will be accounted for in a coming report.

This report is a translation of the SKB report R-13-31 "Koppars korrosion i ultrarent vatten".

Sammanfattning

Det har hävdats att metallisk koppar kan korrodera i avsevärd grad till och med i syrgasfritt vatten och då ge vätgas vilket, om det vore korrekt, skulle kunna ha menliga konsekvenser för kärnbränslehanteringen som SKB ansvarar för. I avsikt att kasta nytt ljus på frågeställningen har vi utfört en oberoende vetenskaplig undersökning av systemet Cu-H_2O vid 50 °C med användande av ultrarena komponenter, nämligen 99,9999 % koppar och vatten av ppt-renhet. Experimenten har baserats på två typer av uppställning, en där gasutvecklingen kunde följas och en där oxidationsprodukter hos koppar kunde undersökas efter olika tider, i det senare fallet möjligt endast efter att utrustningen tagits isär. I bägge fallen utgjordes reaktionskammaren av ett kärl av rostfritt stål, helt gastätt så när som på att en yttre palladiumfolie fungerade som ett selektivt membran varigenom endast vätgas kan passera. Reaktionskammaren innehöll en bägare av borosilikatglas (Duran) med vatten försedd med en insats av kvartsglas som hållare för kopparbleck. Tre uppställningar anslöts individuellt till ett system för kontinuerlig loggning av data. Två av dessa uppställningar var referenssystem (de saknade kopparbleck) men skilde sig åt genom olika material i gastätningen.

Innan experimenten startade renades kopparen i tre steg: Elektropolering för att skapa en slät yta utan repor, vätgasreduktion för att avlägsna ett kvarvarande tunt oxidskikt, och slutligen värmebehandling för att driva av överskott vätgas och reducera mekaniska spänningar. Kvalitén kontrollerades med olika analystekniker (XPS, ERDA) vilka visade dels att metallen var befriad från oxid, dels att inte vätehalten hade ökat genom behandlingen. Att reningen av vattnet från inlöst syrgas var effektiv följdes och kontrollerades med en särskild optisk sond. Alla reaktionsexperiment genomfördes i en handskbox med torr kvävgas i avsikt att förhindra kontamination av syrgas, såväl vid start som vid brytande av experiment. Avgörande för att garantera att renheten bevarades var gastäta behållare för transport in och ut ur boxen, en helt nödvändig åtgärd för att säkra kvalitén på materialen själva och analyserna av dem.

Vi har följt den gradvisa tryckförändringen som funktion av tid i tre utrustningar (varav två referenssystem) och har med masspektrometri visat att gasfasen utgörs av vätgas. Det visar sig att den initiala tryckökningen vid experimentens start tycks mycket lika varandra, oavsett om koppar i vatten finns närvarande eller inte. Visserligen är det skillnader i maximalt uppnått tryck, men dessa kan inte enkelt korreleras till observationen att även referenssystemen uppvisar nästan identiska förlopp vad gäller vätgasutvecklingen. En källa till vätgasproduktion förutom från eventuell korrosion av koppar bör vara de komponenter av rostfritt stål som ingår.

Vi har öppnat utrustningarna utan tryckmätning efter 1, 3 och 6 månader och förutsatt att vätgas utvecklats även där. I de fallen har endast vätgas kunnat passera palladiummembranet sedan experimenten startats då reaktionskammaren var fylld med handskboxens kvävgas. Därför har ingen extern kontamination kunnat äga rum, och det faktum att vätgas hela tiden avlägsnas bör driva en kopparkorrosionsprocess vidare, förbi jämvikt. Vi har analyserat kopparblecken, vattnet samt glaset i kontakt med vattnet, allt för att fastlägga i vad mån koppar har reagerat. Det sker med tiden en ökande upplösning av olika ämnen in i vattnet, inklusive stigande kopparhalt. Emellertid måste någon del av denna ökning härröra från glaset: Det innehåller koppar som lakas ur allteftersom. Faktum är att ökningen i koppar- och järnhalter följer samma trend om än i mycket låga koncentrationer (analyserade med ICP-MS).

Det mest avgörande analysresultatet berör bildandet av korrosionsprodukter på ytan av kopparen, varvid den känsligaste analystekniken, Augerspektroskopi, inte har kunnat påvisa någon förväntad Cu_2O. Den enda signalen i Augerspektrum från Cu *LMM* kommer från metallisk koppar. Mycket svaga syrespektra detekterades visserligen, men dessa kan inte hänföras till någon kopparoxid utan snarast till syreinnehållande ämnen som adsorberats, ty syresignalernas intensitet ökade till och med inne i spektrometerns ultrahögvakuum under 30 minuter. Detta illustrerar känsligheten och detektionsgränsen: Delar av monolager är tillräcklig täckning av ytan för att ge mätbara signaler.

Vi misstänker starkt att de kopparhalter som uppmätts i vattnet med ICP-MS till del beror av glasets korrosion, ty XRF har tydligt visat att glaset innehåller bland annat koppar. Till yttermera visso ökar koppar- och järnkoncentrationerna med ungefär samma hastighet (ur jämförelse mellan 1, 3

och 6 månaders exponering). Därför blir kopparhalter såsom enbart härrörande från koppars kontakt med vatten överestimerade. Data från Augerspektroskopi från sexmånadersprovet ger vid handen att en eventuell beläggning av kopparoxid måste vara betydligt tunnare än 1 nm, med tanke på den extrema ytkänsligheten och på att endast metallisk koppar detekterades.

Utifrån olika analysdata och med hänsyn tagna till faktorer enligt ovan drar vi slutsatsen att korrosionshastigheten hos ren koppar i rent vatten är mycket låg, troligen mindre än 1 nm/år.

Denna rapport utgör en delrapport utifrån utvärdering av tryckförsök och analys av korrosionsprodukter efter sex månader. Arbetet går vidare med ytterligare analyser av pågående långtidskorrosionsförsök. Dessutom skall nya tryckmätningar utföras efter viss omkonstruktion av apparaturen i avsikt att eliminera utläckning och minimera bakgrundsvärdena av vätgas. Resultaten av dessa insatser redovisas i en kommande rapport.

Denna rapport är en översättning av SKB rapport R-13-31 "Koppars korrosion i ultrarent vatten".

Contents

1 Introduction

1.1 Background

SKB intends to dispose nuclear fuel in copper canisters with an iron insert. These are to be deposited in an anaerobic environment in underground caverns, enclosed in bentonite clay (SKB 1978).

The method has been questioned recently, however, by different experiments showing that hydrogen gas seems to be formed by copper in contact with water, which is interpreted as a corrosion process with water as the only oxidant.

A series of such studies have been performed since experimental data in an article from 1986 seemed to support the notion that copper corrodes at a non-negligible speed with pure water as the oxidant (Hultquist 1986, Szakálos et al. 2007, Hultquist et al. 2009, 2011). These and other experiments have mainly measured hydrogen evolution through the pressure increase in a chamber that is connected to the test chamber via a palladium membrane permeable to hydrogen gas only. The amount of hydrogen gas evolved has then been used to calculate the amount of copper assumed to have oxidised to the same degree. The amount of hydrogen gas evolved would thus mean that the copper canisters corrode considerably faster than predicted by previous calculations based on well recognized thermodynamic data.

The results have been questioned by various researchers. Accordingly, attempts have been made to reproduce the results with similar experimental set-ups (Simpson and Schenk 1987, Eriksen et al. 1989, Becker and Hermansson 2011). As the experiments deviate from recognized thermodynamic preconditions, they have also been criticised in so far as the interpretations have been strongly questioned (Werme and Korzhavyi 2010, Johansson 2008).

1.2 Mission and purpose

Through these controversial results, the Department of Materials Chemistry, now extended with a change of name to the Department of Chemistry – Ångström Laboratory, was commissioned by SKB to make independent experiments for investigation purposes. These were, however, to be performed as a basic research assignment with as refined conditions as possible, that is, with as pure copper and as clean water as is economically justifiable, in order to confirm or refute the proposed hypotheses. In consequence, the new experiments serve to reproduce neither the conditions on which the laboratory results are based nor the conditions that will prevail at the final disposal of the copper canisters. This choice means, instead, a refinement of the experiments in so far as both components – copper and water – should have the highest purity to avoid additional parameters (sometimes intractable) that could influence the hypothetical corrosion process and thereby affect the results. Well-defined material grades and accurately developed and well-described working procedures guarantee that the experiments shall be reproducible. Details in that respect are to be found in the enclosed appendices.

1.3 Structure of the report

The report is made up of two basic parts, a main text and an appendix with various sub-appendices. The appendix provides a number of details concerning the experiments, details that are not necessary to follow the report through to its conclusion but that clarify both technical and performance aspects of the study. In the text, reference is made to the specific appendix that contains details on that part of the text.

The main text is divided into different sections that illustrate the procedure from preparation to completion of the work:

Section 1 (Introduction), Section 2 (Preparation), Section 3 (Descriptions of the experimental set-ups), Section 4 (Chemical characterisation methods), Section 5 (Results of pressure measurements and chemical analyses), Section 6 (Discussion and conclusions), Section 7 (Summary).

The main text ends with a reference list for the entire report.

The appendix is similarly divided into different sections with details relating to the main text:

Appendix A (Quality control), Appendix B (Equipment), Appendix C (Performance details), Appendix D (Descriptions of the analysis techniques), Appendix E (Calculations and estimations).

2 Preparatory work

The preparatory work evolved in several stages. Unique conditions apply for experiments where one must handle and protect components of the utmost purity at the beginning of the experiments. All experiments must then be carried out in such a way that the purity is maintained when they are initiated and that no contamination takes place either in the course of the experiments or in connection with their interruption for an evaluation of results. It must be possible to carry out analyses in a reliable way for the measurement of small amounts and contents using approaches that can complement each other and result in a consistent interpretation of the outcome. All measurements and parameter controls must be carried out with the highest precision and accuracy. This includes on the one hand continuous measurements and adjustments during the tests (which must be secured against e.g. power failure), and on the other analyses of starting components, products from the alleged corrosion process and materials that have been in chemical contact with these substances during the course of the tests.

2.1 Strategy for monitoring the processes

It was crucial to be able to guarantee the quality in all steps of the experiments through appropriate treatment and follow-up with different parallel and overlapping analytical methods. The use of a glove box with a controlled inert atmosphere was utterly essential. Previous studies have focused on pressure changes, whereas in this study it was considered absolutely necessary to correlate the gas evolution with a characterisation of reaction products so as to be able to claim both that the pressure increase is caused only by hydrogen gas and that this must derive from the corrosion of copper.

The design of the experiments must permit an analysis of all three aggregation states:

(*s*) solid phase, (*l*) liquid phase, and (*g*) gas phase. The following figure illustrates the analysis strategy concerning the effects of copper in contact with water, with analyses also of components in contact with this system, such as glass surfaces and palladium membranes.
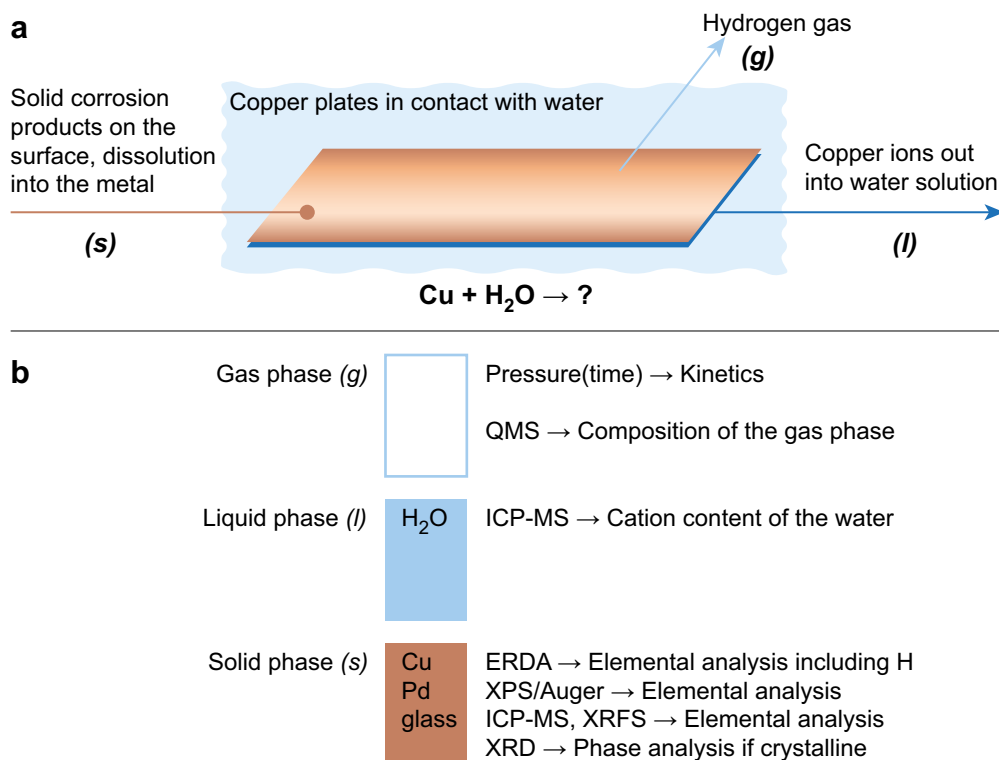
Figure 2-1. *Schematic outline of (a) the problem and (b) the related analysis strategy.*

2.2 Selection and treatment of materials

2.2.1 Copper

The copper grade that was selected contained 99.9999% Cu in the form of a foil in two thicknesses, 0.25 and 0.50 mm (for supply reasons). However, the contaminants declared by the supplier (see Appendix A) never include surface contamination. The copper was therefore surface cleaned in three steps:

1) electropolishing, 2) hydrogen reduction and 3) heating in vacuum.

Unlike all forms of mechanical polishing, electropolishing creates a very even surface with a reproducible method. With a mechanical grinding of such a soft metal, there is, in addition, always a risk that the polishing agent adheres to the surface and contaminates the sample. The electropolishing was performed in phosphoric acid (*pro analysi*) whereby a continuous piece was purified. This piece had been partly cut through in grooves so that it could then be split into smaller parts (20×10 mm and 47×12.5 mm respectively) without running the risk of contaminating the metal through cutting (Figure 2-2). The larger plates, selected to yield larger amounts of corrosion products, were too large to fit into the analytical instruments for solid products. The oxide contaminants on the surface were removed through hydrogen reduction (99.9999% H_2) for an hour during heating to 300°C (Figure 2-3). Its efficiency could be monitored a posteriori with electron spectroscopy (XPS; see Results). Finally, the temperature was raised to 400°C in UHV (10^{-8} Torr) for two hours whereby the remaining hydrogen gas was baked out. This process was monitored using mass spectrometry in order to guarantee that the material was exhausted of all hydrogen before it was interrupted. The copper was transported to the glove box in a sealed tube without breaking the vacuum (Methodology details in Appendix C).

Copper was also used as a sealing gasket (of CF type, also silver plated) between the reaction chamber and its lid. Its hydrogen content was 0.9 ppm according to melting analysis (Appendix D1).

2.2.2 Water

The water used in the experiments was of ppt quality (Specification in Appendix A) which was difficult to check. For instance, pH-measurements cannot be carried out due to extremely low buffer capacity. After opening in the glove box, dissolved gases were removed (O_2, CO_2) through bubbling with high purity nitrogen (> 99.9999% N_2). This method was considered superior to other methods such as pumping out (Butler et al. 1994).

The purification effect could be monitored in real time (Figure 2-4) using an optical instrument (Appendix B3), and after just over an hour the oxygen content was under the detection limit (< 1 ppb) of the instrument. Analysis of the water with ICP-MS gave no detectable amounts of dissolved elements in addition to those from the glass. No significant difference was detected between "virgin water" and degassed water.

2.2.3 Glass

In order to follow previous studies to some extent but also make sure that dissolution of water was kept to a minimum, we selected borosilicate glass (Duran) for the containers intended to contain the water and copper samples (Appendix A and references therein). However, the holders that were in direct contact with the copper samples were made of quartz glass.

Figure 2-5 shows a test chamber of stainless steel with a Duran glass beaker and an insert of quartz glass. This was where the copper pieces used in both types of corrosion experiment set-up were placed, both for pressure measurements and for investigation of corrosion products. Glass sheets (also made of Duran glass) were likewise placed there with a view to later analysis. All glass ware was cleaned with nitric acid before the experiments (see Appendix C).

2.2.4 Steel

The material in the metal containers was stainless steel 304L, and the reaction chamber was produced in one piece. The sealing was a CF-63 flange that was lathe machined from the chamber. The sealing lid was a blind flange (CF-63) in 304L steel with, a KF-16 flange (likewise in 304L steel) welded on. As seal to the lid, a copper CF-63 gasket was used (see Figure 2-5 and Figure 2-6).

The material in most parts of the vacuum chamber that were in contact with the reaction chamber was, however, stainless steel 304L, and the seal was CF-15. The leak valve was made in 316L (see Appendix B).
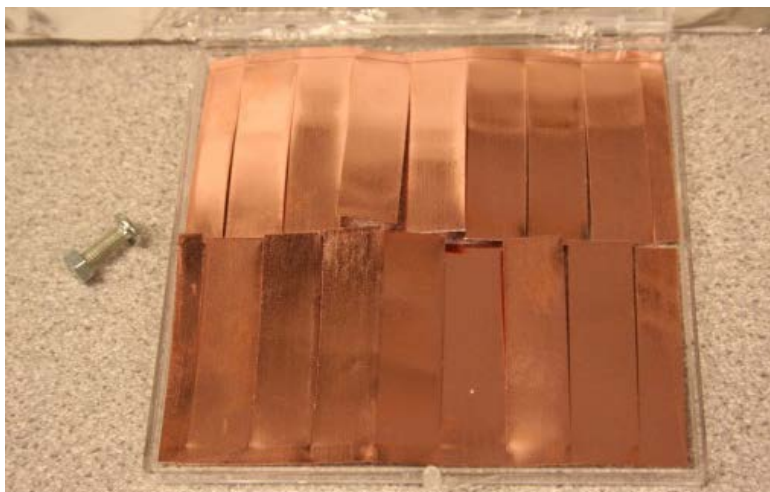
Figure 2-2. Copper plates from cut-outs of larger sheets of copper.
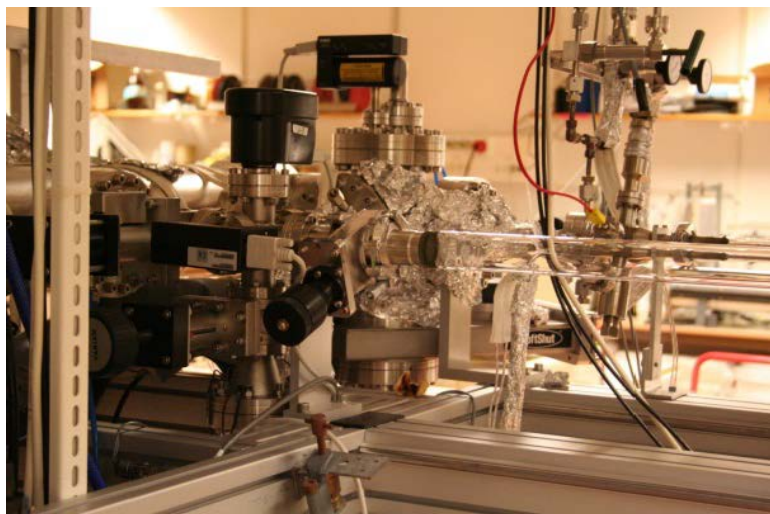
Figure 2-3. UHV oven for surface cleaning of copper samples.
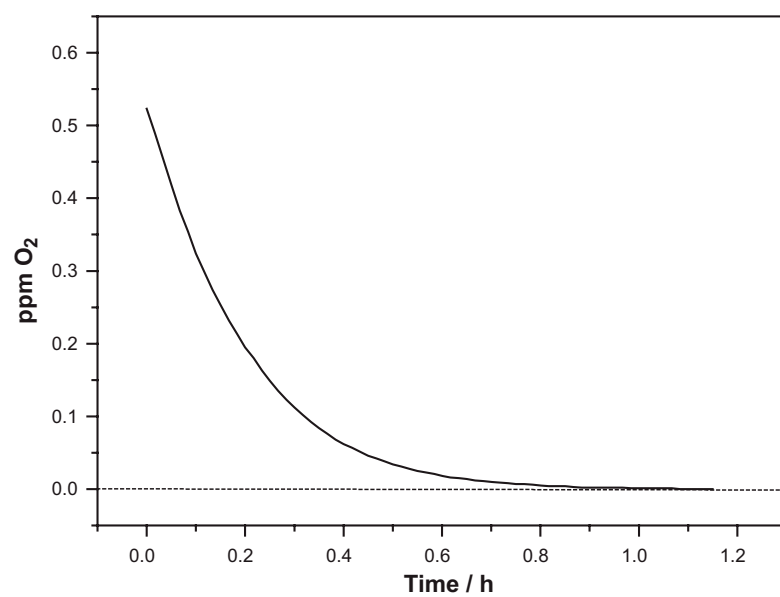
Figure 2-4. The oxygen content of the water during bubbling.

Figure 2-5. *The reaction chamber with beaker and insert holder with an inserted copper plate.*

Figure 2-6. *From left to right: Glass beakers to be filled with 100 ml water; insert of quartz glass as holder for glass sheets and copper plates; reaction chamber of stainless steel where the beaker with insert is placed together with the chamber lid with copper gasket (CF 63).*

2.2.5 Palladium membrane

The seal between the reaction chamber and the vacuum chamber was constituted of a 0.1 mm thick palladium foil (> 99.99%, see Appendix A). A membrane with a diameter of 23 mm was die-cut and used as a selective gas filter and seal. The membrane was squeezed against the KF-16 flange with a Helicoflex-gasket in aluminium. The aluminium gasket was only exposed to the vacuum chamber, and not to the reaction chamber.

2.3 Experimental strategy

In order to avoid contamination as much as possible, the experiments were set up inside a glove box. These were in principle equivalent but still of two types, one for *continuous monitoring* of gas pressure (including reference system) and another without this connection for the *repeated analysis* of the copper samples and their immediate environments (Figure 2-7). A part of the overall strategy was to open the latter type of set-up at different times without putting the long-term tests with pressure monitoring at risk. As these were also equipped with Pd membranes, the systems were "open" in the sense that the formed hydrogen gas could escape without the build-up of a counter pressure. This situation would mean that a local chemical equilibrium would be shifted towards the formation of more reaction products than in a closed pressure-monitoring system, because hydrogen was removed continuously with unchanged kinetics.

The larger plates, 8 pieces (see Section 2.2.1 concerning dimensions), was used in pressure test Main 1 (total surface area of 96 cm^2). The smaller plates, 7 pieces, were loaded together with a glass sheet in each of the five long-term tests (see Figure 2-7).

By breaking the containers that were not connected to the pressure-gauge equipment, it was also possible to get successive feedback of the appropriateness of different procedures and the possibilities of different analysis methods, a bonus effect of using this strategy. The plan was to break the first set-up after one month and the remainder after three, six, nine, and twelve months, respectively.

Glove box
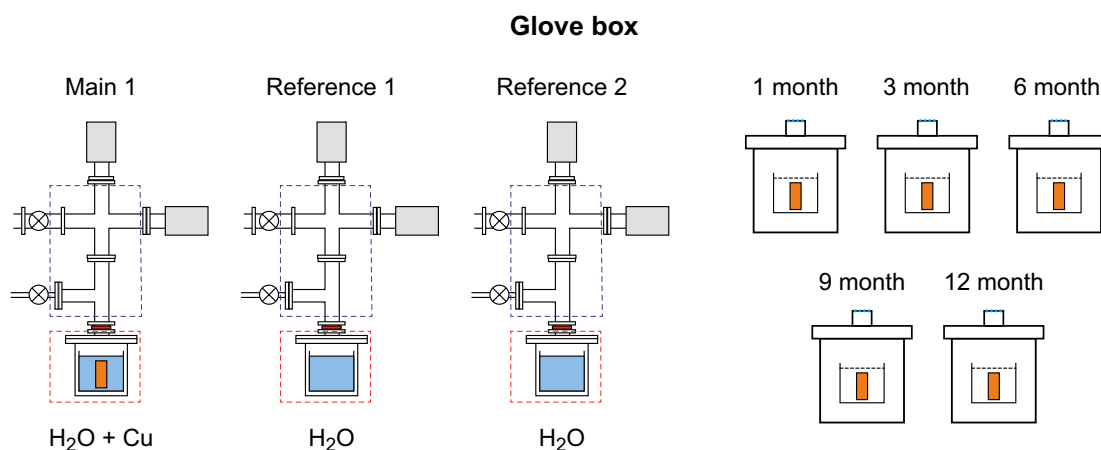
Figure 2-7. Schematic view of experimental set-ups of two types, three with and five without pressure monitoring. Reference systems 1 and 2 lack copper plates but are otherwise as Main 1.

3   Description of experimental set-up and procedure

3.1   Set-up

3.1.1   Glove box

The test set-ups were arranged in a glove box of nitrogen atmosphere, in which also the steel containers were loaded and opened. In this way contamination by oxygen gas would be avoided. The guaranteed purity of the nitrogen gas is 99.9999% but in fact it is normally a factor of ten higher. Also, oxygen and water were removed from the glove box atmosphere. The results of an initial test of the capacity of the glove box are illustrated in Figure 3-1. After about 5 days oxygen and water contents below the detection level (0.1 ppm) were achieved. See further Appendix B, Performance. Evacuable transferring vessels were utilised to move samples in and out.

3.1.2   The steel containers with inserts

All steel containers were of the same type, equipped with lids with palladium membranes and heating jackets (Figures 3-2 and 3-3); see also Appendix B). The temperature of the reaction vessel was selected at 50°C, while the temperature of the membrane was slightly higher (55°C) – heated by a separate heating tape – to counteract water condensation. The chamber and the lid (with the membrane) were each equipped with a thermocouple element for temperature control/measurement. The temperature was controlled by means of a computerised temperature control system.

Three of the containers were equipped with a connection for simultaneous pressure measurement (designations according to Figure 2-7). The other containers, intended for the monitoring of the formation of reaction products (see section 2.3), had in fact a membrane but lacked this extension equipment. Irrespective of set-up they were (in the glove box) equipped with an inner glass beaker that was filled with ultrapure water and an insert of quartz glass with samples of Duran glass, quartz glass, and (except in the reference setups) copper plates (see Appendix A for details). In the insert the samples were arranged vertically and entirely lowered into the water without contact with each other (Figure 2-6). After loading, the lid was screwed on under controlled conditions (torque wrench) to achieve reproducibility.

Above the membrane, in the first type of set-up, there is an initially evacuated volume of 76 cm^3 and two pressure gauges with different operating ranges: The maximum values are 1 Torr and 50 mTorr, respectively. The latter can register pressure differences of about 0.02 mTorr, which corresponds to a leak rate of 10^{-12} Torr L/s, lower than the detection limit of a helium leak detector.
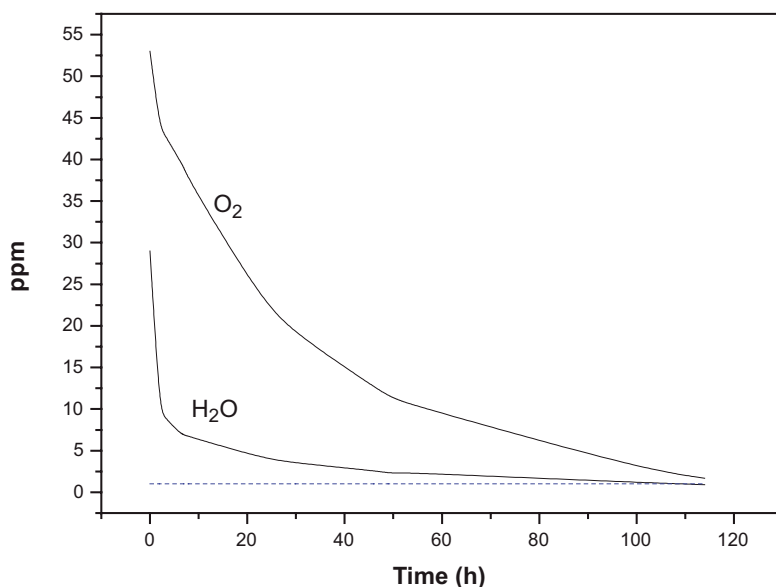
Figure 3-1. Oxygen and water content in the glove box after start.
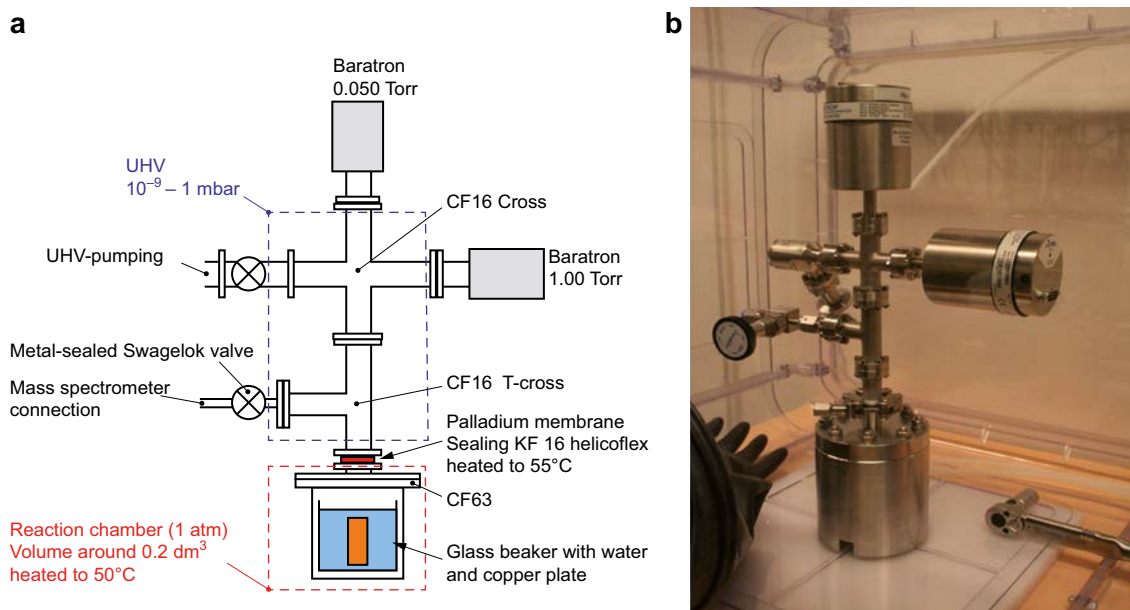
Figure 3-2a–b. (a) Exploded view drawing of a planned reaction chamber with connection for pressure measurements. b) Photograph of the actual design before connecting to the logging system.

Figure 3-3. Interior of the glove box with three connected containers (Main 1, Reference 1, Reference 2).

3.1.3 Parametric control and data logging

The hardware was purchased from National Instruments. The experiments were controlled and monitored by a logging system from Rowaco AB that controls and records both temperature and pressure parameters from a total of 24 thermocouple elements and 8 pressure sensors. Besides logging data, the system warns if data significantly deviate from reference values, and the system is also equipped with a backup safety system including a UPS system in case of power failure (see Appendix B).

Figure 3-4 shows schematically how the gas-phase investigations with pressure measurements and mass spectrometer analyses were performed. Besides referring to the different reaction vessels (the same designations as in Figure 2-7) a rough progression over time is indicated. In consequence, the mass spectrometer analysis of the gas phase could not take place initially but later, following modification of the spectrometer to allow its connection to the system.

3.2 Procedure details

3.2.1 Seal

The geometry of the seal between the reaction chamber (at the bottom) and the vacuum section (uppermost) is schematically illustrated in Figure 3-5. The palladium membrane (red in the figure) is squeezed where the sealing ring of aluminium (Helicoflex) faces the vacuum section. The ring (in blue) has a wall thickness of ~1.4 mm. The copper seal between the reaction chamber and its lids is illustrated in Figure 2-5 and Figure 2-6.

The vacuum systems were leak tested by an Agilent VSRR022 leak detector. None of the systems gave detectable signals when leak tested by a helium leak detector, which means that the inleakage rates for all of them were lower than 10^{-11} Torr L/s. For the performance of the pressure gauges, see section 3.1 and Appendix B for additional details.
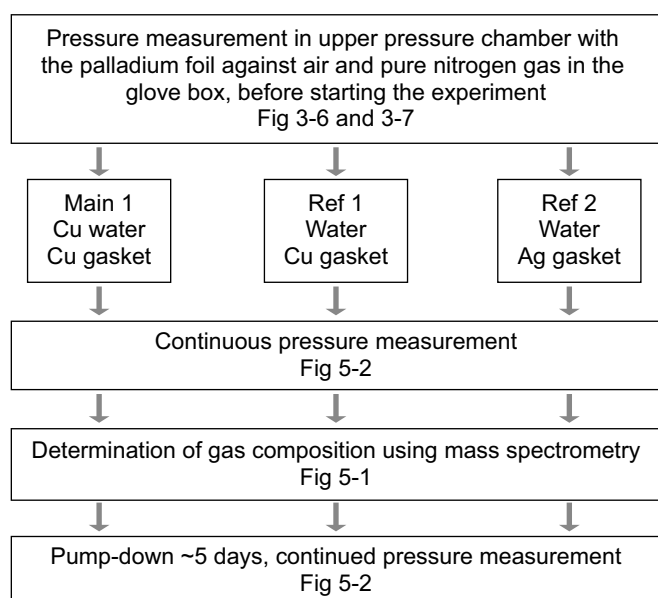
Figure 3-4. *Schematic view of the experimental set-ups for the studies of the gas phase by pressure monitoring and chemical analysis (Main 1, Reference 1, Reference 2). The arrows give a rough indication of the progress over time.*

Figure 3-5. *Sketch of sealing ring of the palladium membrane (left) and photographs of the installation (right).*

3.2.2 Bake-out of the vacuum equipment

A low and stable pressure must be reached before starting the experiments. The pressure systems were therefore baked, and the increase in pressure subsequently measured. As the palladium membrane is in contact with the atmosphere, the lowest possible pressure should be limited by the hydrogen content in the air, i.e., 0.4 mTorr (Novelli et al. 1999).

The bake-out of the vacuum systems, that is, the upper section in Figure 3-2, which was not yet connected to the reaction chambers, was very time-consuming. The pressure gauges do not withstand temperatures higher than 70°C, and therefore the bake-out was initially limited to 120°C, and the pressure gauges were not baked. Ten days of bake-out turned out to be insufficient for reaching a stable starting pressure below 10 mTorr. The pressure increased continuously for one month, which was believed to be caused by water degassing during an insufficient bake-out time at the selected temperature. A modification of the procedure was therefore required:

The heated section could be insulated such that the temperature at the pressure gauges did not exceed 70°C, and therefore it was possible to increase the bake-out temperature to 150°C. This turned out to be efficient (stable pressure after four days) and was therefore applied to the connections to both the main cylinder (Main 1) and the reference set-ups (Reference 1 and Reference 2).

After the 150°C bake-out the pressure in the vacuum sections reached stable levels of ~9 mTorr for Main 1 and Reference 1 and ~3 mTorr for Reference 2 (with Ag-plated copper in the reaction chamber lid). Following stabilisation a considerably slower pressure increase, $< 2 \cdot 10^{-11}$ Torr L/s, was observed. The slow pressure increase was considered to be acceptable, as it would only contribute to the total pressure increase by 2 mTorr/year in the vacuum systems.

3.2.3 Pressure stabilisation before starting the experiments

The bake-outs and evacuations of the three vacuum chambers (upper section according to Figure 3-2a) were all performed in an open glove box by a UHV system. The next step was to assemble the different parts into a complete measurement system. When the glass pane of the glove box was mounted and the box was started, it turned out that the pressure in the vacuum chambers dropped after the change of atmosphere outside the membrane to dry nitrogen gas. At this stage, the reaction chambers were not yet connected. The pressure in the vacuum chamber intended for Main 1 changed from just below 9 mTorr to 3 mTorr (see Figure 3-6); for Reference 1 it changed from slightly more than 9 mTorr to 4 mTorr whereas it dropped only slightly from an already lower level for Reference 2 (see Figure 3-7).

As only hydrogen gas can pass the palladium foil, the pressure difference must indicate that hydrogen gas exits the vacuum chamber into the glove box. A hypothesis is that a reduced hydrogen activity on the outside of the foil (from air to dry nitrogen gas) creates a driving force for out-diffusion. On the outside of the Pd foil, the content of hydrogen gas (in 99.99999% nitrogen gas) should be very small – the partial pressure in air is about 0.4 mTorr (Novelli et al. 1999). That hydrogen gas was the entirely dominating species could be determined in a later phase (Section 5) when it was possible to connect a mass spectrometer first after a modification.
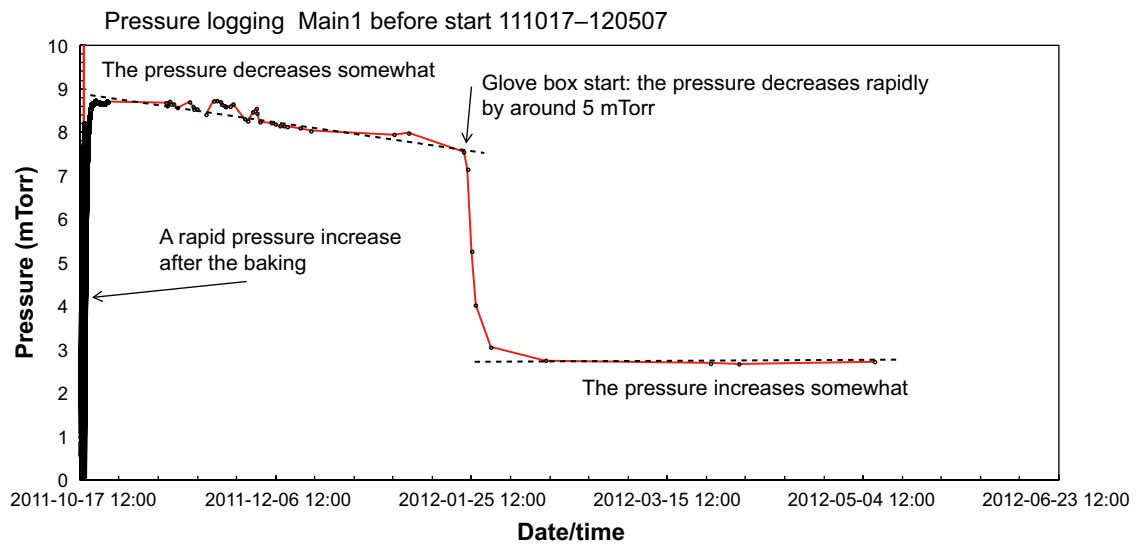
Figure 3-6. *Pressure change in the vacuum section of Main 1 after bake-out and when starting the glove box. Note that the reaction chamber was not yet connected.*
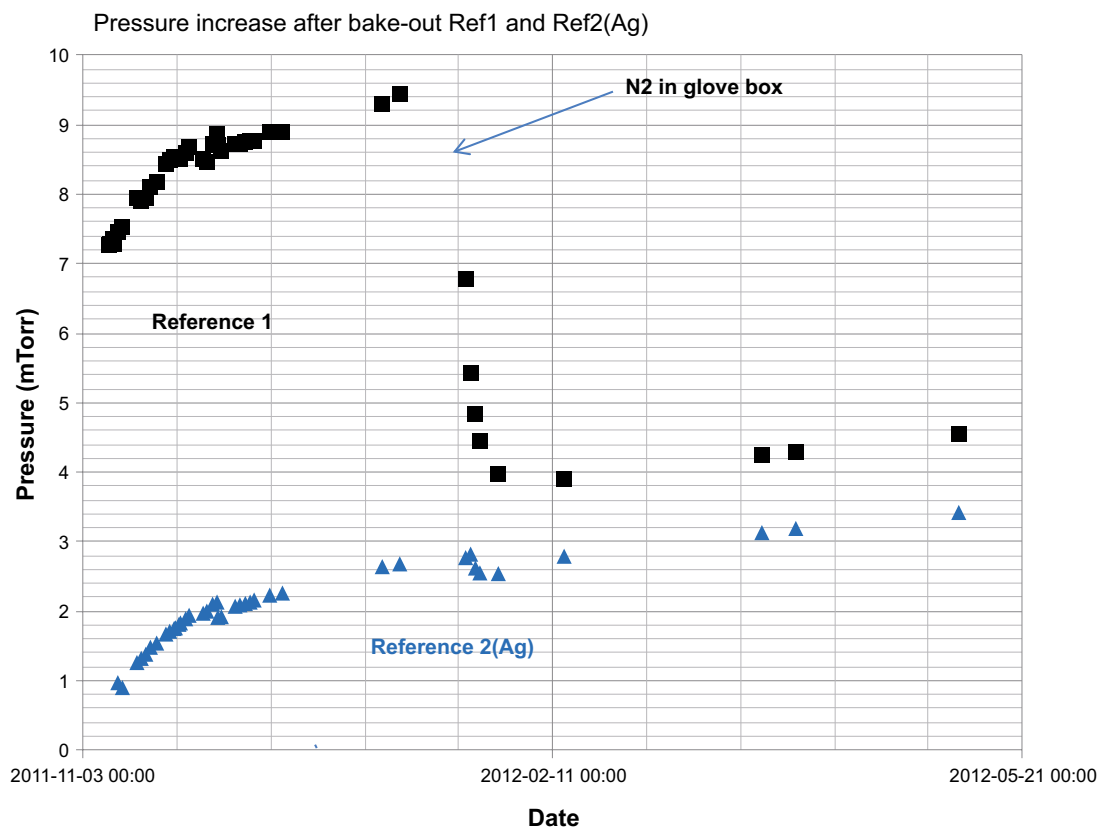
Figure 3-7. *Corresponding pressure changes for Reference 1 and Reference 2. The designation "Ag" for Reference 2 means that in this equipment the copper ring of the lid (Figure 3-3) was replaced later by a silver-plated ring, which is of no importance here.*

4 Chemical characterisation methods

The chemical characterisation of aggregation states requires different methods. For the solid state, we have primarily utilised so-called non-destructive techniques, diffraction and spectroscopy using equipment available at the Ångström laboratory, unless otherwise specified. Mass spectrometry was used for gas-phase analysis. The ICP technique (experiments performed at the Department of Chemistry at the Biomedical Centre (BMC)) required transformation into liquid phase if the samples were not liquid to start with. See Appendix D for details about some of the methods.

4.1 Electron spectroscopy

Two electron spectroscopy techniques were utilised: XPS (X-ray photoelectron spectroscopy) and Auger spectroscopy. Both methods are mainly utilised for elemental analysis but they also give some information about chemical bonds.

The sample is irradiated with X-rays – or electrons for Auger, in a special instrument – in a high-vacuum system. In both cases the outgoing electrons are analysed with regard to their energies. These are photo-electrons (in XPS) or Auger electrons; the latter are caused by interaction between electrons in the material after excitation of the material by X-ray photons (or high-energy electrons).

The methods are highly surface-sensitive owing to the strong absorption of electrons, and the Auger method is even more sensitive than XPS, in both cases by fractions of monolayers (Xing et al. 2007). The analysis depth is ~1–10 nm for XPS and ~1–3 nm for Auger spectroscopy (Vickerman and Gilmore 2009). Electron spectroscopy samples are therefore often treated in vacuum in the spectro-meter in ways to create a "fresh" surface, e.g. through breaking, stripping, and peeling. In some cases it is possible to "blast" with an inert gas, argon sputtering. By this means the outer atomic layers can be removed; however, in the worst case this technique may give rise to chemical modifications. It is highly important that the sample exposure time to reactive atmospheres is kept as short as possible. Here, a canister with an inert atmosphere has been utilised for transfers from glove box to spectrometer.

The spectrometers utilised were a Perkin Elmer Phi 5500 and a Scienta with a SES 200 analyser, the latter for the 1-month sample of copper. Both operated with monochromatic AlKα radiation, and the electron energies are expressed either as binding energy (for XPS) or as kinetic energy (for Auger). The energy ranges that were studied for the copper samples – apart from the initial overview spectra – comprise spectra of Cu *2p*, C *1s* and O *1s* (XPS) as well as Cu *LMM* (Auger). Auger spectra are, in contrast to XPS spectra of corresponding elements, more complicated but serve also more as finger-prints for a phase analysis rather than an elemental analysis: While Cu *2p* spectra are nearly identical for Cu and Cu_2O, their Auger spectra are different.

4.2 X-ray fluorescence spectroscopy (XRF)

The method resembles electron spectroscopy techniques in the sense that solids are irradiated with X-rays whereby electrons in the material are excited. In XRF, it is the subsequent emission of X-ray photons in the relaxation phase down to the ground level that is utilised. This means a considerably increased analysis depth compared to XPS, 30–50 μm. The energy of the outgoing X-ray radiation can directly be related to differing atomic species; hence, this method is suited for elemental analysis.

The element-specific radiation can be analysed either in terms of its energy or its wavelength. The intensity of the signal is a measure of the amount. We have utilised energy dispersion of the signals (often shortened ED) and used an instrument in which the intensity measurement is optimised through the use of a secondary source (PAN Epsilon 5). For accurate measurement, calibration to materials with known amounts is required. Contents down to the ppm level can in this way be determined. Equipment and methodology details can be found in Appendix D.

4.3   Elastic Recoil Detection Analysis (ERDA)

Elastic Recoil Detection Analysis (ERDA) is an analysis method based on ion-beam technology and is particularly suited for the depth profile analysis of light elements (Tesmer et al. 1995) which generally is difficult to perform quantitatively. The samples are placed in an ultra-high vacuum chamber with a pressure of $< 10^{-6}$ mbar. In ERDA analyses, high-energy heavy ions are used; that is, the energy is some hundreds of keV per atomic mass unit. The ions that impinge on the sample surface at a low angle knock atoms and ions from the sample, and these ions and atoms are then detected. The energies of the knocked-out atoms and ions depend on their atomic masses and the depth from which they recoil. Specific depth profiles for each atomic species can be obtained from a single measurement by using a combination of TOF technology (time-of-flight technology) and conventional solid-state detectors.

The experiments were performed at the tandem accelerator in a TOF/ ERDA set-up at the Ångström Laboratory, Uppsala University (Zhang et al. 1999, Petersson 2010). The instrument was adapted for the determination of hydrogen content and other contaminants in copper and palladium. An ion beam of I^{8+} with the energy 36 MeV was used, as it gives the best yield for the elements in our study. The contents of elements with atomic numbers lower than ~30 can be determined down to depths of 150–200 nm. The resolution of the depth profile is ~15 nm for the studied elements. Before the analyses were started, the detectors were calibrated for light particles (Zhang et al. 1999).

4.4   Melting analysis

The method is based on the heating of metal samples such that incorporated gases are emitted from the whole sample. Here, the method was used to determine the hydrogen content of copper. The hydrogen gas is transported in a carrier-gas flow of nitrogen gas and is detected by changes in thermal conductivity. The system is calibrated to standard samples of known hydrogen content. Hydrogen can be determined in very small amounts (< 0.1 ppm) with high sensitivity. The analysis was made by Bruker with a Bruker Galileo.

4.5   X-ray diffraction (XRD)

Diffraction phenomena are most appropriate to crystalline phases, and the information provides a *phase identification*. Solid corrosion products that are formed on metallic copper can be detected and identified if two conditions are fulfilled: firstly that they are crystalline, and secondly that they exist in sufficient amounts (the layer has sufficient thickness). A synchrotron source (MAX-lab Laboratory; Lund) has been utilised for the grazing incidence measurements, a procedure that is particularly suited to studies of thin layers. With this technology, crystalline copper oxide with a thickness of about 5–10 nm should be clearly detectable.

As the radiation source is far away from the experimental set-up (implying that the time aspect is not negligible) a special transfer technique must be applied. The sample was mounted in a vacuum-tight sample chamber of stainless steel with a beryllium dome (CF seal) in the nitrogen atmosphere of the glove box. The closed sample chamber permits the radiation to get in and out, and therefore no contamination by air can take place. The dome-shaped lid of beryllium absorbs X-ray radiation to a minor extent.

4.6   Mass spectrometry (MS)

Apart from the special application for liquid analysis below (ICP-MS), the technique is used for gas analysis:

A quadrupole mass spectrometer MKS Cirrus (LM99) triple mass filter 1–200 amu with an SEM detector was used (SEM denotes here secondary emission mass). The system was modified for UHV by increasing the inlet holes from 4×15 μm to 4×100 μm through a blinded bypass. In this way, the base pressure was reduced to $\leq 10^{-9}$ Torr. The mass spectrometer was connected to the pressure logging

system with a 1/8" gas line of stainless steel. The flow to the mass spectrometer was regulated by an UHV valve which means that the measurement takes place during pump-down. This means that the levels of gases with higher mass numbers will be slightly underestimated, as the pressure is lowered during measurement. The measurement sensitivity depends on the flow to the mass spectrometer. The pump-down speed was chosen such that the total pressure was reduced by about 10–30% during a measurement. The sensitivity was estimated at $\sim 5 \cdot 10^{-5}$ Torr in the pressure logging system (the corresponding pressure in the mass spectrometer is $\sim 5 \cdot 10^{-10}$ Torr).

4.7 Inductively Coupled Plasma Mass Spectrometry (ICP-MS)

The acronym ICP-MS stands for Inductively Coupled Plasma Mass Spectrometry, a spectroscopic technique for the measurement of low element content in a liquid sample. This is analysed after transfer to an aerosol (fine liquid droplets) that in turn is influenced by argon plasma such that more or less only atomic constituents remain and are ionised. The analysis is performed with a mass spectrometer that separates ions according to the mass/charge ratio (m/z). The amount of ions per time period can be related to the concentration of the element of concern.

The possibility to determine elements with ICP-MS is limited by the degree of ionization, by overlapping m/z-values of isotopes of other elements and by the presence of molecules that are abundant or difficult to decompose. Interference problems can be suppressed by, for example, selecting special isotopes for the study. A control of the reliability can be obtained in that different isotopes should yield the same concentration value (after correction for relative abundances), as used in the copper analysis (special test for ^{63}Cu and ^{65}Cu). Details are provided in Appendix D.
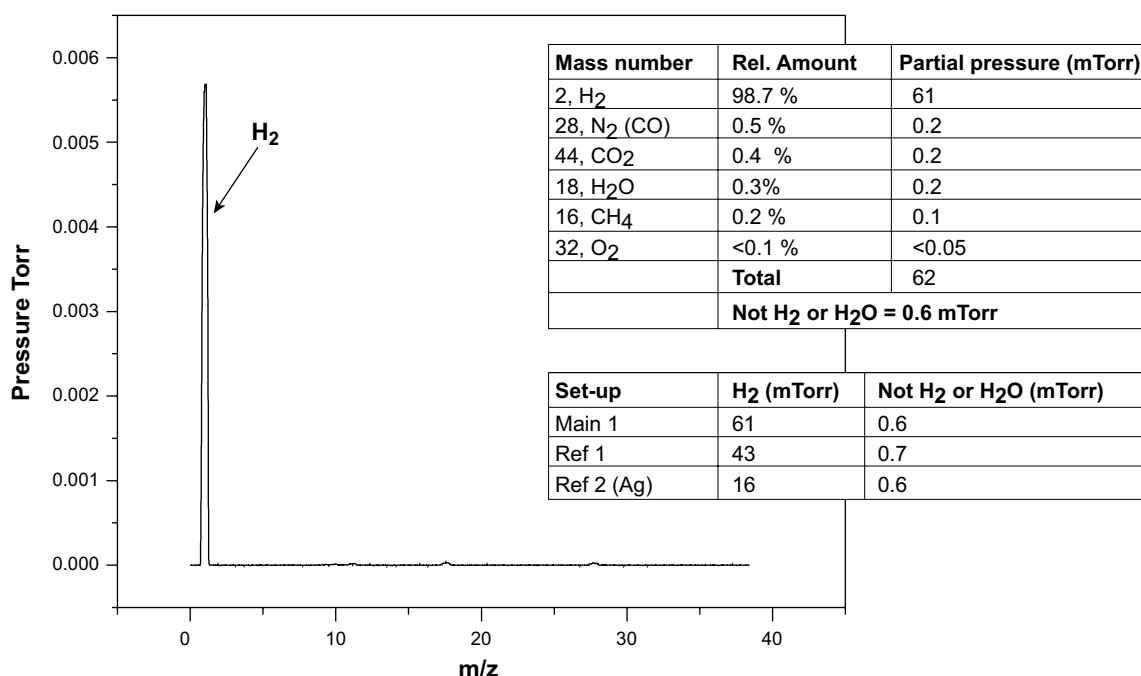
5 Results of continuous measurement and discrete chemical analyses

As it was necessary to test both the experimental equipment and the analysis methods during the performance of the long-term test, the systems without connected pressure measurement were evaluated at specific time points at an earlier stage, primarily after about a month, in contrast to those where pressure was measured continuously. This measurement was followed by equivalent measurements after three and six months.

5.1 Gas phase

The pressure measurements indicated a pressure increase both in the main cylinder (Main 1) and in a reference cylinder (Reference 1) with only a vessel of water with a glass insert but without added copper. This led to the hypothesis that the copper ring that constitutes the seal against the lid (see Figure 2-5) could also participate in a corrosion process. In consequence, a parallel blind test in which the copper seal was replaced with a silver-plated copper seal was started later (Reference 2).

In all three arrangements, hydrogen gas could be registered (Figure 5-1) with traces of CO (N_2), CO_2, CH_4, and H_2O that gave rise to an observed pressure increase to a maximum followed by a slow pressure drop (Figure 5-2). In all set-ups (see the lower table inset in Figure 5-1) the pressures of species other than hydrogen gas are approximately the same irrespective of the total pressure, which may indicate that they constitute remains left from the bake-out of the upper chamber, explained by the fact that the pressure-measurement system could not be heated. That hydrogen gas is the major species was not known at the start of the experiments, as a mass spectrometer could be connected only after redesigning the equipment.

Mass number	Rel. Amount	Partial pressure (mTorr)
2, H_2	98.7 %	61
28, N_2 (CO)	0.5 %	0.2
44, CO_2	0.4 %	0.2
18, H_2O	0.3%	0.2
16, CH_4	0.2 %	0.1
32, O_2	<0.1 %	<0.05
	Total	62
	Not H_2 or H_2O = 0.6 mTorr	

Set-up	H_2 (mTorr)	Not H_2 or H_2O (mTorr)
Main 1	61	0.6
Ref 1	43	0.7
Ref 2 (Ag)	16	0.6

Figure 5-1. Results of mass spectrometry studies of the gas phase in the upper chamber. In the inset tables, data from species (of low content) other than hydrogen gas are presented. The upper table is related to Main 1. In the lower table the three arrangements are compared. The values on the pressure axis in the graph are not relevant other than on a relative scale as only a small fraction is taken out for QMS analysis.
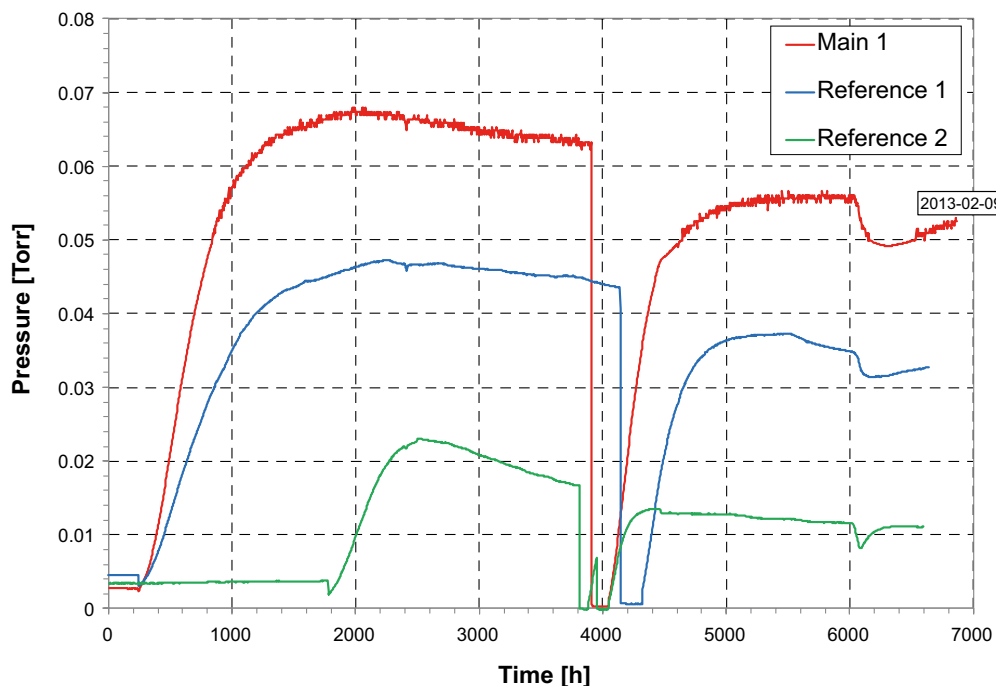
Figure 5-2. *Gas pressure as a function of time in the three arrangements that were connected to pressure-measurement systems. Reference 2 was added at a later stage because it was equipped with another seal.*

In the three setups, after about 4,000 hours, the upper chamber section was pumped, which also emptied the corresponding lower chamber as the palladium membrane permits hydrogen to pass through from there. Following pumping, the pressure rises back to levels that correspond to an extrapolation from an unpumped state. The kink in the curves at about 6,000 hours is an effect of an external operational failure in the form of a temporary air intake in the nitrogen line to the glove box (> 250 ppm oxygen), followed by a gradual recovery.

The initial growth of the curves indicates that hydrogen pressure is built up through production in the system. The palladium foil permits hydrogen gas to pass between the vacuum chamber and the reaction chamber, so in fact it is not possible to say where the generation takes place. The size of the initial growth, that is, the pressure increase per time unit, becomes a measure of the generation. An analysis of the curve shape during growth indicates that there is an inflection point after which growth decreases. The pressure increase rate decreases as the driving force of diffusion through the palladium membrane decreases. If the hydrogen-generating process reaches equilibrium at a sufficiently high pressure it is anticipated that the curves will level out.

The maximum pressure increase rate occurs at somewhat different points in time in Main 1 and the two reference set-ups, as shown in Figures 5-3 and 5-4, respectively, after 300–400 hours. The highest slopes before and after (see Figure 5-2) the pump-down that was performed at approximately 4,000 hours for the three set-ups are shown in Table 5-1. It appears that the initial slopes are almost equal after the pump-down.

Table 5-1. Maximal pressure increase of hydrogen gas.

Equipment	Maximal slope (Torr/h)	Ditto after pumping (Torr/h)
Main 1	$1.1 \cdot 10^{-4}$	$1.4 \cdot 10^{-4}$
Reference 1	$4.6 \cdot 10^{-5}$	$1.1 \cdot 10^{-4}$
Reference 2	$5.3 \cdot 10^{-5}$	$8.5 \cdot 10^{-5}$
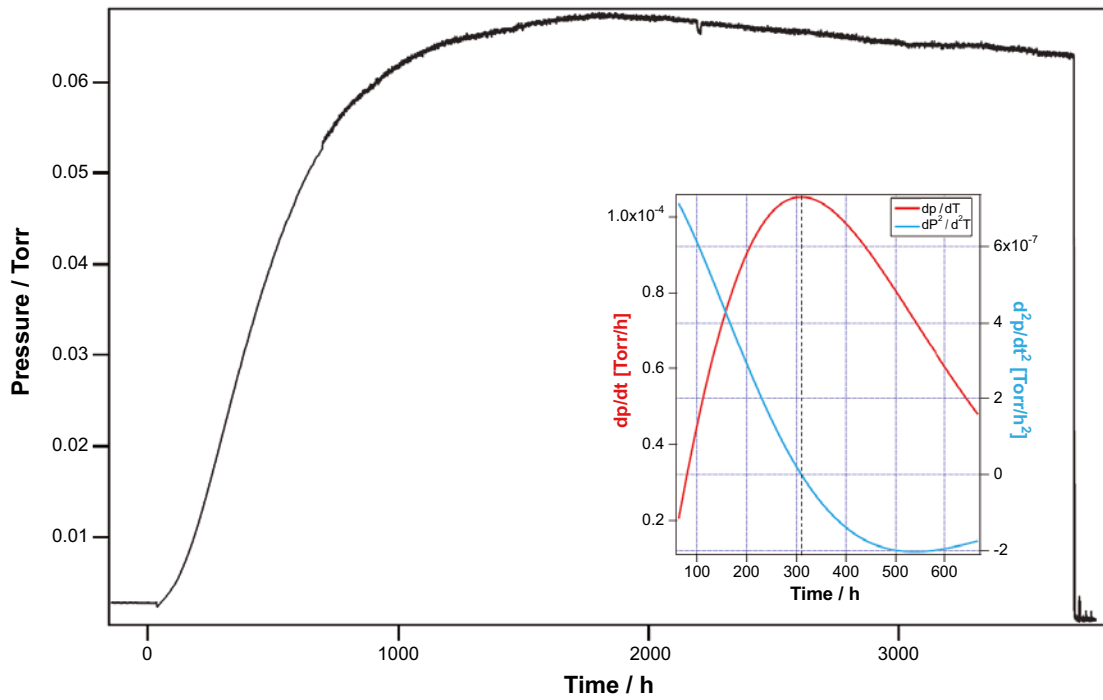
Figure 5-3. *Pressure development in Main 1 vs. hours from start. The small inset graph presents an analysis of the initial development, expressed in terms of derivatives (cf Figure 5-2).*
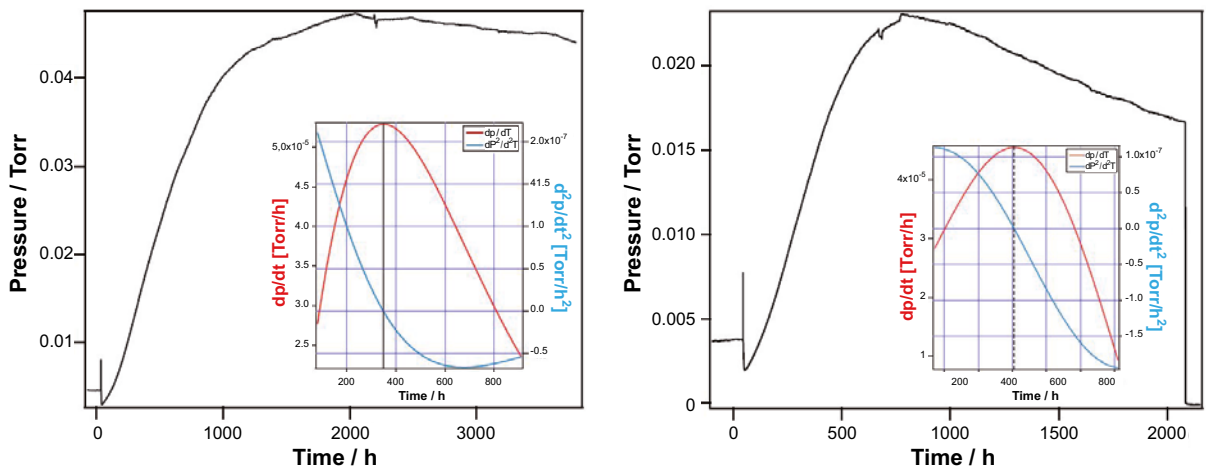
Figure 5-4. *Pressure development in Reference 1 (left) and Reference 2 (right). The graphs are analogous with the previous figure. Reference 2 was started approximately 1,500 hours after Main 1 and Reference 1 (Figure 5-2), so the zero point is shifted in relation to them.*
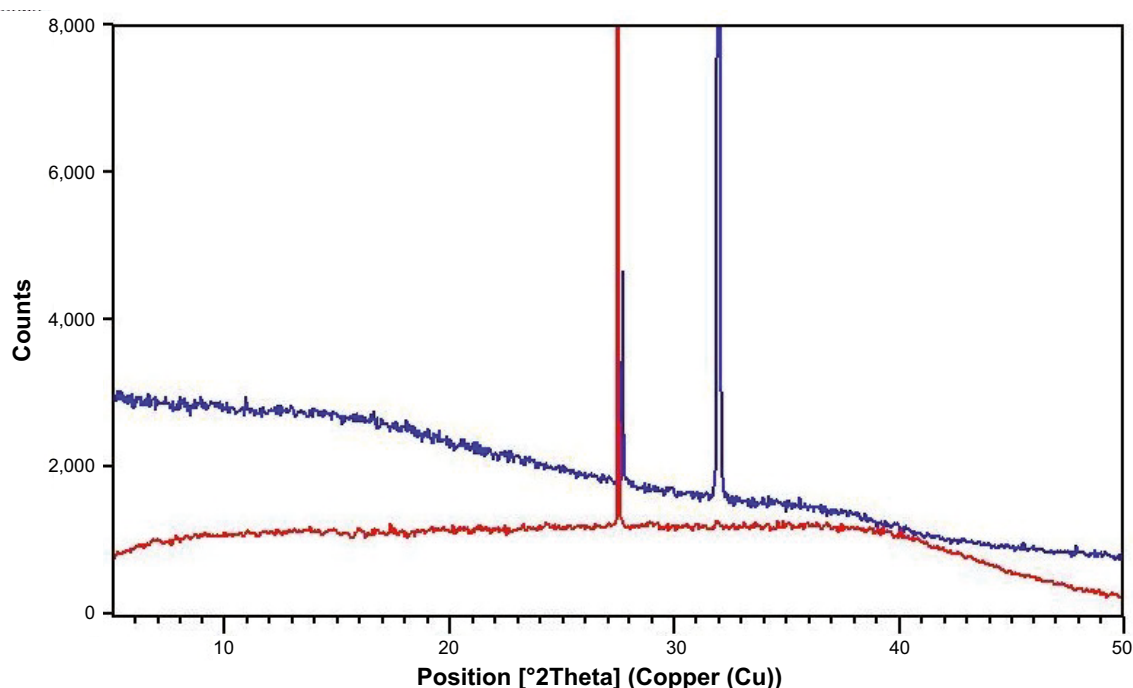
5.2 Copper plates

5.2.1 X-ray diffraction (XRD)

One of the set-ups without pressure logging (see outline diagram in Figure 3-2, lower chamber) was opened after one month, and two different copper plates (0 and 1 month) were tested using XRD at the MAX IV Laboratory in Lund. No crystalline copper oxide was detected, even though grazing incidence was used to more easily study the surface coating. A layer of a couple of nanometres would have been detectable. The peaks that were observed correspond to metallic copper. The difference between the patterns of the two samples (Figure 5-5) is due to the somewhat different textures of the metal. The outcome of the experiments indicates that the method is not suitable for the small amounts of solid corrosion products that may have been formed. No more XRD experiments were performed on the samples that were opened later as it was supposed that it would not be possible to analyse a coating on these samples either, in particular as the requirement of crystallinity must be satisfied. Electron spectroscopy is more sensitive with respect to the detection of a product on the surface, but the requirement of phase-identifying this product remains.

5.2.2 Electron spectroscopy

XPS was performed with AlKα as the X-ray source. In addition to the overview spectra, partial spectra of Cu *2p* and O *1s* were recorded. The analysis included metallic copper before the hydrogen purification step and at the start of the tests. All XPS spectra are reported in intensities on an arbitrary scale vs. binding energy in eV.

Figure 5-6 is an overview spectrum in the 0–1,400 eV binding energy regime from a copper sample after hydrogen cleaning ("treated") and the original copper after electropolishing ("untreated"). An elemental analysis of major peaks shows the presence of copper, oxygen, and carbon. After the hydrogen purification step ("treated") a small phosphorus peak (around 135 eV, seen in the uppermost spectrum in the figure only after magnification) is entirely gone, and the carbon and oxygen peaks are significantly reduced. By using argon sputtering *in situ* ("treated sputtered") the surface presence of carbon and oxygen can be further reduced. As an extra check that the residual gas in the spectrometer (UHV) had not contaminated the sample during recording of individual spectra, the sputtering was repeated ("…after the measurement"). The 575–800 eV region stems from Cu Auger processes, the energies of which end up here with this choice of X-ray source.


Figure 5-5. *Diffraction patterns from copper plates with grazing incidence. Blue curve: Copper after hydrogen reduction; Red curve: Copper after 1 month in water.*
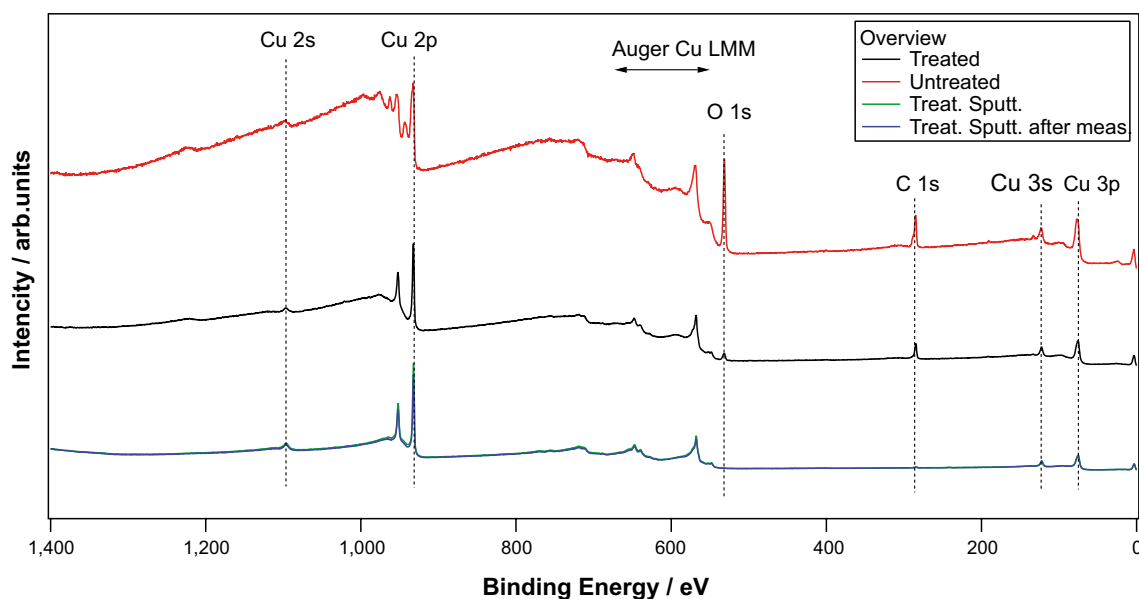
Figure 5-6. *XPS spectra from different copper samples before the tests using AlKα as the X-ray source For designations, see the text.*

Magnified copper spectra in 930–970 eV region (Figure 5-7) shows with satisfactory clarity the change that the hydrogen cleaning has caused. Before this, in addition to the contributions of metallic copper shown in the lower spectrum, both shifted main peaks (see arrows) and satellites (to Cu $2p_{1/2}$ and Cu $2p_{3/2}$) are clearly observable. The latter gives evidence for Cu(II) as wide structures at 943 eV and 963 eV. Consequently, a coating of a Cu(II)-compound, was removed by the hydrogen gas cleaning. There was no change visible following sputtering.

Oxygen spectra from XPS (Figure 5-8) in the first versions of the analysis did not result in a reliable interpretation. Oxygen and carbon are to some extent always observed in XPS spectra. If there are different chemical species that all contain oxygen, it is also a difficult matter to decompose the total spectrum into independent contributions.
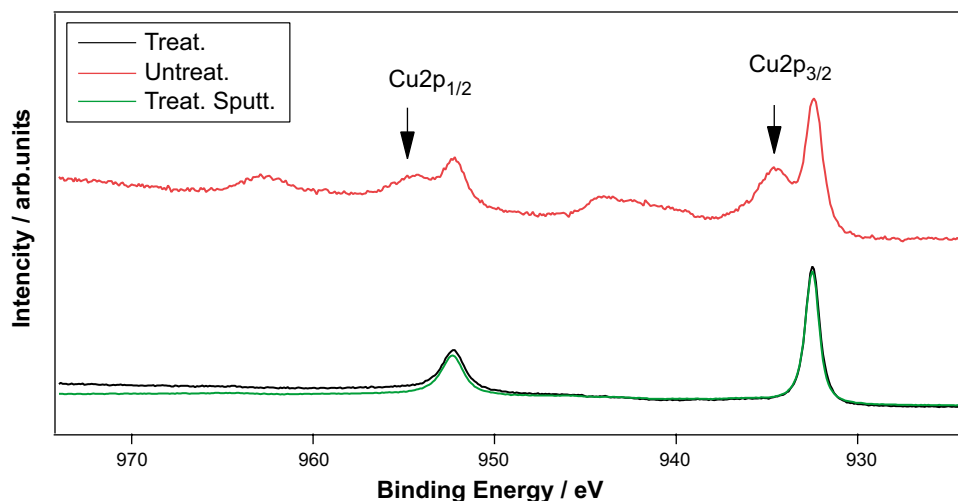
Figure 5-7. *Cu 2p spectra before and after the cleansing step (cf. Figure 5-6). The arrows indicate Cu 2p peaks from a surface species. The wide peaks that disappear after hydrogen purification are satellites to these.*
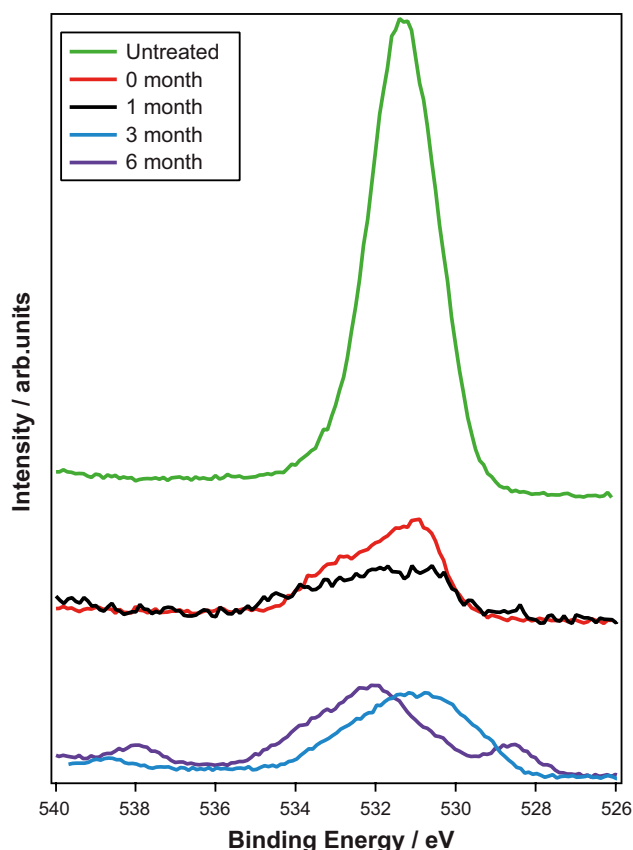
Figure 5-8. *O 1s spectra from copper.*

The peak positions are sensitive to the calibration (instrument dependent), which in this case is done by relating to the carbon peak position (285.0 eV). The relative intensities must be handled with care in the interpretation, especially as the measurements, unfortunately, had to be made on different instruments. The relative intensities give only a semi-quantitative idea of the relative amounts, yet it may be concluded from Figure 5-8 that no significant change in oxygen content occurred during the 0–6 month time interval. The registered oxygen is not necessarily chemically bonded but can also arise from physisorption on the surface, especially if the surface is exposed to an oxygen-containing gas phase (even inside the spectrometer) before measurement can begin. Figure 5-9 reproduces in detail the oxygen spectrum from the six-month exposure wherein it is apparent that oxygen is effectively removed by sputtering inside the spectrometer. This suggests the presence of adsorbed species, such as H_2O or CO. The sample was taken directly from the water and was transferred to the spectrometer without contact with any oxygen-containing gas phase. Surface adsorption of oxygen species may have occurred in the spectrometer during the recording of the copper spectra (approximately 30 minutes), or it may stem from some species dissolved in the water.

Besides the O *1s* contribution, there are two peaks enclosing the oxygen peak, interpreted as antimony contributions (Sb $3d_{5/2}$ and Sb $3d_{3/2}$), where the peak energy difference corresponds to a spin-orbit coupling of 9.5 eV. A weaker contribution from Sb can be detected in the three-month sample. There seems be a correlation with the exposure time in water, which fully agrees with the ICP-MS data of the water phase (see below) indicating that the glass may be the antimony source (see Table 5-5). Antimony is also removed by sputtering; meaning that it occurs only within a thin layer. Here it must be stressed that the antimony content in the water phase is very low, and hence the magnitude of the oxygen peak also corresponds to a very small amount.

After exposure of copper to liquid water (1, 3, and 6 months, respectively) no satellite peaks could be observed in the Cu *2p* spectrum. In Figure 5-10 it can be seen that their spectra are largely identical, and, furthermore, they are not altered from the situation immediately after the cleaning. Here they have been normalised with respect to background to facilitate comparison. There is no detectable
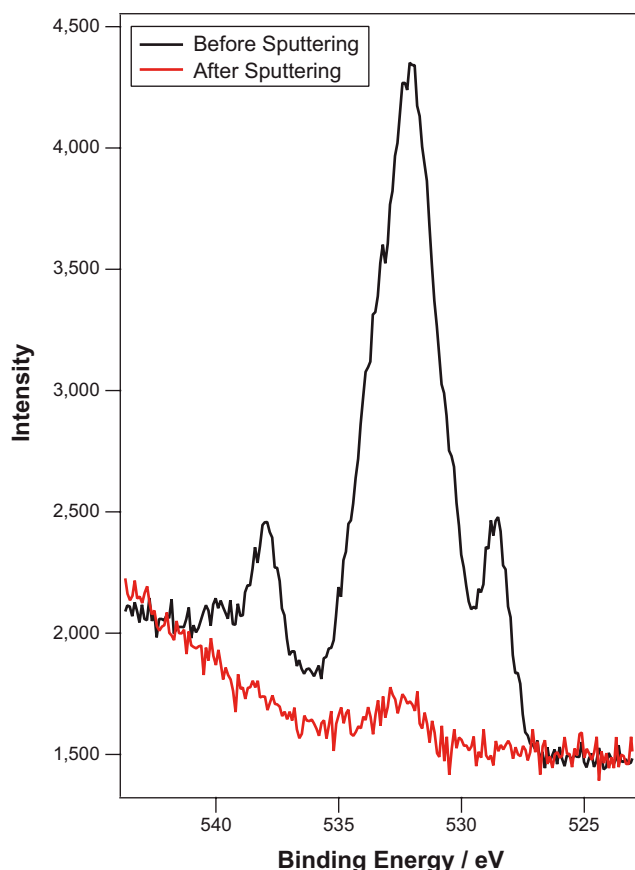
*Figure 5-9.* *Oxygen spectrum for the 6-month sample.*

amount of CuO on the surface as the typical Cu(II)-structures are absent (compared with the upper-most spectrum). Unfortunately, the presence of Cu(I) in the form of Cu_2O or other similar Cu(I)-species cannot be entirely excluded, as their copper spectra are almost identical to the spectrum of pure copper.

One conclusion of these attempts was that XPS could not give an adequate phase analysis. However, one could suspect that Auger spectroscopy might provide a solution to this problem, but then great care must be taken to ensure that the sample is by no means exposed to influences after taking it out of the sample chamber and before transferring it into the spectrometer, as this technique is particu-larly surface sensitive. Thus arose completely crucial requirements concerning the logistics follow-ing the opening of a sample chamber, and these were observed when opening the six-month sample: It was therefore agreed with the persons handling the analyses that they should be carried out with the smallest possible risk for contamination. After opening, the copper samples were therefore immediately transferred, without being exposed to air, directly into the electron spectrometer, and the exposure to air was limited to a couple of minutes when loading the ERDA spectrometer.

Figure 5-11a shows Cu *LMM* Auger spectra (three different electrons are involved), both directly from the sample chamber ("before sputter") and after sputtering in the spectrometer. The two spectra are more or less identical. They are background corrected and intensity normalised. The difference (zero is the lowest value) shows that there are no other Auger peaks of major importance since the contributing significance as the difference does not show any structure. The deviation at the largest maximum is only an effect of the normalisation and the counting statistics. As opposed to XPS, where Cu and Cu_2O give almost identical Cu *2p* spectra, Cu_2O in the Auger technique would have made a separate distinguishable contribution in the form of a Cu *LMM* spectrum with a wide maxi-mum around 917 eV, that would have been reflected in the difference. The interpretation of the two identical spectra as metallic copper features is entirely in accordance with the literature data in Figure 5-11b (Yano et al. 2003). A thin layer of Cu_2O yielding total coverage seems unlikely. The information depth of the Auger copper peaks is around 8 Å (Lindau and Spicer 1974).
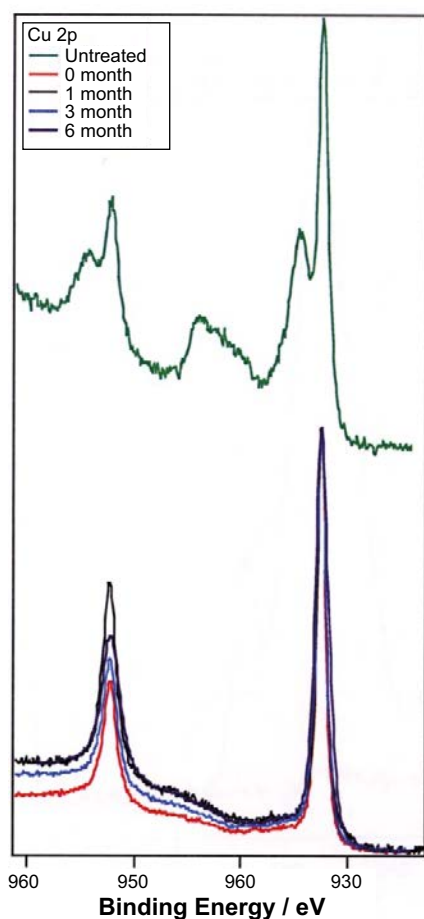
Figure 5-10. *Cu 2p spectra of copper samples, both before cleansing (cf. Figure 5-7) and for hydrogen-gas cleansed samples after 0–6 months in water.*
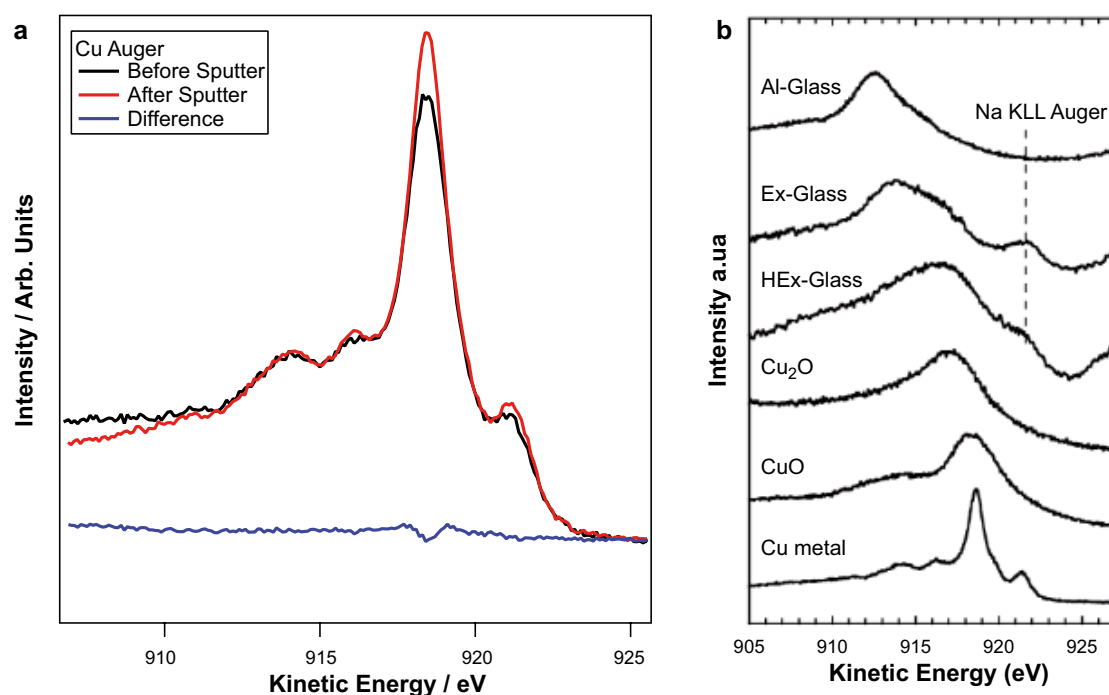

Figure 5-11a–b. *Auger spectra from 6-month sample (a), and for e.g. copper and its oxides (b) (from Yano et al. 2003).*

## 5.2.3   Elastic Recoil Detection Analysis (ERDA)

The method was used for hydrogen determination in the copper since XPS can by no means be used for the analysis of light elements. In Appendix D2 (Figure A) a typical raw time-energy spectrum from the measurements is shown. Each region or trace in the spectrum corresponds to detected atoms with a defined mass. These spectra are usually analysed with standard software whereby concentrations can be determined down to levels of 0.1 atomic per cent (Janson 2004). In Figure 5-12, results for a copper plate in water for six months are shown. As the bulk hydrogen content in the copper samples is lower than 0.1%, no acceptable measurement values can be obtained below that limit, which here corresponds to a depth of only about 25 nm. The observed levels of hydrogen, carbon, and oxygen at the surface stem from adsorbed molecules, probably water and hydrocarbon. Depth profiling can in principle be achieved down to 150 nm, but for these copper samples the limit is set by the concentration value 0.1%. To obtain reliable measurement data below this limit, i.e., to provide content data from deeper regions in the sample, another, more sensitive, analysis method (SIMNRA) must be applied. It is based on simulations that are compared to registered data, which may lead to uncertainties in the obtained values (Mayer 1999).

Figure 5-13 shows the hydrogen distribution in the same sample in another way that permits registration of data from greater depths in the sample. Here, the horizontal axis is an energy scale, and the highest energy corresponds to the conditions at the surface. Registered hydrogen also includes hydrogen atoms in surface-adsorbed molecules, in this case primarily water. This prevails is in the form of a thin layer. SIMNRA simulations give curves wherein the variation in electronic cross-sections and detector sensitivity are taken into account, both as a function of energy, and the process depends on the hydrogen content. The program does not allow a direct mathematical fit, but instead calculations (simulations) are carried out for various stepwise predetermined contents and the results are compared to the experiments. The experimental measurements (single points that have been connected) show – as the signals are weak – an apparent periodic, but in reality random, spread (in the vertical direction) of the yield from the collision processes. The red curve reproduces the best result (within the spread of the measurement range) for 300 ppm relative atomic ratios (< 5 ppm parts per weight) in the bulk and for a surface layer that has been assumed to be 1.5 ML (ML stands for monolayers) of adsorbed water molecules. Another chosen constant value in the calculations would displace the curve outside the envelope region that is defined by the individual measurement data points. The fact that the curve turns upwards to the left thus does not reflect a variation in hydrogen content but is rather a consequence of different energy dependencies; the curve is calculated based on a constant content for the whole energy range within the 150 nm depth that has been possible to analyse. This value may, as for the other non-destructive analysis techniques, represent the bulk content. More details can be found in Appendix D2.
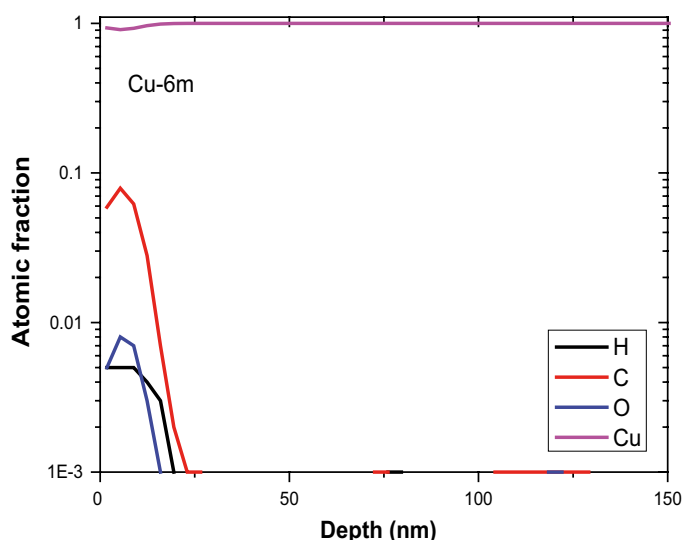
Figure 5-12. *Depth profiles for copper (6 months) for hydrogen, carbon, and oxygen, as well as copper (in principle 100%). No data could be obtained for concentrations below 10^{-3} (that is, deeper than 25 nm) with a conventional assessment method.*
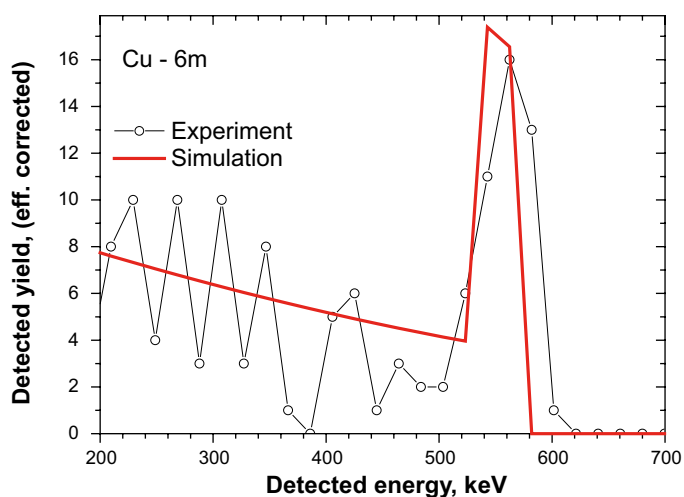
Figure 5-13. *Best simulation result for hydrogen compared to experimental data (6 months).*

Corresponding analyses were also made on copper samples that were not incorporated in the corrosion set-ups, and are reported together in Table 5-2 including the results from a palladium foil. As can be deduced from the table (contents in mass or atomic ratios) the calculations provide the best fit for a constant hydrogen content. At this level of analysis the content does not seem to have changed during the six months in water compared to the initial state after the electropolishing (elsewhere denoted as 0 months). The measurement data can only be given with one significant figure due to the error sources of the method.

Table 5-2. Analysis result from copper samples and the palladium foil with ERDA.

Sample	Cu-untreated[a]	Cu-EP[b]	Cu-HC[c]	Cu-6m[d]	Pd[e]	Pd[f]
H conc. (weight)	6 ppm	5 ppm	5 ppm	5 ppm	40 ppm	40 ppm
H conc. (atomic)	400 ppm	300 ppm	300 ppm	300 ppm	4,000 ppm	4,000 ppm
Remarks:					2% oxygen	2% oxygen

[a] Untreated copper, such as received.
[b] The same after electropolishing.
[c] After electropolishing followed by hydrogen reduction.
[d] Copper plate after 6 months in water.
[e] Palladium foil after 6 months in test set-up.
[f] Palladium foil when starting.

5.2.4 Melting analysis

The ERDA analyses are not representative of the total content and give only the composition down to a certain depth in the material (see Figure 5-12). To get a more correct picture of the total content, melting analyses were performed on different copper samples (Appendix D). The results are shown in Table 5-3 in which the samples have the same designations as in the ERDA table, e.g. Cu-1m means a copper sample after a month in water.

Table 5-3. Analysis results of copper samples in melting analysis (Bruker Corp.).

Sample	Cu-untreated[a]	Cu-EP	Cu-HC	Cu-1m[b]
H conc. (weight)	4.3 ppm	1 ppm[c]	2 ppm[c]	3.4 ppm

[a] Hydrogen content according to specification in Appendix A2 < 0.1 ppm.
[b] Copper plate after 1 month in water.
[c] Only one measurement, thus a large uncertainty in the measured value.

5.3 Glass

Duran glass sheets in contact with the water phase were first analysed by XPS and then by ICP-MS. The latter method requires, however, dissolution to a liquid phase that is injected in a flame. XPS showed presence of copper on the glass surface at a coverage of a few per cent, and sputtering for a couple of minutes made the signal disappear.

After leaching with HNO_3 to create a liquid phase, traces of copper were detected also with ICP-MS. However, the evaluation must be regarded as unsatisfactory as the spread in measurement data between glass sheets of the same type was larger than the precision in individual measurements. Here concentrated HNO_3 was used to dissolve potentially existing copper on the glass surface. The acid solution was then diluted to 1.4 M and was sprayed directly into the flame.

XRF gave a clearer picture of the conditions (see Appendix D): The copper surface concentration was measured such that the contents are quantified by means of a standard of known amount (thickness). The measurement was background corrected against a blank material (very clean electronics silicon). For copper films thinner than 100 nm, the thickness (the amount) is proportional to the intensity of the CuKα peak at 8.04 keV (Figure 5-14). Germanium was used as secondary radiation source to give high sensitivity in the copper determination. Details about instruments and methods are given in Appendix D.

The sensitivity of copper at 360 s measurement time was estimated to about $2 \cdot 10^{-10}$ mole/cm^2, which corresponds to a significantly lower coverage than a complete monolayer (approximately 1/10 ML). The measurements were normalised against a standard sample, a glass sheet coated with copper.
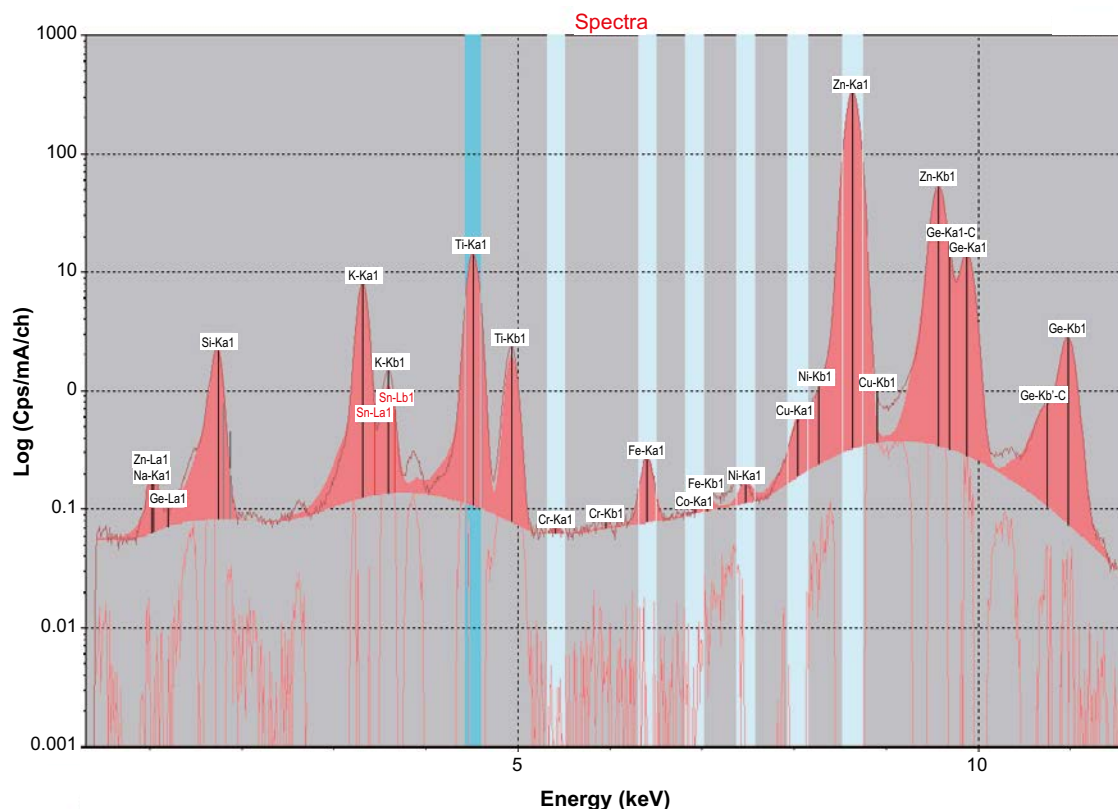
Figure 5-14. X-ray fluorescence spectrum on an energy scale.

In Table 5-4, the results of measurements on glass sheets that were immersed in water 1 or 6 months and a glass sheet that was not incorporated into the tests (blank). The intensity value is obtained from the integrated peak area. There is, however, an error source from the fact that the glass turned out to contain zinc, the fluorescence radiation of which is so close in energy that its presence can affect calculation of the copper intensity. For the reference sample with a 35 nm copper coating, a value of 133 cps/mA was obtained as a measure of the intensity, which corresponds to $3.80 \text{ cps} \cdot \text{mA}^{-1} \cdot \text{nm}^{-1}$. From this, the analysis values could be calculated. Details can be found in Appendix D4.

A corresponding XRF analysis could not be made on the glass beakers in a reliable way, as this analysis method requires surfaces to be flat.

Table 5-4. Summary of measurement results of glass that was immersed in water (1 and 6 months) together with copper plate and reference materials (glass, silicon, and copper-coated glass).

Sample	Glass – 6 month	Glass – 1 month	Glass blank	Si blank	Reference sample
Intensity (cps/mA)[b] raw data	1.98; 2.13[a]	1.86	1.86	1.78	133
Thickness (nm) "gross"[c]	0.05-0.07	0.02	0.02	–	35.0
Thickness (nm) "net"[d]	0.03–0.05				

[a] Measurements were performed on both sides of the same sheet.
[b] The intensity is normalised to the tube current.
[c] After background correction from the reference sample sensitivity.
[d] Alteration after exposure compared with glass blank.

5.4 Liquid phase

The water phase was analysed with ICP-MS. The methodology is sensitive in two aspects. On the one hand, low contents can be measured; on the other hand, systematic errors are very hard to control. Samples can very easily be contaminated by the surrounding environment, and this particularly applies to the element zinc, which is a widely spread trace element. As a step in the analysis, different isotopes of the same element were in some cases used to yield a consistent picture or simply overcome disrupting interferences from species that are generated in the plasma (see Appendix D). The latter methodology is illustrated by the determination of iron, for which ^{57}Fe must be used.

The analysis method is not capable of showing how the different elements have been bound, and the dominating elements in the water phase originate in the glass (Figure 5-15). This is actually an amorphous salt that is influenced by the ultrapure water (see Appendix A). It is therefore not surprising that the dominating elements, which were dissolved in the water after being in contact with the glass, are elements that therein constitute cations (Na, K, Ca, Mg), anions (Cl), or are included in complex silicate ions (Si, B, Al, P) that are decomposed in the plasma. The measured copper content in the water phase is very low and of considerably lower magnitude than most elements that with certainty stem from the corrosion of the glass.

Figure 5-16 shows how the amount of copper in the water phase changes with exposure time in the tests where copper and glass are in contact with water (see also Appendix D3). The copper contents are very small, and after a month, the levels of antimony, iron, and zinc are even greater (Table 5-5). The change during a month gives a larger relative increase of copper than of e.g. zinc. We have no information about dissolution rates from glass and cannot easily correlate the increasing copper content over time with an increasing metal corrosion. From a pure thermodynamic perspective the dissolution of the metal would certainly contribute to the obtained values but is not the only source as copper was measured in the glass that was in contact with the water.

Table 5-5. Measured contents (part by mass) of selected elements for pure water and for 1-month tests. Data for iron have low accuracy, and are therefore put in brackets.

Sample situation	Cu (ppb)	Zn (ppb)	Fe (ppb)	Sb (ppb)
Pure water	0.02	1.0	0.1	0.00
Reference sample	0.08	3.70	(0.27)	5.52
Sample with copper	1.56	7.00	(1.87)	4.46
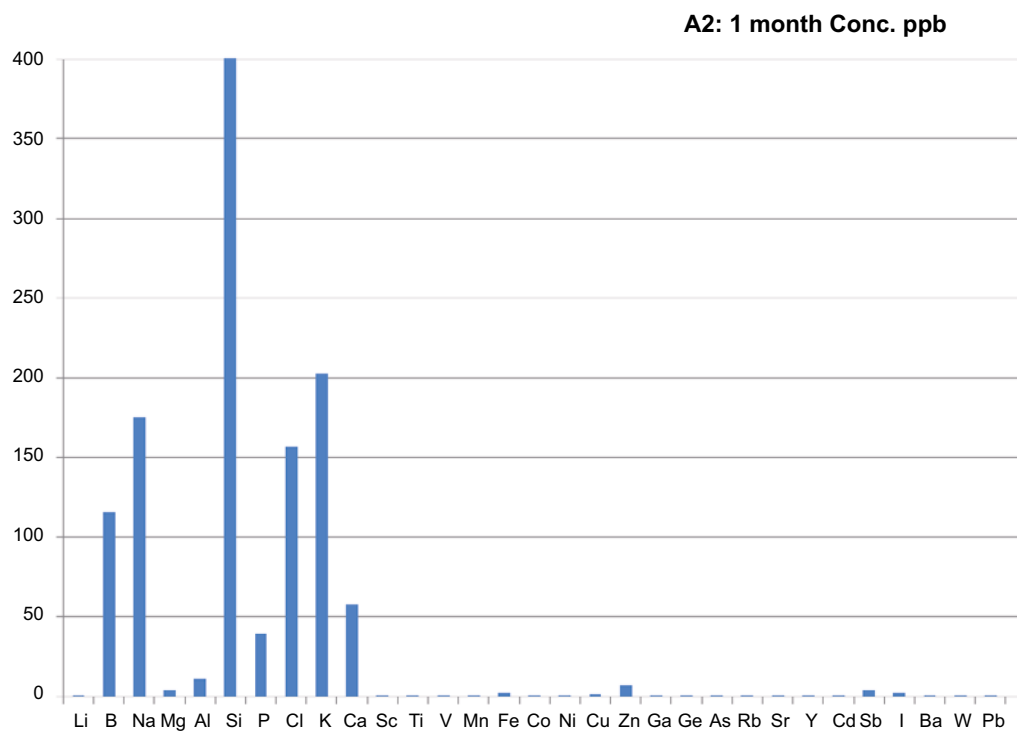
Figure 5-15. *Contents in ppb (part by mass) of different elements that have been measured in the water phase after one month of exposure. The column for silicon (from complex silicates) has been cut (from the value 1,290) to make it possible to show low contents in the chart.*
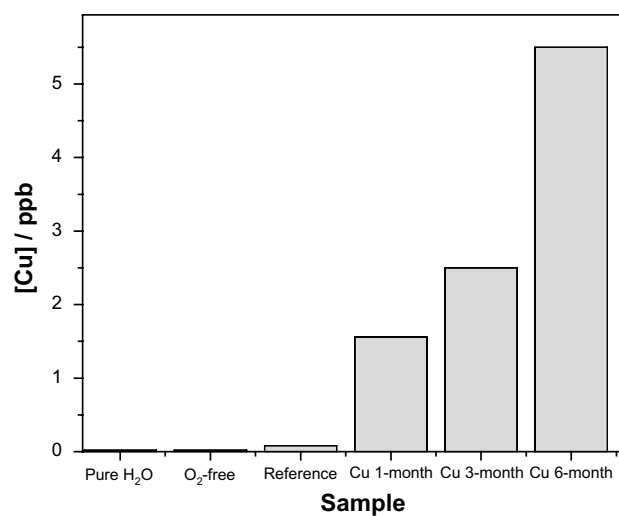

Figure 5-16. *Copper content in the water as a function of the exposure time in water (1, 3, 6 months).*

In Figure 5-17 are shown the measurement data from the 6-month sample, the sample that this far should give the best measurement statistics, with sampling at two points in the water phase, at the bottom and at the top. The reason for the sampling was to examine if particles could settle to the bottom (e.g. from detached flakes of oxide). That seems not to be the case. See also Appendix D3 for other exposure times. Since palladium is also present in the system, in contact with steam, this element was also measured, even using three different isotopes, with non-detectable amounts (< 0.01 ppb) as a result.

The concentrations are given here as µg/L, and the bar chart is supplemented by specifications of the estimated error limits. The accuracy in the measurement of the copper content is illustrated by the fact that the measured values from available isotopes are not significantly different, which indicates that disturbances from plasma effects are absent. The measurement data of these two isotopes are in Figure 5-17 normalised to the isotope abundance so that both ^{63}Cu and ^{65}Cu give measures of the total content.

Iron is probed with ^{57}Fe to avoid interferences from primarily ^{40}Ar^{16}O for the most common iron isotope, ^{56}Fe. The natural isotope abundance of ^{57}Fe is of the order of 2%, from which the values from the measurement were recalculated to represent the total iron content.
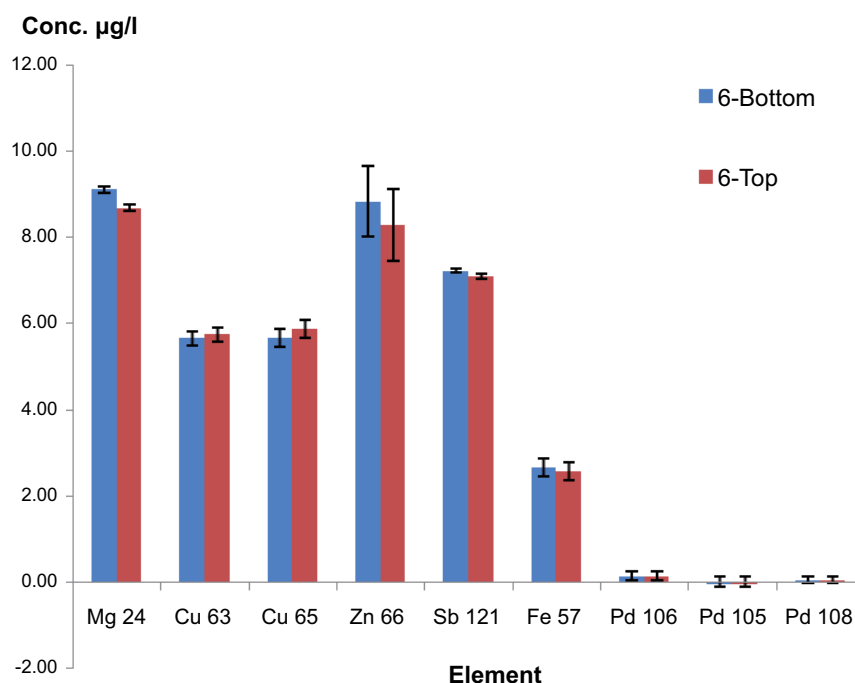

Figure 5-17. *Comparative measurement data (here in µg/L, numerically equivalent to ppb) with sampling both from an upper and a lower part in the beaker for the 6-month sample. (NOTE! For palladium, the error limits are larger than the analysis values.)*

6 Discussion and conclusions

6.1 Thermodynamic background to the experiments

The overall conclusion of our investigations is that we have registered production of hydrogen gas from the reaction chamber, globally indicated by pressure measurements and in detail analysed by mass spectrometry. The presence of other gases is at a very low level and of constant content independent of the set-up (Main 1, Reference 1, Reference 2), which implies that they originate in the vacuum section. Their presence does not affect the results adversely. What is complicating the interpretation is, however, that hydrogen gas is registered in almost as high a degree in the reference set-ups (Reference 1 and Reference 2) – without copper plates in the water – as in the active set-up (Main 1).

It should be possible to thermodynamically link the evolution of hydrogen gas to a copper corrosion process:

$$2Cu(s) + H_2O(l) \rightarrow Cu_2O(s) + H_2(g)$$
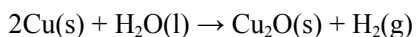
All chemical processes can in closed systems be regarded as equilibria and be described mathematically by an equilibrium equation, in this case:

$$\frac{a(Cu_2O) \cdot a(H_2)}{a^2(Cu) \cdot a(H_2O)} = K$$

The activity value $a = 1$ (dimensionless) applies to condensed states of pure compounds, to a first approximation applies to copper, copper oxide, and water. Deviations occur at possible compositional changes via dissolution, but such processes may be considered to be of minor significance in this system and should also have a highly marginal effect on the activity values. The activity on the hydrogen gas can be translated into partial pressure, which affects the dimension and the value of the equilibrium constant K. Its temperature dependence is expressed as a temperature dependence of the partial hydrogen gas pressure illustrated in Figure 6-1 (Noläng 1983). As shown in Figure 6-1, the equilibrium pressure of hydrogen gas in the copper-water system is very low (about 10^{-14} mbar at room temperature), which also has been pointed out by other researchers (SSM 2011).

In the presence of water-soluble copper ions (in hydrate complexes), the equilibrium shifts so that more hydrogen gas is formed. Such a scenario should occur to a larger extent in the presence of stronger complex formers, e.g. chloride ions, which exist in natural water. Figure 6-1 gives an indication of the smallest amount of hydrogen gas that is formed at equilibrium without such water-soluble species.
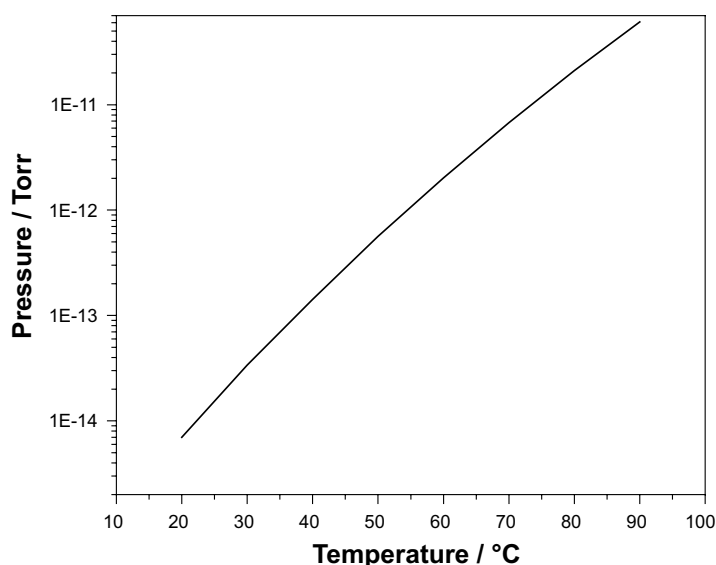
Figure 6-1. The temperature dependence of hydrogen pressure at equilibrium between water and copper.

In this system, the equilibrium constant is very small (its numeric value is set by the choice of pressure unit), whereby the reaction is strongly shifted to the left.

We observed hydrogen evolution in the experimental set-ups in which pressure was registered, but it is assumed that this also occurred in the set-ups that were not connected to the logging system. It is, however, stressed that the amount of hydrogen gas is not the same per time unit which partly is related to the fact that the set-ups without connected pressure measurement means are *open systems*, in the sense that hydrogen gas is always permitted to leave the reaction vessel.

Despite a global non-equilibrium, we can still draw conclusions from the above equilibrium expression and draw the conclusion – empirically according to Le Chatelier's principle – that removal of a product on the right side of the equal sign drives the reaction towards formation of more products, that is, more hydrogen gas and more copper oxide may be formed. During a given time period, the configuration should therefore lead to the formation of more products than if the system were closed. We assumed then that the local kinetic conditions, which might be influenced by the metal surface microstructure, are independent of whether the system is open or closed.

In the set-ups with connected pressure gauges, the reaction chamber is connected to the vacuum chamber, to which only hydrogen gas can pass. Here as well, hydrogen gas leaves the system in the reaction chamber, but the set-up is arranged such that hydrogen gas after start will be on both sides of the Pd membrane. Consequently the detectable hydrogen gas pressure that can be recorded will eventually be equal on both sides, and then there will no longer be a driving force for diffusion from one chamber to the other, and the pressure should stabilise at a certain value.

This was not what we observed; instead, we found that the pressure decreased with time after a maximum had been formed. The explanation to these observations may be a leak at the rim of the palladium foil (see Figure 6-2), an effect that we at an early stage assessed to be of minor importance for the principal outcome of the experiment. Calculations based only on the diffusion process show in fact that the *lateral* flow rate inside the palladium foil, which was permitted by our design of the seal, would constitute a mere per mille of the *normal* flow rate against the foil. As we, by means of the highly accurate pressure measurements that our equipment allows, were able to observe a pressure decrease (see Figure 5-2), there must be other processes involved than pure diffusion in a solid phase. If a hydrogen pressure of the same order is applied to both sides of the membrane (at the pressure maximum), hydrogen gas can still get a free outlet path to the sides as the only possibility for a net flow and lead to a pressure decrease if the hydrogen gas evolution in the system is weaker. The small pressure decrease we are able to measure indicates therefore that either the kinetics or the rate of hydrogen gas production decreases. In other words, these three experimental set-ups were in fact to some extent also open.

6.2 Recording the amount of hydrogen

As a consequence of such a leakage, albeit small, the measured amounts of hydrogen are certainly underestimated, while at the same time also this "open" system drives the reaction further to the right than at equilibrium. In the beginning of the process, one should be able to rely on the hydrogen evolution basically being equal in Main 1 and in the set-ups without connected pressure measurement means. This relation is needed to estimate the evolved amount of gas in the open systems. The maximum pressure increase of the Main 1 process (Table 5-1) may be used to calculate one year of hydrogen production, yielding this corresponds to $4 \cdot 10^{-6}$ moles of H_2. Here no consideration is made for the possible inclusion of hydrogen in the palladium.
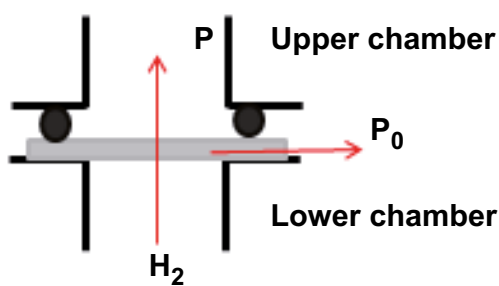

Figure 6-2. *The membrane and indicated normal and lateral flows.*

In addition to the gas phase, some hydrogen may be in the palladium foil ($7 \cdot 10^{-6}$ mole H_2 from ERDA analysis) and dissolved in the copper (estimated $3 \cdot 10^{-6}$ mole H_2), in both cases as atomic hydrogen. Hydrogen gas can certainly be dissolved in the water phase, but the solubility at 50°C is 0.0013 g H_2/kg, that is, 0.0007 mole H_2/L at atmospheric pressure (Blackman and Gahan 2013). Here, the water volume was 100 ml and the pressure was much lower, which together result in a negligible amount of dissolved hydrogen in the water phase. Taken together the amounts of hydrogen become $14 \cdot 10^{-6}$ mole H_2 or at least no more than $\sim 2 \cdot 10^{-5}$ mole H_2 if we consider that the amount of hydrogen probably is underestimated, partly through continuous lateral leakage, and partly due to the fact that the effect of the Pd foil has not been incorporated. The number is an estimated upper limit based on analyses. For details of the calculations, see Appendix E.

6.3   Correlation to observed amounts of oxidised copper

In the above reaction formula it has been assumed that the redox reaction for the formation of hydrogen gas would produce Cu_2O. This is not the only possibility but, in any case, some kind of oxidation product of copper must be formed in a corrosion process, that is, one or more species where the copper oxidation state is higher than zero. Such spieces can occur in different forms in the corrosion process, both as a surface coating on the metallic copper (that may be detached through deficient adhesion) and as copper in dissolved form in the water phase. Also, we have accounted for the (unlikely) possibility that the glass acts as an efficient ion exchanger and depletes the water phase of copper.

Through analysis, copper from solid particles from the bottom of the reaction vessel can be determined. One cannot determine, however, if such particles (which are dissolved in an acid) consist of surface-layer material that has been detached or if they possibly consist of scraped-off metal from the moment when the copper substrates were loaded in the reaction vessel. To avoid such error sources, glass sheets were placed in parallel in the same vertical position as the copper plates, to serve as substrate for possible precipitation from the solution. According to classical nucleation theory, precipitation on solid surfaces (heterogeneous nucleation) is associated with a much lower activation energy than homogeneous nucleation (which occurs in the liquid phase). Both cases require supersaturation which, however, is less for heterogeneous nucleation.

We have analysed these alternatives:

a) Surface layers on the copper plates by electron spectroscopy.

b) Dissolved copper in the water phase by ICP-MS.

c) Dissolved (or precipitated) copper in the glass using XRFS.

Calculated from a stoichiometric approach in a redox reaction, $2 \cdot 10^{-5}$ moles of formed hydrogen gas would correspond to $4 \cdot 10^{-5}$ moles of copper in the form of Cu(I). Instead, using the analysed copper contents (Section 5) from the six months of exposure, we calculated the amount of copper that would exist in these forms per year (mole Cu/years). As XPS does not give indications about the presence of Cu(II), we have assumed a tentative surface layer of Cu_2O. In a water solution based on pure water, Cu^+ cannot exist in high amounts but is bound in the form of Cu_2O if this is formed. The estimates reported in Table 6-1 are made using analysis methods independent of the form in which copper exists in solution, however, and are instead based on an area of 100 cm^2 on glass surfaces and copper surfaces (rounded off from the real value 96 cm^2 for the pressure set-ups) and a water volume of 100 cm^3, respectively.

Table 6-1. Comparison between product amount and outcome of analyses.

Source of Cu	Measured[a]	Number of mole Cu/year
Copper(I)oxide	< 1 nm/year	$1.5 \cdot 10^{-7}$ mole/year
Cu-ions in water solution[b]	< 10 ppb/year	$1.6 \cdot 10^{-8}$ mole/year
Cu on the glass[c]	< 0.1 nm/year	$1.4 \cdot 10^{-7}$ mole/year
In total		**$3.1 \cdot 10^{-7}$ mole/year**

[a] Extrapolated values from exposure time of investigated samples.
[b] Partly from the glass.
[c] Copper is also inherently present in the glass from the start (see Table 5-4).
The variation in the copper content between different sheets causes some uncertainty in the measurement data.

The most reliable electron-spectroscopy assessment is the one performed after 6 months using Auger spectroscopy. Based on the fact that we cannot detect any copper oxide from the Cu *LMM* spectrum (Figure 5-11), such a layer must be thinner than 1 nm. In the table this thickness is thus set at < 1 nm for one year of exposure.

The copper content of the water seems partly to depend on the glass; thus, from an increasing copper content in the water phase over time it cannot be concluded that the metal is the single source. The glass erodes also more over time. ICP analyses of copper from glass that are not incorporated in the tests (leached with nitric acid) showed that the copper content varied between the samples. We are therefore also unable to adjust the measured copper content for the influence from the glass. The value of 10 ppb as a measure of the corrosion process of copper is therefore probably overestimated. It was confirmed by XRF that the glass contains copper. In that case, the measured signal strength was translated into values of copper content as if occurring as a layer on the glass surface.

From the summation in Table 6-1 the released amount appears to be $3 \cdot 10^{-7}$ mole Cu/year, which differs considerably (1%) from the amount calculated from the observed amount of hydrogen gas ($4 \cdot 10^{-5}$ mole Cu/year).

Speculations that the antimony registered by XPS on the copper might inhibit the corrosion process do not seem particularly likely. We are uncertain of what the source of antimony is. Antimony was not detected with XPS in the used glass sheets, although the content in the water phase was of the same magnitude as the copper and zinc. In the XPS experiment it is likely that the antimony stems from an attached thin film of water, as the sample was transferred directly to the vacuum chamber of the spectrometer. An estimate based on observed XPS intensities anticipates that the antimony coverage on the metallic copper would correspond to around 0.3% of the whole surface, an order of magnitude that would not inhibit surface reactions (corrosion) even if the antimony were strongly bonded (alloyed). The total content is extremely small.

6.4 Study of the leakage in the palladium foil

As mentioned above, we expected that the hydrogen pressure would stabilize at a certain level. One might interpret the deviation as due to a dependence on a lateral hydrogen gas flow through the palladium membrane. With the purpose of obtaining an understanding of the sizes of the normal and lateral flows, experiments in which hydrogen gas was added to the upper part (the vacuum chamber) were performed. By doing so the pressure became greater above the palladium foil (in the vacuum chamber) than below the foil (in the reaction chamber). Consequently this generated a driving force for diffusion. Compared with the situation in Figure 6-2, this implies instead that hydrogen gas flows in the opposite direction through the foil, and that the pressure drops in the upper chamber. Figure 6-3 shows a pressure-equalisation process that in principle has two components, a rapid process (= larger flow rate) followed by a slower process. Our interpretation is that, initially, normal flow to the membrane entirely dominates the pressure equalisation, after which a tail corresponding to a considerably lower flow rate, a small lateral leak, follows.

The tests were performed out of sheer curiosity under not too rigorous scientific conditions, as this would have required a modification comprising gas lines made of metal. Now, a polymer hose was used, with the consequence that a small amount of air probably also was added when hydrogen gas was supplied to the Reference 1 chamber. This explains why the pressure did not get back to the initial value (blue curve), as neither oxygen nor nitrogen can pass through the palladium membrane, but it should not affect the lateral leakage.

6.5 Hydrogen formation with and without copper

We have, like others who have investigated the Cu–H_2O system, observed that hydrogen gas is actually formed, supported by mass spectrometry findings. We can, however, not find an adequate correlation between the amount of formed hydrogen gas and the amount of formed products based on the corrosion of copper.
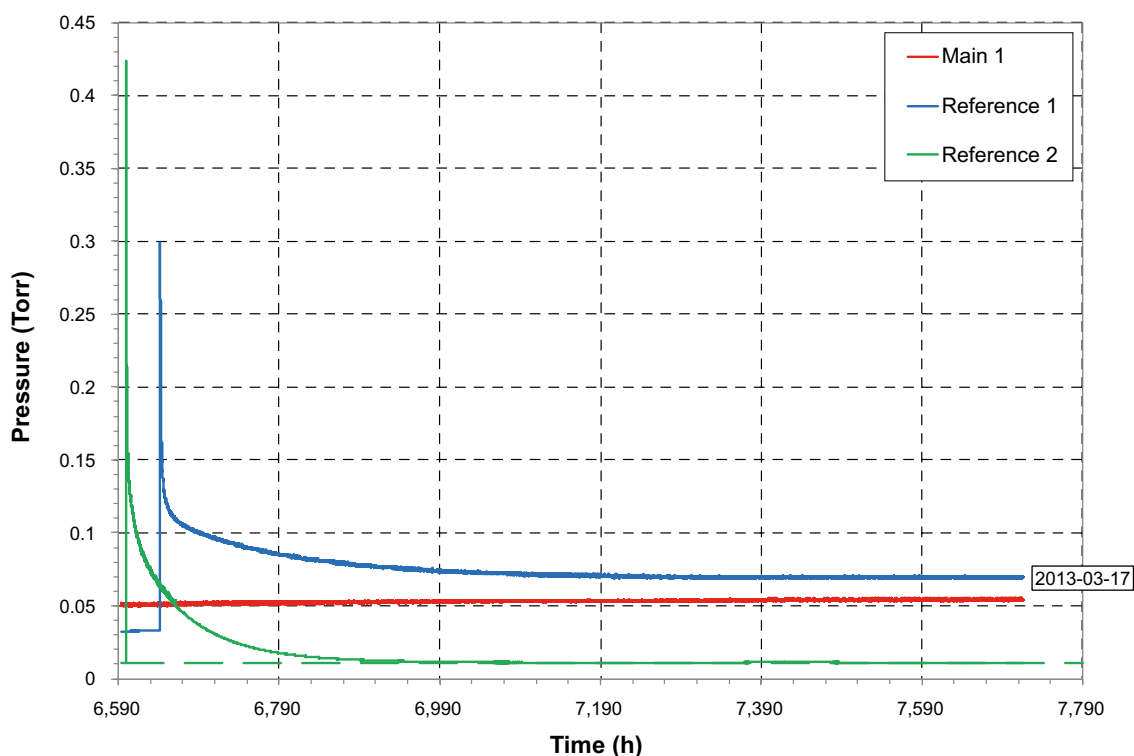
Figure 6-3. *Pressure equalisation between the vacuum chamber and the reaction chamber in References 1 and 2 after supplying hydrogen gas. In the same figure, the simultaneous logging of Main 1 is also drawn.*

In Section 5.1, the pressure increase is presented both graphically for an extended period of time (Figure 5-2) and in the form of a table (Table 5-1) concerning the maximum rate of formation for Main 1 and the two reference set-ups.

In all three set-ups, hydrogen gas is formed to approximately the same final pressure, although the reference set-ups completely lack immersed copper in the water. Reference 2 was created by ending an equivalent set-up to Main 1 as a result of Reference 1 not deviating much from Main 1 (Figure 5-2). A suspicion arose that the copper gasket that constitutes the seal between the reaction chamber and the lid contributed to the hydrogen formation despite the fact that it was not exposed to liquid water. In Reference 2 this copper gasket was thus replaced by a silver-plated gasket, but in other respects Reference 2 is as Reference 1. In spite of this hydrogen gas forms also in this case, although to a lower pressure before the maximum is attained.

The value of the maximum may depend on the palladium membranes being different. If instead the initiation of the hydrogen-formation process is examined, the influence from the membrane may become less important since a considerable counterpressure is far away. Then, Table 5-1 gives an interesting answer:

After pump-down of the set-ups, the maximum slope of the pressure increase rate is almost equal for all three set-ups; that is, the data constitute a strong indication that the hydrogen gas formation rate does not depend that much on copper being present or not. From this fact one can draw the conclusion that the maximum annual hydrogen production ($2 \cdot 10^{-5}$ moles) that was calculated from the maximum slope of Main 1 should considerably overestimate the expected amount of copper corrosion products. In other words, the copper corrosion rate cannot be directly inferred from the observed rates of formation for hydrogen gas. We have not been able to assess the significance of the stainless steel in detail, nor can we rule out the effect of the pressure gauges, which could not be baked out. There are strong indications that a significant hydrogen production has the vacuum system (mainly the stainless steel) as source wherein it dominates the background.

The absence of a significant amount of corrosion products containing copper agrees very well with the slopes being almost equal. The values in Table 6-1, that the amount of corroded copper corresponds to about 1% of the copper amount that can be calculated from the amount of hydrogen gas, are therefore completely in agreement with the fact that the initial slopes do not vary much.

7 Summary of conclusions

This study differs in essential aspects from similar studies aiming to clarify whether copper can corrode in oxygen-free water by water acting as an oxidant. The assignment was given a basic-research character, which is why great emphasis has been put on working with as clean components as possible, and, in a performance perspective, in such a way that no contamination can alter the cleanness and no material properties modifications are induced. Special methodologies have been utilised to avoid reactions with the surrounding air both during the course of the experiments and prior to the subsequent analysis steps. The latter has implied that experiments have been performed in a glove box with a controlled inert atmosphere, and that materials have been transported in vacuum or protective gas in tailor-made containers.

The results have been described in detail and discussed in Sections 5 and 6, respectively. The results can be summarised in three single statements:

- In those experiments where pressure is measured, we have observed a pressure increase as a function of time.

- Using mass spectrometry we have been able to conclude that the reason for this can be ascribed solely to hydrogen gas.

- We have not found any plausible stoichiometric relation (from a redox reaction) between the measured amount of hydrogen and the amount of product in the form of oxidised copper.

From ERDA analysis it was found that there are no significant changes in the hydrogen content of the metallic copper even after six months, while melting analysis data indicate that there is some increase; however, that trend is ostensible and can be attributed to deficient measurement statistics. Using Auger spectroscopy, no significant formation of oxide on the metal surface can be can found. The single indication that copper participates in a redox reaction is a weak increase of the copper content in the water, but these are extremely small amounts, which is why we cannot exclude that some of this originates from the glass that has been in contact with the water. Ultrapure water has a strong corrosive effect on glass, even though we have selected a glass grade that should give the lowest effect, yet provably contains copper to some extent. If so, it is a matter of copper ions from the glass being dissolved, which is not linked to a redox reaction but is an expected result from the effect water has on a salt (the glass material is in fact a complex amorphous borosilicate material; that is, boron is substitutionally included in the silicate network). ICP-MS shows clearly that other ions are released to a much higher degree, and elements such as potassium, calcium, and sodium have been included as cations while aluminium, boron, silicon, chlorine, and phosphorus have been included in anions that are decomposed in the plasma. We have no information about release rates from the glass, but it is noted that both the copper content and the iron content (elements that are in the glass according to analyses) in the water increase with approximately the same factor in the analysis from 6 months exposure compared to 3 months exposure (Appendix D3), and the increasing iron content can hardly result from release from the metallic copper. Therefore, we cannot exclude effects from the glass.

The products in which copper should be in an oxidised state (Cu^I or Cu^{II}) have been analysed from set-ups that were not connected to the pressure-measurement system, but that otherwise were designed in the same way regarding materials and temperature. Then, based on a redox reaction, a simple proportionality is anticipated between the molar amount of oxidised copper and the corresponding amount of evolved hydrogen gas. We have however observed a considerably larger amount of hydrogen gas than what can be calculated from the observed amounts of oxidation products. As presented in Table 6-1, the molar amount of copper in corrosion products is only of the order of 1% of the hydrogen gas we observe, which we believe to large extent originates in the stainless steel.

By considering these chemical analysis data, which are based on a battery of sophisticated methods and investigations of different phases, the creation of oxidation products from copper corrosion can be translated into an estimated corrosion rate of copper at the maximum 1 nm/year.

This report constitutes a progress report of the evaluation of pressure tests and the analysis of corrosion products after six months. The work moves on with further analyses of ongoing corrosion tests as well as evaluations of new pressure tests after some redesigning of the equipment in order to eliminate release leakage and keeping the background levels of hydrogen gas at a minimum. The results of these efforts will be reported in a forthcoming report.

8 Acknowledgements

References

SKB's (Svensk Kärnbränslehantering AB) publications can be found at www.skb.se/publications.

Bansal N P, Doremus R H, 1986. Handbook of glass properties. Orlando, FL: Academic Press.

Becker R, Hermansson H-P, 2011. Evolution of hydrogen by copper in ultrapure water without dissolved oxygen. Report 2011:34, Strålsäkerhetsmyndigheten.

Blackman A, Gahan L, 2013. Aylward and Findlay's SI chemical data. 7. uppl. Wiley.

Bunker B C, Arnold G W, Beauchamp E K, Day D E, 1983. Mechanisms for alkali leaching in mixed Na-K silicate glasses. Journal of Non-Crystalline Solids 58, 259–322.

Butler I B, Schoonen M A, Rickard D T, 1994. Removal of dissolved oxygen from water: a comparison of four common techniques. Talanta 41, 211–215.

Eriksen T E, Ndalamba P, Grenthe I, 1989. On the corrosion of copper in pure water. Corrosion Science 29, 1241–1250.

Flanagan T, Kishimoto S, Biehl G, 1981. Hysteresis in supported Pd-H2 systems. I Gokcen N A (red). Chemical metallurgy – a tribute to Carl Wagner: proceedings of a symposium / sponsored by the TMS-AIME Physical chemistry committee, the Copper, nickel, cobalt, and precious metals committee, and the ASM-MSD Thermodynamic activity committee at the 110th AIME Annual meeting, Chicago, Illinois, 23–25 February. Warrendale, PA: Metallurgical Society of AIME, 471.

Hench L L, 1975. Characterization of glass corrosion and durability. Journal of Non-Crystalline Solids 19, 27–39.

Hench L L, Clark D E, 1978. Physical chemistry of glass surfaces. Journal of Non-Crystalline Solids 28, 83–105.

Hultquist G, 1986. Hydrogen evolution in corrosion of copper in pure water. Corrosion Science 26, 173–177.

Hultquist G, Chuah G K, Tan K L, 1989. Comments on hydrogen evolution from the corrosion of pure copper. Corrosion Science 29, 1371–1377.

Hultquist G, Szakálos P, Graham M J, Belonoshko A B, Sproule G I, Gråsjö L, Dorogokupets P, Danilov B, Aastrup T, Wikmark G, Chuah G-K, Eriksson J-C, Rosengren A, 2009. Water corrodes copper. Catalysis Letters 132, 311–316.

Hultquist G, Graham M J, Szakálos P, Sproule G I, Rosengren A, Gråsjö L, 2011. Hydrogen gas production during corrosion of copper by water. Corrosion Science 53, 310–319.

Janson M S, 2004. CONTES, Conversion of Time-Energy Spectra, a program for ERDA data analysis. Instruction manual. Internal Report, Uppsala University.

Johansson L-G, 2008. Comment on "Corrosion of copper by water". Electrochemical and Solid-State Letters 11, S1.

Lanford W A, Davis K, Lamarche P, Laursen T, Groleau R, Doremus R H, 1979. Hydration of soda-lime glass. Journal of Non-Crystalline Solids 33, 249–266.

Lindau I, Spicer W E, 1974. The probing depth in photoemission and auger-electron spectroscopy. Journal of Electron Spectroscopy and Related Phenomena 3, 409–415.

Luo S, Flanagan T B, 2002. Thermodynamics of hydrogen solution and hydride formation for different microstructures of Pd. Journal of Alloys and Compounds 330–332, 29–33.

Luo S, Flanagan T B, 2006. Supersaturation and hydride formation in the dilute phase of Pd–H and Pd–Mn–H alloys. Journal of Alloys and Compounds 419, 110–117.

Mayer M, 1999. SIMNRA, a simulation program for the analysis of NRA, RBS and ERDA. I Duggan J L, Morgan I L (red). Proceedings of the 15th International Conference on the Application of Accelerators in Research and Industry, Denton, TX, 4–7 November 1998. American Institute of Physics Conference Proceedings 475, 541–544.

Morey G W, 1925. The corrosion of glass surfaces. Industrial and Engineering Chemistry 17, 389–392.

Möller K, 1995. Kopparkorrosion i rent syrefritt vatten. SKI Rapport 95:72, Statens kärnkraft-inspektion. (In Swedish.)

Noläng B, 1983. Application of equilibrium computations to chemical vapour transport and related systems. Doktorsavh. Uppsala universitet. (Acta Universitatis Upsaliensis 691).

Novelli P C, Lang P M, Masarie K A, Hurst D F, Myers R, Elkins J W, 1999. Molecular hydro-gen in the troposphere: global distribution and budget. Journal of Geophysical Research 104, 30427–30444.

Pederson L R, Baer D R, McVay G L, Engelhard M H, 1986. Reaction of soda lime silicate glass in isotopically labelled water. Journal of Non-Crystalline Solids 86, 369–380.

Petersson P, 2010. Ion beam analysis of first wall materials exposed to plasma in fusion devices. Doktorsavh. Uppsala universitet.

Simpson J P, Schenk R, 1987. Hydrogen evolution from corrosion of pure copper. Corrosion Science 27, 1365–1370.

SKB, 1978. Copper as a canister material for unreprocessed nuclear waste – evaluation with respect to corrosion. KBS TR 90, Svensk Kärnbränsleförsörjning/Kärnbränslesäkerhet.

SSM, 2011. Is copper immune to corrosion when in contact with water and aqueous solutions? Report 2011:09, Strålsäkerhetsmyndigheten.

Szakálos P, Hultquist G, Wikmark G, 2007. Corrosion of copper by water corrosion, passivation, and anodic films. Electrochemical and Solid-State Letters 10, C63–C67.

Tanner S D, Baranov V I, Bandura D R, 2002. Reaction cells and collision cells for ICP-MS: a tutorial review. Spectrochimica Acta B 57, 1361−1452.

Tengberg A, Hovdenes H, Andersson J, Brocandel O, Diaz R, Hebert D, Arnerich T, Huber C, Körtzinger A, Khripounoff A, Rey F, Rönning C, Schimanski J, Sommer S, Stangelmayer A, 2006. Evaluation of a lifetime-based optode to measure oxygen in aquatic systems. Limnology and Oceanography: Methods 4, 7–17.

Tesmer J R, Nastasi M, Barbour J C (eds), 1995. Handbook of modern ion beam materials analysis. Pittsburgh, PA: Materials Research Society.

Tsong I S T, Houser C A, White W B, Power G L, Tong S S C, 1980. Glass leaching studies by sputter-induced photon spectrometry (SIPS). Journal of Non-Crystalline Solids 38–39, 649–654.

Vickerman J C, Gilmore I C, 2009. Surface analysis: the principal techniques. 2. uppl. Hoboken, NJ: Wiley.

Werme L O, Korzhavyi P A, 2010. Comments on Hultquist et al. " Water corrodes copper". Catalysis Letters 135, 165–166.

Wilmad-LabGlass, u å. Technical information: cleaning glassware. Tillgänglig: http://www.wilmad-labglass.com/uploadedFiles/Main_Site/Pages/Support/cleaning_glassware.pdf [17 September 2013].

Xing Y, Dementev N, Borguet E, 2007. Chemical labeling for quantitative characterization of surface chemistry. Current Opinion in Solid State and Materials Science 11, 86–91.

Yano T, Ebizuka M, Shibata S, Yamane M, 2003. Anomalous chemical shifts of Cu 2p and Cu LMM Auger spectra of silicate glasses. Journal of Electron Spectroscopy and Related Phenomena 131–132, 133–144.

Zhang Y W, Whitlow H J, Winzell T, Bubb I F, Sajavaara T, Arstila K, Keinonen J, 1999. Detection efficiency of time-of-flight energy elastic recoil detection analysis systems. Nuclear Instruments and Methods in Physics Research B 149, 477–489.

Quality control of starting components

A1   Glass corrosion in relation to copper corrosion experiments

Literature study: Erika Widenkvist (Editing and supplements: Rolf Berger).

A1.1   Glass corrosion

Silicate glasses are among the most chemically inert of commercial materials and are therefore used in a wide range of applications. They react with almost no liquids or gases at low temperatures (below ~300°C). However, one very important exception is water (Bansal and Doremus 1986). The reaction of alkali silicate glasses with aqueous solutions is usually interpreted as a result of a combination of two independent processes: initial diffusion-controlled extraction of alkali ions out of the glass matrix, and the dissolution of the glass matrix itself. The first reaction is described as an ion-exchange (interdiffusion Na^+/H_3O^+ or Na^+/H^+) process or as a result of water diffusion into the glass network. As the rate of extraction decreases with increasing depth of alkali depletion, the second reaction of matrix dissolution becomes the dominant one (Bansal and Doremus 1986, Bunker et al. 1983, Pederson et al. 1986). The result is an increase in alkali ions and pH in the aqueous solution as well as release of decomposition products from the silicate glass.

The overall rate of attack on silicate glass by aqueous solutions depends on several factors, such as e.g. pH of the solution, its volume in contact with the glass, solution concentrations, and glass composition (Lanford et al. 1979, Morey 1925). The compositional effects are used for making glassware more durable. Oxide additives prohibiting alkali diffusion and oxides reinforcing the silicate matrix are used to increase the corrosion resistance (Tsong et al. 1980, Hench 1975, Hench and Clark 1978).

A1.2   Laboratory glassware

Laboratory glassware is commercially available in a variety of glass compositions; two commonly used glass types are shown in tabell A-1. Due to the importance of chemical resistance in e.g. pharmaceutical applications and glass in contact with foodstuff, several standards and classifications are available to guide in the choice of glassware. In tabell A-1 the class of hydrolytic resistance (DIN ISO 719), acid resistance (DIN 12 116), and alkali resistance (DIN ISO 695) are presented for the tabulated glasses.

Newly manufactured glassware can be slightly alkaline and should be soaked for several hours in acid water (a 1% solution of hydrochloric or nitric acid) and washed before use (Wilmad-LabGlass, n d).

A1.3   Glass in copper corrosion experiments

In previous copper corrosion experiments performed by Hultquist et al. soda-glass was used (Hultquist 1986, Hultquist et al. 1989, 2011) or occasionally Duran glass (Szakálos et al. 2007). The glass type was not stated for all experiments (Hultquist et al. 2009, 2011, Szakálos et al. 2007). Due to the long exposure times, glass leaching can be a factor that needs to be taken into account when interpreting the results. In fact, different results were observed for quartz-glass or soda-lime glass tubes (Möller 1995). From this short literature survey, borosilicate glassware appears to be a good choice of container material for long term exposure to water. By using Duran® beakers, any contamination due to glass leaching should be smaller than that expected for soda-glass beakers.

Tabell A-1. Composition and chemical resistance of glass (source: http://www.duran-group.com). Class I represents the highest resistance.

Glass type	SiO_2	B_2O_3	Na_2O+K_2O	Al_2O_3	BaO	CaO	MgO	Hydrolytic class (I–V)	Acid class (I–IV)	Alkali class (I–III)
Soda-Lime glass	69	1	16 (13+3)	4	2	5	3	III	I	II
Borosilicate glass (Duran®)	81	13	4	2				I	I	II

A2   Copper quality: Analysis certificate

Certificate of Analysis

Alfa Aesar®
A Johnson Matthey Company

Copper foil, 0.25mm (0.01in) thick, Puratronic®, 99.9999% (metals basis)

Stock Number: 42974
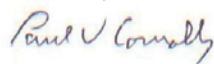**Lot Number: D13U048**

Analysis

Cu   99.99991 %

Ag	< 0.01	Al	0.012	As	< 0.002	Au	< 0.5
B	< 0.0005	Ba	< 0.0005	Be	< 0.001	Bi	< 0.002
Br	< 0.005	Ca	< 0.005	Cd	< 0.05	Ce	< 0.001
Cl	0.0025	Co	< 0.0005	Cr	< 0.002	Cs	< 0.005
F	< 0.002	Fe	0.0081	Ga	< 0.005	Ge	< 0.02
Hf	< 0.001	Hg	< 0.01	I	< 0.002	In	< 0.05
Ir	< 0.001	K	< 0.005	La	< 0.01	Li	< 0.001
Mg	< 0.001	Mn	< 0.001	Mo	< 0.002	Na	< 0.001
Nb	< 0.0005	Nd	< 0.005	Ni	< 0.005	O	1.6
Os	< 0.001	P	< 0.002	Pb	0.0037	Pd	< 0.002
Pt	< 0.001	Rb	< 0.001	Re	< 0.001	Ru	< 0.005
S	0.052	Sb	< 0.005	Sc	< 0.0002	Se	0.016
Si	< 0.005	Sn	< 0.01	Sr	< 0.0001	Ta*	< 5
Te	< 0.05	Th	< 0.0001	Ti	0.0072	Tl	< 0.001
U	< 0.0002	V	< 0.0002	W	< 0.002	Y	< 0.0002
Zn	< 0.05	Zr	< 0.0005				

Values given in ppm unless otherwise noted
Analysis method: GDMS
* denotes instrument contamination

Certified by:

Paul V Connolly

Quality Control

www.alfa.com

Analysis certificate for copper, 0.25 mm thickness; analysis by GDMS.

Certificate of Analysis

Alfa Aesar®
A Johnson Matthey Company

Copper foil, 0.25mm (0.01in) thick, Puratronic®, 99.9999% (metals basis)

Stock Number: 42974
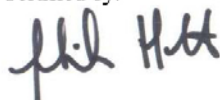**Lot Number: D20W015**

Analysis

Cu   99.99991 %

Ag	< 0.01	Al	0.012	As	< 0.002	Au	< 0.5
B	< 0.0005	Ba	< 0.0005	Be	< 0.001	Bi	< 0.002
Br	< 0.005	Ca	< 0.005	Cd	< 0.05	Ce	< 0.001
Cl	0.0025	Co	< 0.0005	Cr	< 0.002	Cs	< 0.005
F	< 0.002	Fe	0.0081	Ga	< 0.005	Ge	< 0.02
Hf	< 0.001	Hg	< 0.01	I	< 0.002	In	< 0.05
Ir	< 0.001	K	< 0.005	La	< 0.01	Li	< 0.001
Mg	< 0.001	Mn	< 0.001	Mo	< 0.002	Na	< 0.001
Nb	< 0.0005	Nd	< 0.005	Ni	< 0.005	O	1.6
Os	< 0.001	P	< 0.002	Pb	0.0037	Pd	< 0.002
Pt	< 0.001	Rb	< 0.001	Re	< 0.001	Ru	< 0.005
S	0.052	Sb	< 0.005	Sc	< 0.0002	Se	0.016
Si	< 0.005	Sn	< 0.01	Sr	< 0.0001	Ta*	< 5
Te	< 0.05	Th	< 0.0001	Ti	0.0072	Tl	< 0.001
U	< 0.0002	V	< 0.0002	W	< 0.002	Y	< 0.0002
Zn	< 0.05	Zr	< 0.0005				

Values given in ppm unless otherwise noted
Analysis method: GDMS
* Instrument contamination

Certified by:

Quality Control

Analysis certificate for copper, 0.25 mm thickness; analysis by GDMS.

Certificate of Analysis

Alfa Aesar®
A Johnson Matthey Company

Copper foil, 0.25mm (0.01in) thick, Puratronic®, 99.9999% (metals basis)

Stock Number: 42974
Lot Number: F14W027

Analysis

Cu   99.99991 %

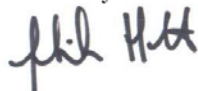|							
Ag	< 0.01	Al	< 0.021	As	< 0.002	Au	< 0.5
B	< 0.0005	Ba	< 0.0005	Be	< 0.001	Bi	< 0.002
Br	< 0.005	Ca	< 0.005	Cd	< 0.05	Ce	< 0.001
Cl	0.006	Co	< 0.0005	Cr	< 0.002	Cs	< 0.005
F	< 0.002	Fe	0.009	Ga	< 0.005	Ge	< 0.02
Hf	< 0.001	Hg	< 0.01	I	< 0.002	In	< 0.05
Ir	< 0.001	K	< 0.005	La	< 0.01	Li	< 0.001
Mg	< 0.001	Mn	< 0.001	Mo	< 0.002	Na	< 0.001
Nb	< 0.0005	Nd	< 0.005	Ni	< 0.005	O	1.116
Os	< 0.001	P	< 0.002	Pb	< 0.002	Pd	< 0.002
Pt	< 0.001	Rb	< 0.001	Re	< 0.001	Ru	< 0.005
S	0.028	Sb	< 0.005	Sc	< 0.0002	Se	< 0.005
Si	< 0.005	Sn	< 0.01	Sr	< 0.0001	Ta*	< 5
Te	< 0.05	Th	< 0.0001	Ti	0.004	Tl	< 0.001
U	< 0.0002	V	< 0.0002	W	< 0.002	Y	< 0.0002
Zn	< 0.05	Zr	< 0.0005	C	0.252	H	< 0.1
N	< 1						

Values are given in ppm unless otherwise noted
Hydrogen and nitrogen determined by LECO
Analysis method: GDMS
* Instrument contamination

Certified by:

[signature]

Quality Control

Analysis certificate for copper, 0.25 mm thickness; GDMS and melting analysis.

Certificate of Analysis

Alfa Aesar
A Johnson Matthey Company

Copper foil, 0.5mm (0.02in) thick, Puratronic®, 99.9999% (metals basis)

Stock Number: 42975
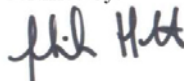**Lot Number: G26W045**

Analysis

Cu   99.9999 %

Ag	< 0.01	Al	0.026	As	< 0.002	Au	< 0.5
B	< 0.0005	Ba	< 0.0005	Be	< 0.001	Bi	< 0.002
Br	< 0.005	Ca	< 0.005	Cd	< 0.05	Ce	< 0.001
Cl	0.0077	Co	< 0.0005	Cr	< 0.002	Cs	< 0.005
F	< 0.002	Fe	0.0082	Ga	< 0.005	Ge	< 0.02
Hf	< 0.001	Hg	< 0.01	I	< 0.002	In	< 0.05
Ir	< 0.001	K	< 0.005	La	< 0.01	Li	< 0.001
Mg	< 0.001	Mn	< 0.001	Mo	< 0.002	Na	0.0057
Nb	< 0.0005	Nd	< 0.005	Ni	< 0.005	O	1.5
Os	< 0.001	P	< 0.002	Pb	< 0.002	Pd	< 0.002
Pt	< 0.001	Rb	< 0.001	Re	< 0.001	Ru	< 0.005
S	0.11	Sb	< 0.005	Sc	< 0.0002	Se	0.026
Si	< 0.005	Sn	< 0.01	Sr	< 0.0001	Ta*	< 5
Te	< 0.05	Th	< 0.0001	Ti	0.0072	Tl	< 0.001
U	< 0.0002	V	< 0.0002	W	< 0.002	Y	< 0.0002
Zn	< 0.05	Zr	< 0.0005				

Values given in ppm unless otherwise noted
Analysis method: GDMS
* Instrument contamination

Certified by:

Quality Control

Analysis certificate for copper, 0.50 mm thickness; analysis by GDMS.

A3   Palladium quality: Analysis certificate

Analysis certificate for palladium foil (Goodfellow)

Palladium foil 0.1 mm no PD000278/1 99.99+%
Foils: LS369989 + LS366153 (identical analysis concentrations[1])

Palladium	Matrix
Al	7 ppm
B	3 ppm
Cu	2 ppm
Fe	10 ppm
Pt	50 ppm
Rh	10 ppm
Si	1 ppm

Copied by Mikael Ottosson 6 March 2012

---

[1] Probably the same foil.

A4   Water quality: Analysis certificate

MERCK

101262 Water

Ultrapur

17 February 2011

Product number	Packaging	Size	Price
1012621000	Plastic bottle	1 l	price on request

Prices are subject to change without notice.

Product information

Hill Formula	H_2O
Chemical formula	H_2O
HS Code	2853 00 10
EC number	231-791-2
Molar mass	18.02 g/mol
CAS number	7732-18-5

Chemical and physical data

Molar mass	18.02 g/mol
Density	1.00 g/cm^3 (20 °C)
pH value	(H_2O, 20 °C) neutral
Boiling point	100 °C (1013 hPa)
Vapor pressure	23 hPa (20 °C)

Safety information

RTECS	ZC0110000
Storage class	10 - 13 Other liquids and solids
WGK	NWG not water endangering
Disposal	28
	Aqueous solutions: Container D.

Analysis certificate of ultrapure water for the experiments.

Specifications

Element	Specification
Ag (Silver)	≤ 50 ppt
Al (Aluminium)	≤ 200 ppt
As (Arsenic)	≤ 50 ppt
Au (Gold)	≤ 50 ppt
B (Boron)	≤ 500 ppt
Ba (Barium)	≤ 50 ppt
Be (Beryllium)	≤ 50 ppt
Bi (Bismuth)	≤ 50 ppt
Ca (Calcium)	≤ 500 ppt
Cd (Cadmium)	≤ 50 ppt
Ce (Cerium)	≤ 20.0 ppt
Co (Cobalt)	≤ 50 ppt
Cr (Chromium)	≤ 50 ppt
Cu (Copper)	≤ 100 ppt
Dy (Dysprosium)	≤ 20.0 ppt
Er (Erbium)	≤ 20.0 ppt
Eu (Europium)	≤ 20.0 ppt
Fe (Iron)	≤ 300 ppt
Ga (Gallium)	≤ 50.0 ppt
Gd (Gadolinium)	≤ 20 ppt
Ge (Germanium)	≤ 50 ppt
Hf (Hafnium)	≤ 10.0 ppt
Ho (Holmium)	≤ 20.0 ppt
In (Indium)	≤ 50.0 ppt
K (Potassium)	≤ 300 ppt
La (Lanthanum)	≤ 20.0 ppt
Li (Lithium)	≤ 50.0 ppt
Lu (Lutetium)	≤ 20.0 ppt
Mg (Magnesium)	≤ 100 ppt
Mn (Manganese)	≤ 50 ppt
Mo (Molybdenum)	≤ 50 ppt
Na (Sodium)	≤ 500 ppt
Nb (Niobium)	≤ 20.0 ppt
Nd (Neodymium)	≤ 20.0 ppt
Ni (Nickel)	≤ 50 ppt
Pb (Lead)	≤ 50 ppt
Pd (Palladium)	≤ 50 ppt
Pr (Praseodym)	≤ 20.0 ppt
Pt (Platinum)	≤ 50 ppt
Rb (Rubidium)	≤ 20.0 ppt
Sb (Antimony)	≤ 50 ppt
Sc (Scandium)	≤ 20 ppt
Si (Silicon)	≤ 500 ppt
Sm (Samarium)	≤ 20.0 ppt
Sn (Tin)	≤ 50 ppt
Sr (Strontium)	≤ 50.0 ppt
Ta (Tantalum)	≤ 50.0 ppt
Tb (Terbium)	≤ 20.0 ppt
Te (Tellur)	≤ 50 ppt
Th (Thorium)	≤ 10.00 ppt
Ti (Titanium)	≤ 50 ppt
Tl (Thallium)	≤ 50.0 ppt
Tm (Thulium)	≤ 20.0 ppt
U (Uranium)	≤ 10.00 ppt
V (Vanadium)	≤ 50 ppt
W (Wolfram)	≤ 100 ppt
Y (Yttrium)	≤ 10.0 ppt
Yb (Ytterbium)	≤ 20.0 ppt
Zn (Zinc)	≤ 500 ppt
Zr (Zirconium)	≤ 50.0 ppt

ICP-MS: Determination after evaporation to dryness with ICP-MS GFAAS: Determination after preconcentration with graphite furnnace AAS Actual analysis values are subject to unavoidable systematic variations in this concentration range.

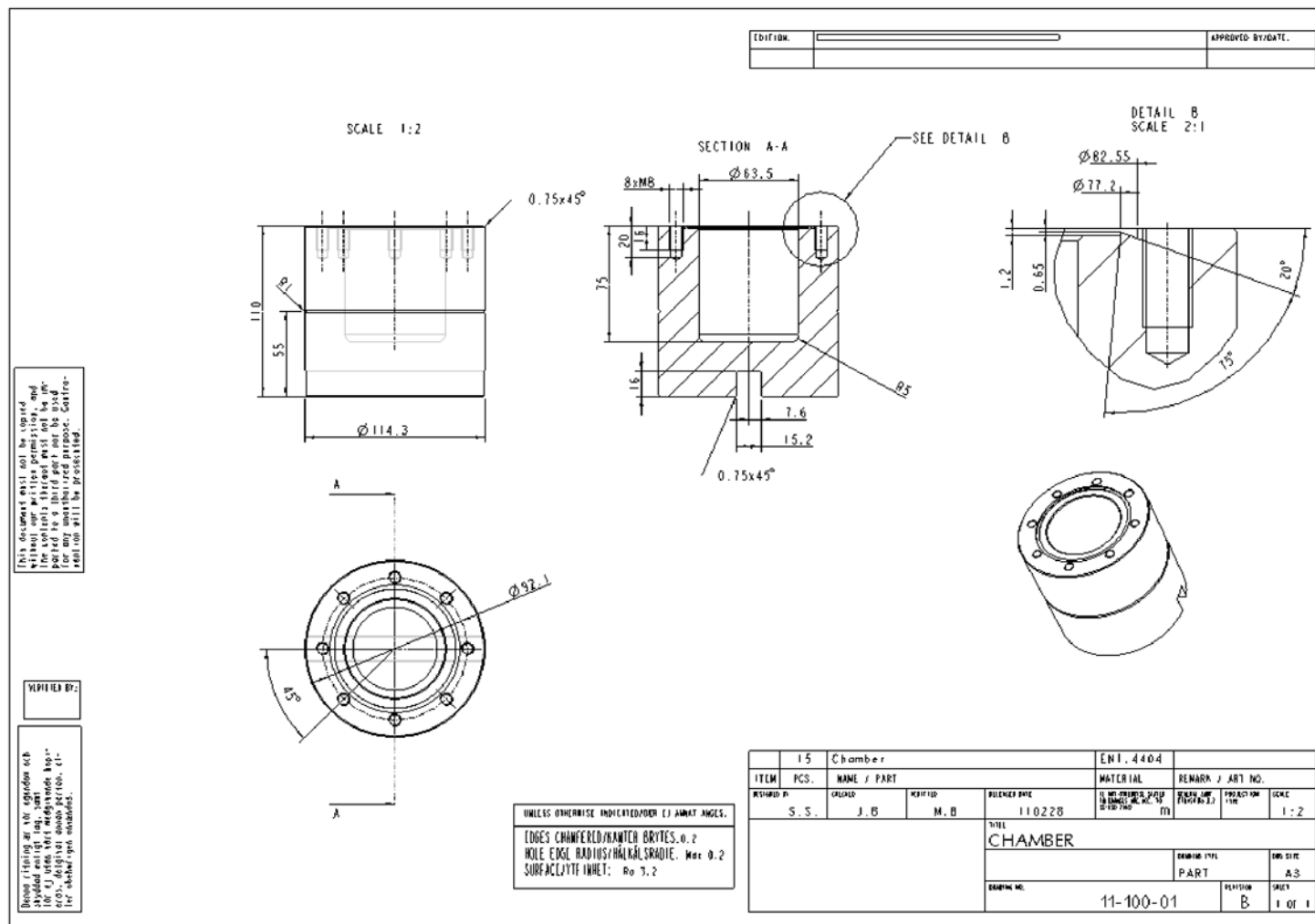*Cont. Analysis certificate of ultrapure water for the experiments.*
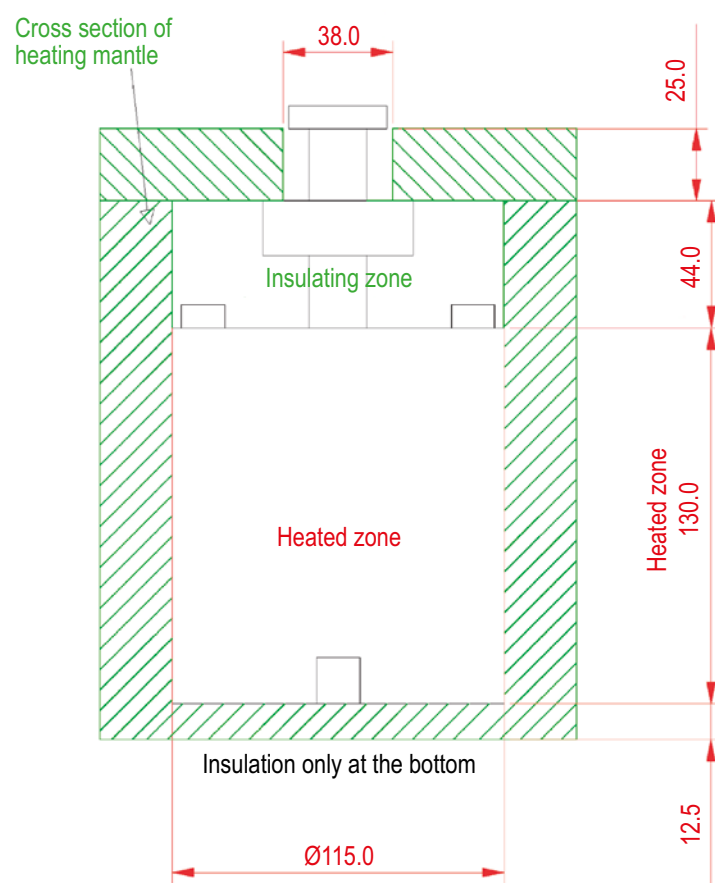
Equipment

B1   Reaction vessel

Drawing

Reaction chamber with CF-63; Materials: Damstahl 304L according to EN4307.

Material specification; heating jacket

Drawing of applied heating jacket for the reaction chamber.

B2   Components vacuum system for pressure measurement

Main 1, Ref. 1, Ref. 2[2]

Standard components

Pressure gauges:

- Capacity manometer, MKS 627B Baratron 0.05 Torr (sensitivity 0.02 mTorr, see below).
- Capacity manometer, MKS 627B Baratron 1.00 Torr.

Pressure readout:

- MKS PR4000B-F (Analogue signal output 0–10 volt for the logging system).

Valves (for bake-out):

- UHV valve ¾ right angle valve NW16CF (SS-304), Agilent 9515014.
- Gas valve (metal-sealed VCR) for QMS, Swagelock SS-4BG-V5 (SS-316).

Vacuum components (SS-304):

- Cross NW16CF, Rowaco FX16/19R.
- T cross NW16CF, Rowaco FT16/19R.
- Adapter NW16CF>KF16, Rowaco CFA16/KF16.
- Adapter NW16CF>KF25, Rowaco CFA16/KF25.

Customised

Manufactured at the Ångström Laboratory workshop:

Welded components (SS-304)

- Lid CF-63 blind with KF-16 flange welded on.
- CF-16 VCR ¼ '' adapter.

Complete manufacturing

- Reaction chamber with CF-63 flange.

Materials: Damstahl 304L according to EN4307.

Specifications

627D Baratron®Heated Absolute Capacitance Manometer
Specifications for pressure gauges

627D Baratron®	
Full Scale Ranges	0.02, 0.05, 0.1, 0.25, 1, 2, 10, 20, 100, 1,000, 2,000, 5,000, 10,000, 15,000, 20,000, 25,000 Torr.
Resolution	0.001% of Full Scale (0.002% of Full Scale for 0.02 and 0.05 Torr).
Accuracy	0.12% of Reading , 0.15% for 0.25, 0.1, and 0.05 Torr (including non-linearity, hysteresis, and non-repeatability).
TemperatureCoefficients	
Zero	0.002% of Full Scale/°C for 1–25,000 Torr range; 0.005% Full Scale/°C for 0.25 and 0.1 Torr, 0.015% Full Scale/°C for 0.05 Torr, 0.03% Full Scale/°C for 0.02 Torr.
Span	0.02% of Reading/°C.
Ambient Operating Temperature	15°C to 40°C.
Volume	6.3 cc.
Warm-Up Time	2 hours for 25,000 Torr Full Scale. 4 hours for 0.1 Torr Full Scale and lower.
Overpressure Limit	45 psia (310 kPa) or 120% Full Scale, whichever is greater.
Materials ExposedtoGases	Inconel®
Input Power Required	± 15 VDC ± 5% @ 0.25 Amps (max.).
Output Signal	Pressure: 0 to +10 VDC into > 10K Ω load.

---

[2] Sealing ring modified with silver coating.

Vacuum systems for high-vacuum pumping

Components

Pressure gauge:

• Full-range pressure gauge Pirani/hot cathode, MKS 979B NW25KF.

Pumps:

• Turbopump V81-T KF40, Agilent.

• Dry pump IDP-3, Agilent.

Vacuum components (SS-304):

• T cross NW25, Rowaco KT25/25.

• Adapter NW25KF NW40KF conical, Rowaco KF40R25/CO.

• Bellow hose NW25KF 1,000 mm, Rowaco FX25/1000.

The system is o-ring sealed and has a base pressure in the low 10^{-7} Torr range.

B3 Gas control

Leak detectors and leak searching

Leak detectors: Agilent VSRR022 No., LL110L022.

Sensitivity: $5 \cdot 10^{-12}$ atm·cm^3/s.

Leak-searching range: 10^{-4}–10^{-11}

Leak testing:

The sensitivity corresponds to: $1.58 \cdot 10^{-4}$ atm·cm^3/year = 0.12 Torr·cm^3/year.

Gas volume in the pressure logging system = 76 cm^3 → 1.6 10^{-3} Torr/year.

Pressure logging systems that were leak tested with helium did not show a detectable signal after tightening.

Oxygen-gas measurement

Instrument:

Fibox 3-trace V3 fibre-optic oxygen meter.

Serial No. S TLA 0003 000032.

Sensor: PSt6 sensitivity: 0–1.8 mg/l.

The method is optical and is based on dynamic "luminescence quenching" with molecular oxygen. A luminophore in an excited state is quenched by molecular oxygen and the luminescence light reduces in intensity in relation to the oxygen content (Tengberg et al. 2006).
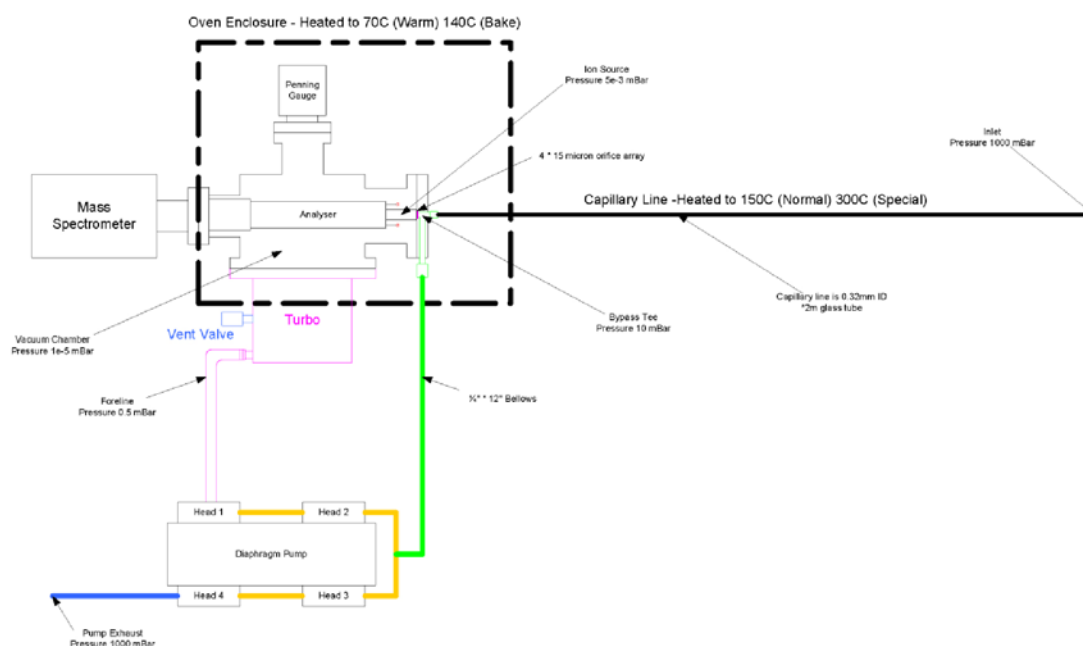
Modification of QMS:

MKS Cirrus (LM99)

Triple mass filter 1–200 amu, Faraday detector and SEM.

Original set-up for atmospheric pressure measurement:

Inlet holes 4×15 μm and bypass.

Gas inlet through 0.32 mm glass capillary with heating to 150°C.

Cirrus vacuum schematic

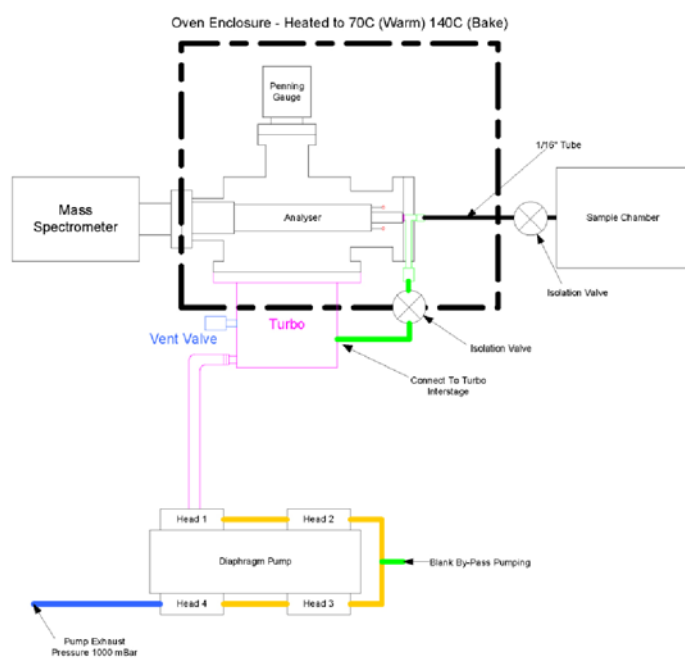**Modification for high vacuum/UHV:**
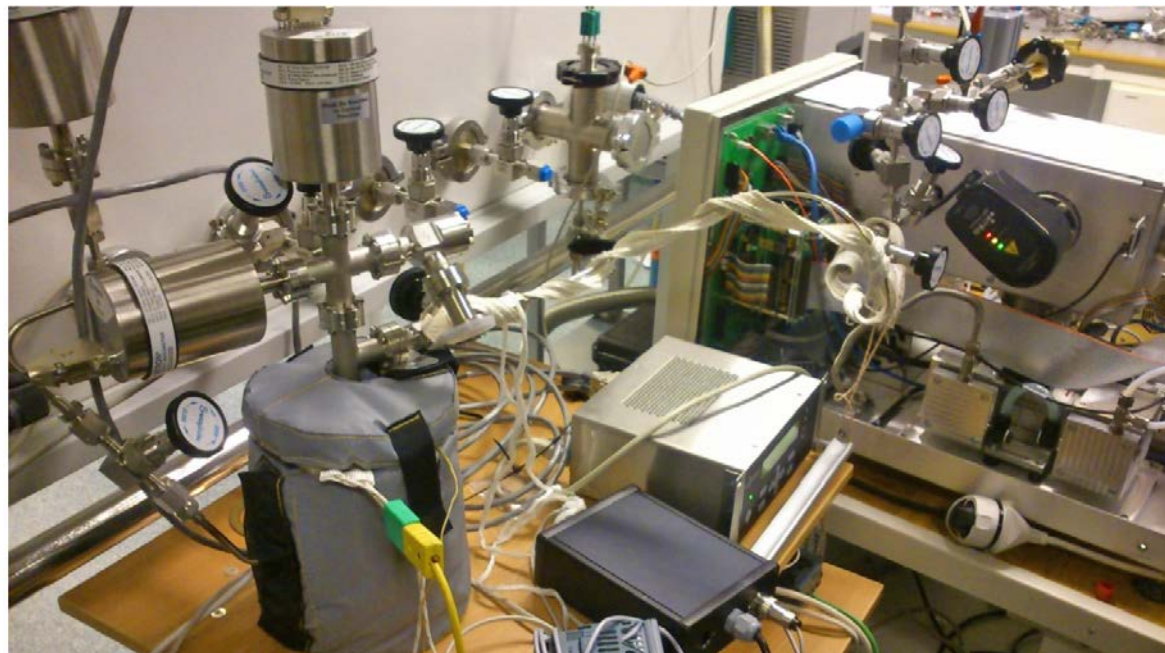
The inlet holes are increased from 4×15 μm to 4×100 μm and the bypass is blinded.

Gas inlet through 1/8" gas line of stainless steel.

Cirrus vacuum schematic

The modified mass spectrometer with system connected.

Background spectra after modification

Base pressure around 10^{-9} Torr (between $8 \cdot 10^{-10}$ and $1.3 \cdot 10^{-9}$ Torr)

Parts of the control-logging system from National Instruments

NI-9201 module: ± 10 V, 12-bit analogue input module

Dissolution = 0.053 volt.

Input signal from MKS PR4000B-F (Analogue signal output 0–10 volt to the logging system).

NI-9476 module: 32-channel digital output module

Relay module for thyristor control supplied with 12 V.

Semiconductor relay: Panasonic AQA 411VL.

75–250 V single phase, current 25 A.

Input 4–32 V direct current.

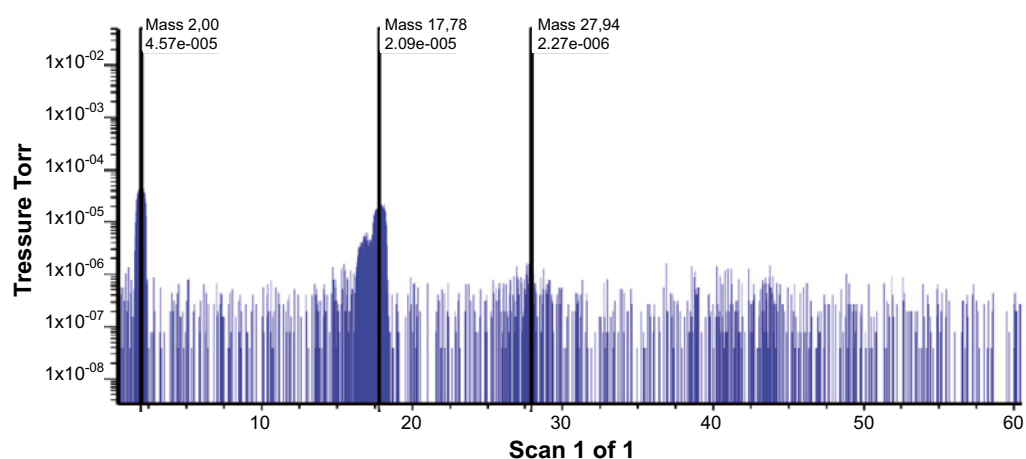### NI-9213 module: 16-channel thermocouple module

For temperature measurement and temperature control of heating jackets and heating tapes.
Sensitivity < 0.02°C.

Cold-Junction compensation accuracy 0.8°C type (1.7°C at most).

Thermocouple element type K from Pentronics (20-23100250).

The three m/z peaks are interpreted as hydrogen gas (2), water (18), and nitrogen gas (28), respectively.

Implementation in control-logging system (Rowaco)

The illustration shows a test of the temperature and pressure monitoring. In this illustration, not all thermocouple elements are connected (giving red windows, which otherwise indicate deviation from reference values).

MBRAUN

M. Braun Inertgas-Systeme GmbH Postfach 1323 D-85741 Garching

Uppsala University
Regementsvägen 1
74237 Uppsala
Sweden

Delivery address:

Uppsala University
Regementsvägen 1
74237 Uppsala
Sweden

Quotation

No.:	AN11-00108		
Date:	20.01.11		
Customer No.:	30242		
VAT-IdNo.:			
Deb.-Ref.			

Responsible
Phone M.Braun: +49(0) 89-32 669 - 0
Sales: Christian Eichner
Tel.-Ext.:   - 221   Fax: - 205   e-mail: c.eichner@mbraun.de
Commercial: Manuela Ernst
Tel.-Ext.:   - 222   Fax: - 205   e-mail: m.ernst@mbraun.de

Pos.	Description	Qty,	Unit	Price-unit	Amount	Currency
10	1500693	1,00	Piece(s)	23.950,00	23.950,00	EUR
	MB-Unilab (1950/780)					
	Glovebox with gas purification system for the work					
	under controlled atmosphere with <1 ppm oxygen and					
	moisture					
	Model: compact system, single user workstation					
	Internal workspace dimensions:					
	1950 mm (W) x 780 mm (D) x 920 mm (H)					
	Material box body: Stainless Steel, 1.4301					
	Gas purifier: 1-filter column, PLC controlled					
	Circulation blower: max. 84 m³/h, inc.					
	water-cooled heat exchanger, frequency controlled					
	Filter column valves: electro-pneum. main valves					
	(PLC-controlled)					
	Filter column regeneration: automatic sequencing					
	program (PLC-controlled)					

Sum carried forward: 23.950,00   EUR

| | | | | Sum carried forward: | 23.950,00 | EUR |

Pos.	Description	Qty,	Unit	Price-unit	Amount	Currency
	Control unit (PLC): Siemens S7-300					
	Automatic box pressure control: -15 to +15 mbar					
	(box can be operated at over- or underpressure)					
	Operation panel: Touch Panel 5.7", monochrome					
	Front window: Polycarbonate with SAPHIR hard coating (resistant to many chemicals and scratches)					
	Gloveport feedthroughs: 4 pcs., diameter 220 mm inc. gloves (Butyl)					
	Standard features (for additional information, please see actual product info):					
	1 pc. Main antechamber, d=390 mm, l=600 mm; inc. sliding tray inside; right side wall manual Evacuation/Refill with ball valve					
	1 pc. Vacuum pump (oil-sealed; 2-stage), approx. 12 m³/h; inc. oil mist filter)					
	6 pcs. Height adjustable shelves					
	1 pc. Electrical feedthrough 230V					
	2 pcs. Flanges DN40 for installation of feedthroughs					
	2 pcs. HEPA H13 dustfilter (gas inlet /-outlet)					
20	1500250 MB-MINI-AC-150-R Mini antechamber Diameter 150 mm, length 400 mm Type: 1/3 inside, 2/3 outside the box Cover: Hinged cover inside and outside Operaiton: manual, 3-way valve Inc. sliding tray	1,00	Piece(s)	1.050,00	1.050,00	EUR
30	1500306 MB-BS-200 Automatic box purging system Unit for inerting (purging) of the workspace with inertgas Operation: via operation panel of the gas purifier automatic (PLC-controlled) Flow rate: max. 200 l/min; inc. manual regulation valve for reduction of the gas flow Functions:	1,00	Piece(s)	930,00	930,00	EUR

| | | | | Sum carried forward: | 25.930,00 | EUR |

mBRAUN

| | | | Sum carried forward: | 25.930,00 | EUR |

Pos.	Description	Qty,	Unit	Price-unit	Amount	Currency
	- Purging ON / OFF					
40	**1500716** MB-OX-EC-PLC Electrochemical Oxygen analyzer Range: 1 to 1000 ppm Sensivity: 10 mV / ppm (range 1) Accuracy: 2% of displayed value, +/- 1 ppm bis 1000 ppm Integrated in Gas circulation piping.	1,00	Piece(s)	3.430,00	3.430,00	EUR
50	**1500685** MB-MO-SE1-PLC Moisture probe, PLC-controlled, measuring range: 0-500vpm, transducer, 0-10V output, 5m cable included.	1,00	Piece(s)	2.830,00	2.830,00	EUR
60	**202** Packing	1,00	Piece(s)	580,00	580,00	EUR
70	**201** Freight	1,00	Piece(s)	1.350,00	1.350,00	EUR
80	**210** Installation by M.Braun Flat-rate payment for set-up and commissioning Instruction of the user in operation and maintenance of M. Braun systems ****** All media supplies must be completely prepared by the customer prior to the installation	1,00	Piece(s)	3.500,00	3.500,00	EUR

| | | | Total: | 37.620,00 | EUR |

Shipping Method: Delivered duty unpaid (DDU) Incoterms 2000
Shipping Agent: SPEDITION
Payment-Terms: 30 days net

We would like to make you aware that according to the Council Regulation (EC) No.
428/2009, Article 22 (10) our products can be dual-use items and are subjected to controls
if exported from the European Community.

Validation of quotation: 90 days after date of issue.
******

Delivery time: approx. 14-16 weeks after date of order and clarification
of all commercial and technical details respectively final approval of the
technical engineering drawings by the buyer.
******

Warranty: 24 months from date of delivery according to the implied warranty
terms and EU-guideline 1999/44/EG.
******

Guarantee: 24 months voluntary supplier's guarantee for all MBraun systems
and components (mechanical, electrical and electronical components), as well
as the workmanship of the systems.

Excluded from any guarantee claim are all parts subject to wear and tear, such
as filters, adsorber material, gloves, etc. as well as customized integrations
such as balances, spincoater, hotplate, dispenser (to be subject of the warranty
and guarantee conditions of the original supplier).

Guarantee starts with the date of delivery / declaration of readiness for
shipment by MBraun.
******

The exporter of the products covered by this document (customs authorisation
no. DE/7600/EA/0020) declares that except where otherwise clearly indicated
these products are of German (EEC) preferential origin.
******

For delivery and sales of M.Braun products, our general terms and conditions of
delivery and sales are effective.
For download, please see:
www.mbraun.de / www.mbraun.com
******

Best regards,
M.Braun Inertgas-Systeme GmbH

i.V. Christian Eichner   i.A. Manuela Ernst
- Deputy Director Sales & Service -   - Sales Assistant -

Performance details

C1 Division of the copper foil before electropolishing

The purchased copper metal was in the form of foils of 100×100 mm in two thicknesses, 0.5 mm and 0.25 mm. The next stage would be to divide these into smaller plates. Since the copper should be surface cleaned by electropolishing, it would become unmanageable to treat each small copper plate individually, and treating a whole sheet followed by mechanical cutting might introduce contaminants from the cutting tool.

By means of milled traces in the metal, one should be able to obtain small plates by breaking the large piece, in the same way postage stamps, connected in sheets via their perforations, conveniently can be removed one by one. While electropolishing a large piece, one could at the same time address the contamination that might have been introduced by the milling.

Grooves were created in the copper foil using a small end mill. The foil sheet was not milled through its entire thickness; about 25% of the thickness was kept. The distance between the grooves was adapted to the test pieces of copper that later would be used in the different experiments, that is, 10×20 mm (for the metal analysis) and 12.5×47 mm (for the pressure-measurement set-ups). The plate dimensions were selected differently depending on whether they would be included in pressure experiments or not. The pressure measurements benefited from using larger plates, while the arrangements that were meant for the analysis of corrosion products were of smaller dimensions to fit properly with the analysis equipment.

The figure below shows an example of a copper sheet with corresponding grooved plates, 12.5×47 mm.

C2   Electropolishing of the copper foil

All glass beakers and measuring cylinders were cleaned in nitric acid of 3% and were rinsed with distilled water before adding electrolyte. The copper foil (that first was given grooves with the end mill; see previous section) was cleaned in 99.5% ethanol (ultrasonic treatment for 1 min) and 2-propanol (ultrasonic treatment for 1 min) to remove grease residues.

The polishing was done in 1.5 L of phosphoric acid:

1 L of 85% phosphoric acid (EMSURE 85% for analysis) was mixed with 0.5 L of distilled water in a 2-litre beaker.

The copper foil was mounted as the anode in a holder of polyethylene between two copper plates that constituted the cathode, in such a way that it was positioned symmetrically between the copper plates (see photograph below). The process had been optimised with copper of lower purity (99.99%) in previous experiments (E. Widenqvist). The polishing was done in two steps, step 1 with 1.7 V (current flowing) for 10 minutes and step 2 with 2.0 V for 10 minutes. The copper foil was then cleaned carefully in distilled water and was finally rinsed by ppb water (see Appendix C4).
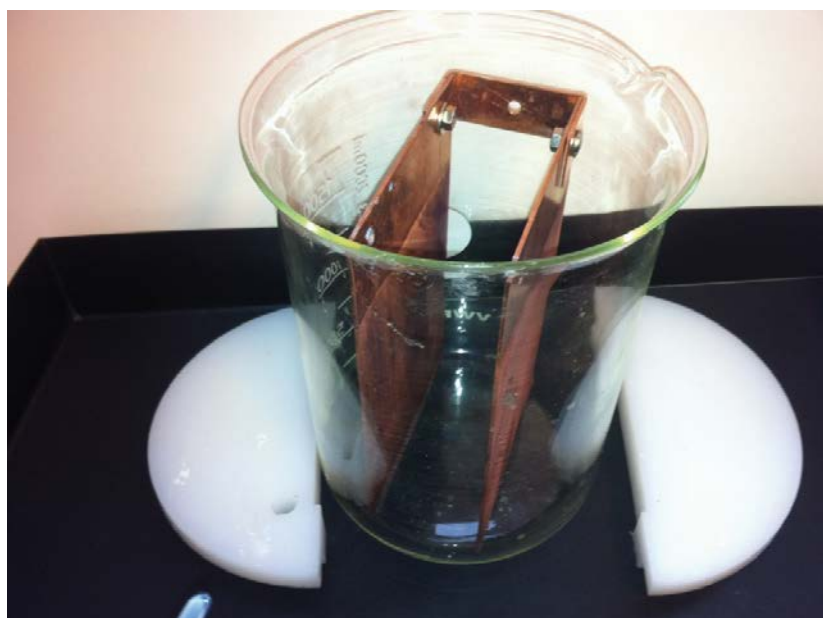
Beaker with copper cathode; the divided polyethylene lid is removed and lies nearby in its two halves. The copper foil was placed between the two copper-cathode plates, mounted in the divided cap.

C3 Heat treatment

C3.1 Description of the ultra-high vacuum oven (UHV oven)

The heat treatments were performed in an ultra-high vacuum system (UHV) where the pressure in the main branch was $< 10^{-10}$ Torr and in the four quartz-glass side pipes, $< 10^{-8}$ Torr. Side pipe II, used for the hydrogen reduction of the copper plates, is connected to a gas system with hydrogen gas and argon. The copper plates from the electropolishing were put inside a quartz-glass tube equipped with a valve at the opening. The metal can then be moved to and from the glove box in a protective argon atmosphere. Before the heat treatment, the empty quartz tube was heated at 150°C for 70 hours and at 600°C for 2 hours. A horizontal tube furnace reaching a temperature of 1,200°C is then pushed over the quartz tube with the sample (Figure C-1).

C3.2 Heat treatment in hydrogen gas

Before the heat treatment, the tube containing the copper plates was filled with argon and pumped three times. It was then filled with hydrogen gas to the nominal pressure of 120 Torr (the pressure gauge that was used is not adapted for hydrogen gas and the real pressure was considerably lower). The temperature was raised for 30 minutes to 300°C, where it was kept for 1 hour whereupon the oven was removed (pushed away). The pressure and the oven temperature were recorded during the cooling-down process. At 300°C the pressure gauge showed 360 Torr. The temperature profile in the oven at the nominal pressure of 360 Torr and an oven temperature of 300°C are shown in Table C-1.

Table C-1. Temperatures recorded at various distances from the centre of the plate. Positive values of x are in the direction towards the oven mouth.

x/cm	T_{oven}/°C	T_{point}/°C	P/Torr
−0.4	300	300	360
0	300	300	360
2	300	298	350
5	300	293	350

C3.3 Heat treatment in vacuum

After the hydrogen reduction, the chamber was purged once with argon and then pumped down to ~10^{-8} Torr. The temperature was raised for 30 minutes from room temperature to 400°C and held there for 2 hours during continued pumping. The pressure was recorded as a function of time, which is shown in Figure C-2. Temperature profile for the oven at 10^{-8} Torr and 400°C, recorded oven temperatures are given in Table C-2. The escaping gases were analysed with a mass spectrometer, and the emitted gases were hydrogen gas, water, and nitrogen gas (Figure C-3). After the heat treatment, the samples were handled in a protective atmosphere.
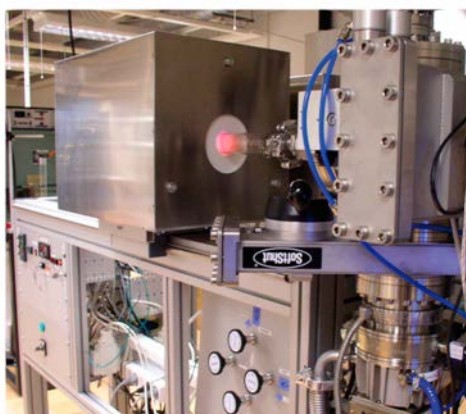
Figure C-1. *Photograph of the UHV oven in operation.*

Table C-2. The temperature is reported from the centre of the plate in the longitudinal direction of the tube. Positive values of x are in the direction towards the oven mouth.

x/cm	T_{oven}/°C	T_{point}/°C
–0.4	400	394
0	400	393
2	400	390
4	400	384
6	400	374
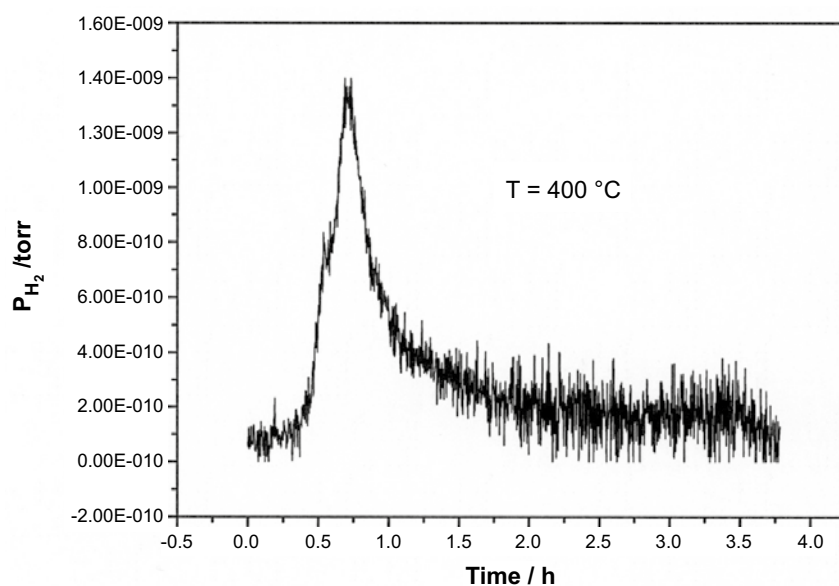
Figure C-2. *The degassing process of H_2 during dehydration of the copper plates. The pressure is recorded on a nominal relative scale.*
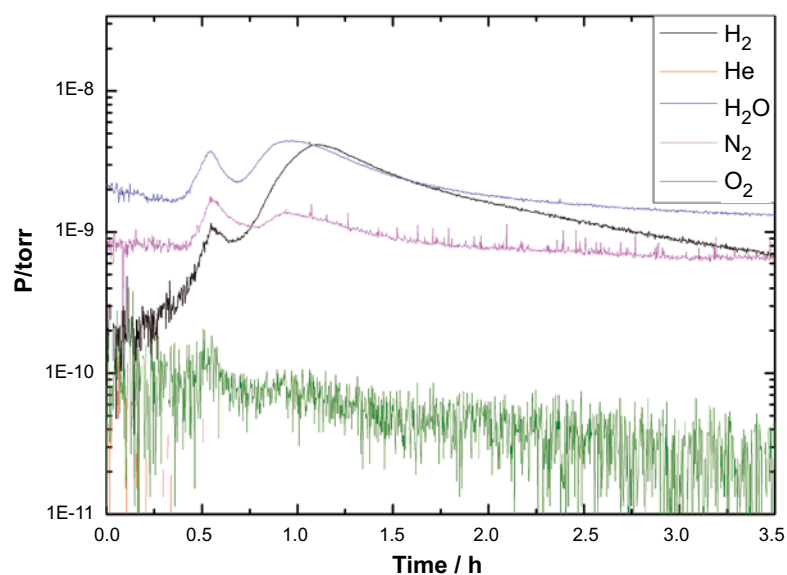
Figure C-3. *Results from mass spectrometer after hydrogen reduction.*

C4   Cleaning of glassware

All glassware used in the experiments was cleaned with ultrapure nitric acid (see the discussion in Appendix A). This applies to both Duran and quartz glassware. The glass was kept in 3M of nitric acid (Suprapur) for 24 hours whereupon it was thoroughly rinsed in deionised water (18 MΩ). Finally, three more rinses were made with specified water of the type "LiChrosolv". After cleaning, the glass was placed in a heating cabinet at 130°C for at least 3 hours before it was transferred to the glove box.

See specifications for the rinse water or the nitric acid, respectively:

Analysis certificate for the used high-purity rinsing water

iM

Specification

1.15333.2500   Water for chromatography LiChrosolv®

Specification		
Spec. conductance at 25 °C (at the time of manufacturing)	≤ 1	µS/cm
Colony forming units	≤ 25	CFU/g
TOC	≤ 30	ppb
Evaporation residue	≤ 5	mg/l
Fluorescence (as quinine at 254 nm)	≤ 1	ppb
Fluorescence (as quinine at 365 nm)	≤ 0.5	ppb
Gradient grade (at 210 nm)	≤ 5	mAU
Gradient grade (at 254 nm)	≤ 0.5	mAU
Gradient grade (basic absorption (210 nm))	≤ 20	mAU

Specification		
Suitable for LC-MS (Bruker esquire 3000 plus); Intensity of background mass peak based on reserpine (APCI/ESI positive)	≤ 1	ppb
Suitable for LC-MS (Bruker esquire 3000 plus); Intensity of background mass peak based on reserpine (APCI/ESI negative)	≤ 20	ppb

Filtered by 0.2µm filter
Suitable for UPLC/UHPLC/Ultra HPLC-instruments

Dr. Reiner Vogt
Responsible laboratory manager quality control

Specification

iM

1.00441.1000   Nitric acid 65% Suprapur®

	Specification	
Assay (acidimetric)	≥ 65.0	%
Chloride (Cl)	≤ 50	ppb
Phosphate (PO₄)	≤ 10	ppb
Sulphate (SO₄)	≤ 200	ppb
Ag (Silver)	≤ 0.5	ppb
Al (Aluminium)	≤ 5.0	ppb
As (Arsenic)	≤ 0.5	ppb
Au (Gold)	≤ 0.1	ppb
Ba (Barium)	≤ 0.5	ppb
Be (Beryllium)	≤ 0.5	ppb
Bi (Bismuth)	≤ 0.5	ppb
Ca (Calcium)	≤ 2.0	ppb
Cd (Cadmium)	≤ 0.5	ppb
Co (Cobalt)	≤ 0.5	ppb
Cr (Chromium)	≤ 1.0	ppb
Cu (Copper)	≤ 0.5	ppb
Fe (Iron)	≤ 2.0	ppb
Ga (Gallium)	≤ 0.1	ppb
Ge (Germanium)	≤ 0.1	ppb
Hg (Mercury)	≤ 1.0	ppb
In (Indium)	≤ 0.5	ppb
K (Potassium)	≤ 2.0	ppb
Li (Lithium)	≤ 0.5	ppb
Mg (Magnesium)	≤ 1.0	ppb
Mn (Manganese)	≤ 0.5	ppb
Mo (Molybdenum)	≤ 0.5	ppb
Na (Sodium)	≤ 10.0	ppb
Ni (Nickel)	≤ 5.0	ppb
Pb (Lead)	≤ 2.0	ppb
Pt (Platinum)	≤ 0.5	ppb
Sb (Antimony)	≤ 0.5	ppb
Sn (Tin)	≤ 0.5	ppb
Sr (Strontium)	≤ 0.5	ppb
Ti (Titanium)	≤ 1.0	ppb
Tl (Thallium)	≤ 0.5	ppb
V (Vanadium)	≤ 0.5	ppb

C5   Ultrasonic cleaning of stainless steel

Equipment: FinnSonic.

Detergent: Tickopur R 33 (see commodity information).

Temperature: 120°C.

Basics for ultrasonic cleaning

General

Ultrasonic cleaning is currently the most effective cleaning technique. The efficiency is ascribed to the creation of cavitation in the cleaning liquid by high frequency vibrations. On the surface of the material object, microscopic cavitation bubbles are formed, exposing the surface to powerful compression waves. The powerful compression waves effectively detach dirt, grease, and other impurities. The cleaning effect reaches also locations where other cleaning methods have no effect. The technology is fast, environmentally friendly, and very effective. Power consumption and detergent consumption are low. Ultrasonic cleaning can easily be automated. Ultrasonic cleaning is the best cleaning method when a high degree of cleaning is required.

Cavitation

Ultrasonic cleaning is based on acoustic cavitation. In ultrasonic cleaning, the cleaning item is lowered into a tank of liquid, and simultaneously exposed to vibrations at ultrasonic frequencies (higher than audibility, i.e. higher than 20 kHz).

The cleaning is not directly caused by vibrations: The ultrasound gives rise to cavitation in the fluid, which gives the desired effect. The ultrasound propagates as compression waves in the fluid, which causes pressure and distraction tensions. The cavitation in the fluid arises when the distraction tensions are so large that bubbles are formed in the fluid. These vacuum bubbles are formed at dirt particles or at other "weak points" in the fluid.

When a cavitation bubble has been formed it grows due to the ultrasound to so-called resonance size, and then it collapses.

In this way, two types of cleaning action are attained:

1. When the bubble is formed it wears on the object surface at resonance frequency until the bubble implodes.

2. When the bubble in the strong ultrasonic field finally implodes, it creates a microscopic but very strong compression wave.

Of these two cleaning effects the latter is very important. When these bubbles collapse, pressures over 1,000 times the atmospheric pressure have been measured. It is this pressure that causes the actual and most important cleaning action.

Factors that affect the cleaning result

1. Mechanical effect = ultrasonic power. The power requirement depends on many factors such as the fluid volume, the mass and geometry of the item to be cleaned, the kind of dirt, and the ultrasonic frequency.

2. Chemical output = cleaning. Common detergent contents are 1–5%. Follow the recommendations of the detergent producer. If the machine has vigorous fluid circulation, do not use a highly foaming detergent.

3. Temperature. Best cleaning effect is normally achieved at about 60–80°C. Follow the recommendations of the detergent producer. The amount of cavitation is lowered drastically at the boiling point of the fluid.

4. Processing time. Common cleaning times are 1–5 minutes. In certain service contexts up to several hours are needed.

General advice to the user

- Note that the ultrasound causes the fluid temperature to rise somewhat during long processes.

- After changing fluid, it is best to let the ultrasound be switched on for a while before articles are cleaned. The ultrasound vents the fluid, and the cleaning action reaches optimum after the deaeration.

- Put the cleaning objects in a basket or holder such that they do not lie on the bottom of the bath.

- The objects to be cleaned should be arranged such that air can come out of cavities. The cleaning objects may need to be turned once during the cleaning process.

- Ultrasonic cleaning is best suited to cleaning hard materials.

- Change the cleaning fluid as soon as the fluid becomes dirty.

- Clean the bath when changing fluid.

- Add cleaning fluid and cleaning agent depending on evaporation and the amount of dirt.

Washing-up liquid

Tickopur and Stammopur

To attain optimal cleaning action in an ultrasonic bath/ultrasonic cleaning machine, a proper cleaning technique in combination with a suitable cleaning agent is required.

Bandelin has developed a number of tailored cleaning agents that all have a very good cleaning effect. They are environmentally friendly and gentle to the ultrasonic bath/cleaning machine and the objects to be cleaned while enhancing the so-called cavitation and thus improving the cleaning effect. Depending on the cleaning task, the following types of agents are available:

- Alkaline, neutral, or acidic.

- Free from surfactants and complex formation agents.

- Disinfecting.

Type of contaminant	Cleaning object	Suitable washing-up liquid	Packaging
General contamination. Grease and oil residues. Soot, ink, waste from drilling, grinding, polishing etc.	Made of glass, ceramic, plastic, rubber, stainless steel, nonferrous metals, precious metals, light metals. Mesh filters, pipettes, circuit boards, respiratory masks, glasses. Be careful with objects that contain tin and zinc.	**Tickopur R 33** General cleaning agent that is anticorrosive. Suitable for laboratory, service, and industrial use. Gentle, faintly alkaline, pH 9.9 in a 1% solution for use. Dosage 1–5%. Cleaning time 1–10 min.	2, 5, 25, and 200 litres.

Analytical methods with comments

D1   Melting analysis

The working principles are made clear by the enclosed analysis report from Bruker having performed melting analysis on five different copper samples. First, a summary is of the important data of the analysis report is given below. It must be noted that the uncertainties of the results are great, particularly for the measurements that could not be duplicated and hence lack standard deviations.

Summary of the analysis report from Bruker: "Hydrogen in copper"

Sample designations:

Alpha untreated: Cu-alpha

After electropolishing: Cu-EP

Ditto + hydrogen cleaning: Cu-HR

Experiments after 1 month: Cu 1m

CF gasket: Cu-CG 64

Table D-1. Results (contents with possible standard deviations in brackets).

| Sample	Content (ppm, mass)	Content (ppm, mole)
Cu-alpha*	4.2 (0.65)	270 (41)
Cu-EP	1.3	80**
Cu-HC	2.4	150**
Cu-1m	3.4 (0.7)	210 (45)
Cu-CG 64	0.9 (0.3)	60 (20)

* Appendix A2: The FM W077 certificate specifies < 0.1 ppm (about 30 atomic ppm).
** Only one measurement per sample.

For the treated copper plates, the difference between the highest and lowest value 3.4–1.3 = 2.1 ppm (parts by weight) is hardly significant if the corresponding standard deviation (0.7 ppm) is taken into consideration. The apparent increasing trend in hydrogen content is therefore misleading.
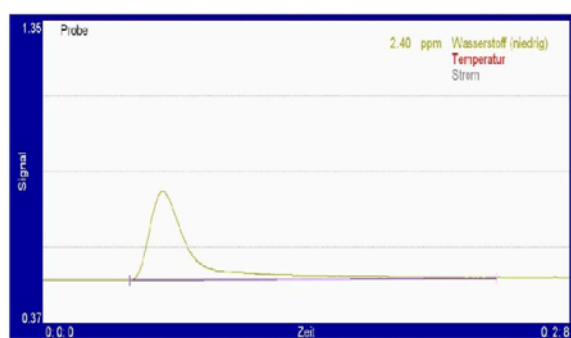
IV.3   Analysis Results for Hydrogen

Sample CuAlfa
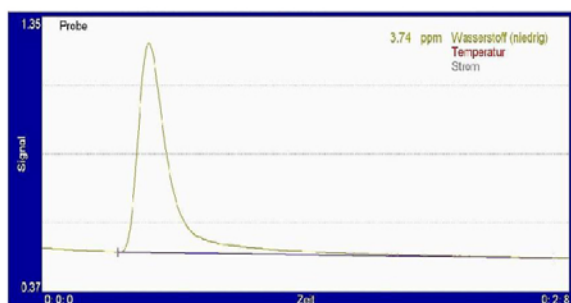
Signal sample "CuAlfa"
(Hydrogen low range)

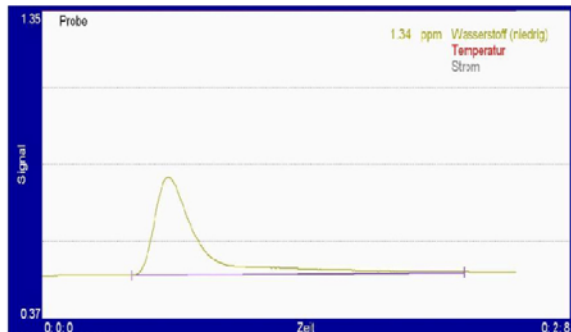| Weight [g]	Hydrogen [ppm]
0.58297	3.7415
0.43762	4.6610
Average	4.2
SD	0.65

Sample CuHR

Signal sample "CuHR"
(Hydrogen low range)

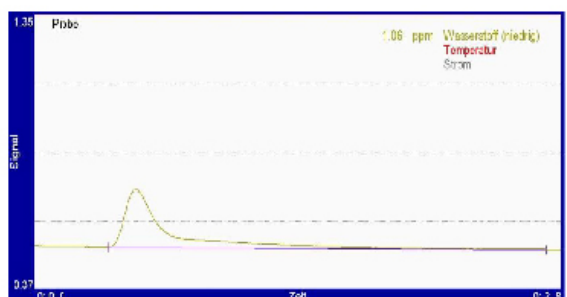| Weight [g]	Hydrogen [ppm]
0.45141	2.3954

Sample CuEP

Signal sample "CuEP"
(Hydrogen low range)

Weight [g]	Hydrogen [ppm]
0.91582	1.3435

Sample Cu1m
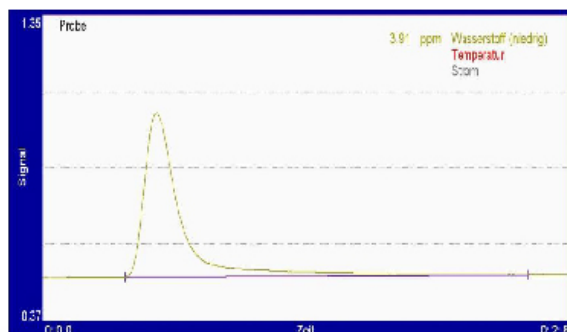
Signal sample "Cu1m"
(Hydrogen low range)

Weight [g]	Hydrogen [ppm]
0.44291	3.9137
0.43813	2.9123
Average	**3.41**
SD	**0.7**

Sample CuCG64

Signal sample "CuCG64"
(Hydrogen low range)

Weight [g]	Hydrogen [ppm]
0.75501	1.0607
0.60995	0.6638
Average	**0.86**
SD	**0.3**

Remark:
One analysis per sample is not representative. Unfortunately no more sample material was available.

For further questions or remarks please do not hesitate to contact us.

We also have the possibility to offer you a demonstration in our Demo- & Application Lab of our analytical instruments, which include CS/NOH analysis instruments and different optical emission spectrometers.

D2 ERDA: Methodology and analysis results

Description of the ERDA technique

Elastic Recoil Detection Analysis (ERDA) is an analysis method based on ion-beam technology, and it is particularly suited to depth profile analysis of light elements (Tesmer et al. 1995 and references given there). The samples are placed in an ultra-high vacuum chamber with a pressure of $< 10^{-6}$ Torr. In the ERDA analysis method heavy ions of high energies (hundreds of keV per atomic mass unit) are used. The ions impinge on the sample surface at a low angle and knock atoms and ions from the sample, and these are detected. The energies of these atoms and ions depend on their atomic masses and the depth from which they are knocked. Specific depth profiles for each atomic species can be obtained from a single measurement by using a combination of TOF technology (time-of-flight technology) and conventional solid-state detectors.

Experimental set-up

The experiments were performed in the tandem accelerator with the TOF/ERDA set-up at the Ångström Laboratory, Uppsala University (Zhang et al. 1999, Petersson 2010). The instrument was adapted for the determination of hydrogen content and other contaminants in copper and palladium. An ion beam of 36 MeV I^{8+} was used, as it gives the highest yield for these elements. The contents of elements with atomic numbers lower than ~30 can be determined down to depths of 150–200 nm. The resolution of the depth profile is ~15 nm for the studied elements. The detectors were calibrated for light particles (Zhang et al. 1999).

Evaluation of the measurement data

In Figure D-1, a time-energy spectrum is shown directly from a measurement, with the x axis approximated as an energy scale and the y axis as an inverse time scale that corresponds to the speed of the particles. Each area or groove in the spectrum corresponds to detected atoms with a definite mass, whereby the lightest atoms, the hydrogen atoms, with high speed and low energy are found in the upper left-hand corner of the spectrum. These spectra are usually analysed with the program CONTES (Janson 2004), in which the concentration can be determined down to 0.1 atomic per cent. For the low hydrogen contents in the present case, a more sensitive assessment method, SIMNRA, must be used which accounts for the detector sensitivity of different atomic species (Mayer 1999).

Measurement on the copper plates

In Figure D-2 are shown CONTES-calculated concentrations of hydrogen, carbon, oxygen, and copper down to a depth of 150 nm in a copper plate after 6 months in pure oxygen-free water. No reliable values could be obtained below around 25 nm, however, as the concentrations at these depths are under the limit of 0.1 at%. On the surface of the copper plate there are relatively high amounts of hydrogen, carbon, and oxygen. A very thin layer of adsorbed water and hydrocarbons remains on the surface, although the measurement is performed in ultra-high vacuum. Deep inside the copper plate, the contents of these elements are too low to be determined with CONTES.

By fitting the spectrum to the SIMNRA program a very good compliance is obtained for 300 ppm (atomic fraction), that is, < 5 ppm parts by weight hydrogen in the copper material and 1.5 monolayers water adsorbed on the copper surface (see Figure D-3). This gives a relatively strong hydrogen signal. The error limits in the measurement data cause a random spread of the data around the reference value.

The same analyses were performed on copper samples that had not been exposed to water, of which the results are reported in Table D-2 along with the analysis results for the palladium filter in the 6-month test. The copper samples showed between themselves no significant differences in hydrogen content. The statistic uncertainty in the data acquisition and the detector sensitivity lead to statistical errors of 50–100 ppm. There may also be systematic errors of the same magnitude.

Measurement on the palladium membrane

Results of ERDA measurements on the palladium filter from the 6-month test are presented in Figure D-4. The results of CONTES and SIMNRA, respectively, agree within the error limits. The hydrogen concentration was determined at 4,000 ppm (atomic fraction), that is, < 40 ppm parts per weight.
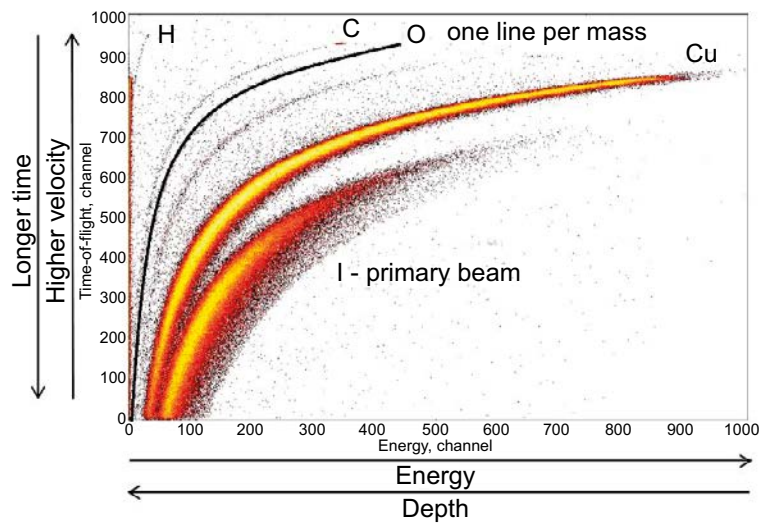
Figure D-1. *TOF-ERDA spectrum of pure Cu: Each atomic mass has a corresponding curve. Here, for clarity's sake, the oxygen curve is accentuated.*
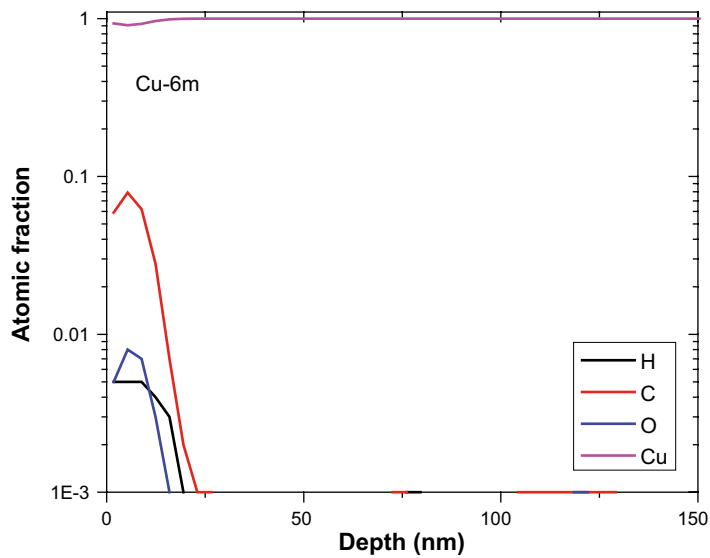
Figure D-2. *Concentration profiles for hydrogen, carbon, oxygen, and copper (100%) measured on a copper plate.*
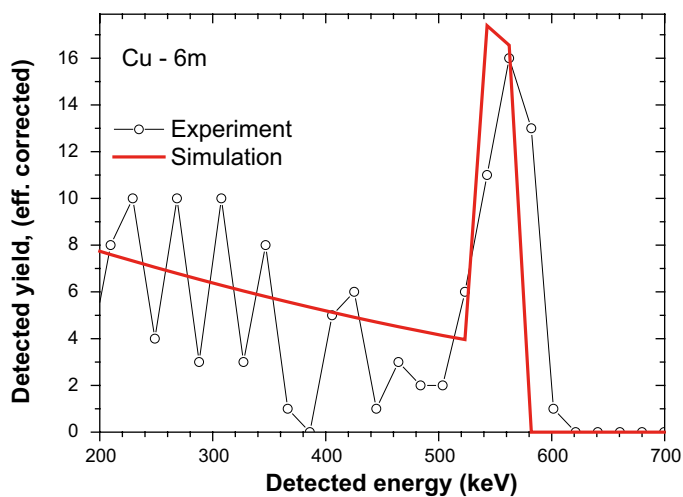
Figure D-3. *Energy spectrum for hydrogen in a copper sample (6 months' exposure). Fit with the program SIMNRA.*

Figure D-4. *Depth-profile concentrations in the palladium membrane after 6 months for hydrogen, boron, carbon, and oxygen. The concentrations are calculated with CONTES.*

Table D-2. Hydrogen concentrations as atomic abundances for copper plates after various treatments and palladium filters after 6 months in the experimental set-up.
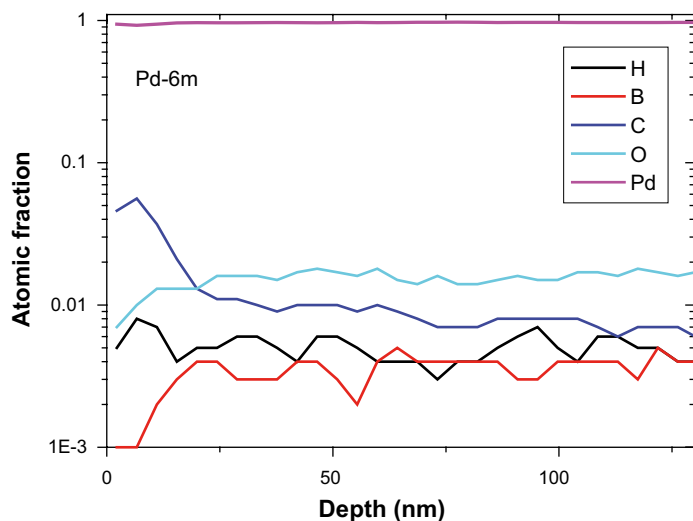
Sample	Cu-untreated[a]	Cu-EP[b]	Cu-HC[c]	Cu-6m[d]	Pd-6m[d]
H concentration.	400 ppm	300 ppm	300 ppm	300 ppm	4,000 ppm
Remarks	2% oxygen				

[a] As new.
[b] Electropolished.
[c] Hydrogen reduced after EP.
[d] 6-month experiment.

Conclusion

The results of the ERDA analyses show that the hydrogen concentrations in the copper plates before and after exposure in oxygen-free clean water for 6 months are equal within the given error limits.

With the ERDA method no differences can be detected.

D3   Analyses with ICP-MS

Brief theory of ICP-MS

ICP-MS (from Inductively Coupled Plasma Mass Spectrometry) is a technique for the measurement of low contents of elements in liquid samples. An ICP-MS measurement starts by introducing the liquid sample by transforming it into an aerosol of liquid drops using a so-called nebuliser and a spray chamber. The aerosol is then sucked into an argon plasma where the liquid is vaporised and the molecules in the sample are decomposed into their atomic constituents due to the high temperature of the plasma. The plasma also ionises some of the atoms, and those ions are guided into a quadrupole mass analyser that separates the ions with respect to mass and charge (m/z). The quadrupole guides ions with a specific m/z-ratio to a detector that registers how many ions impinge on the detector during a specific period of time. The amount of ions per time period can then be related to the concentration of the element in the sample, by first calibrating the instrument to standard solutions with known concentrations and isotopic abundances of the elements to be examined.

The elements that can be determined by ICP-MS are limited by the ionisation degree of the elements, m/z-overlapping isotopes of other elements, and molecules with overlapping m/z that are present in large amounts and hard to decompose. For instance, the analysis of iron is disturbed by argon oxide. The interference problems can be suppressed by using a less disturbed isotope of the same element or by introducing a reaction or collision gas (Tanner et al. 2002) to neutralise the interfering elements or molecules. One can also in some cases theoretically calculate and estimate to what extent a specific element disturbs another element.

Analyses of water samples

A NexION 300D (Perkin Elmer) was used to analyse the water samples, and the instrument was calibrated to multi-element solutions prepared from pure element standards with natural isotopic abundances intended for ICP. As low contents would be investigated, the risk of contamination was high. In consequence, the calibration solutions were prepared in a laminar flow bench ("LAF bench", which functions as a miniature clean room) and powder-free rubber gloves were used when handling all solutions. First, a semi-quantitative method was used to detect which elements were found in water samples A1 and A2 (Figure D-5) and at what magnitude. Most elements, which indeed could be detected, were excluded because of too-low content, because they are abundant in glass, and/or because they are disturbed by interferences, while some elements (Mg, Cu, Zn, Sb, and Fe) were considered to be quantitatively determinable and were selected for further study.

Not even ^{57}Fe was entirely free from problems as an alternative to ^{56}Fe. The fact that most of the samples consisted of water implies that ^{17}O is not negligible in the analyses. To eliminate interferences on ^{57}Fe from ^{40}Ar^{17}O among others, ammonia was used as the reaction gas when ^{57}Fe was measured; and, to make sure that ^{63}Cu was not disturbed by the conceivable presence of PO_2 molecules, ^{65}Cu was also investigated, which is significantly less disturbed by PO_2 molecules. For the 6-month samples Pd was also analysed, and three of the most abundant isotopes were selected to facilitate investigation and exclusion of hypothetical problems related to overlapping molecules. In total, 8 water samples were analysed quantitatively, with the analyses distributed over three separate occasions.
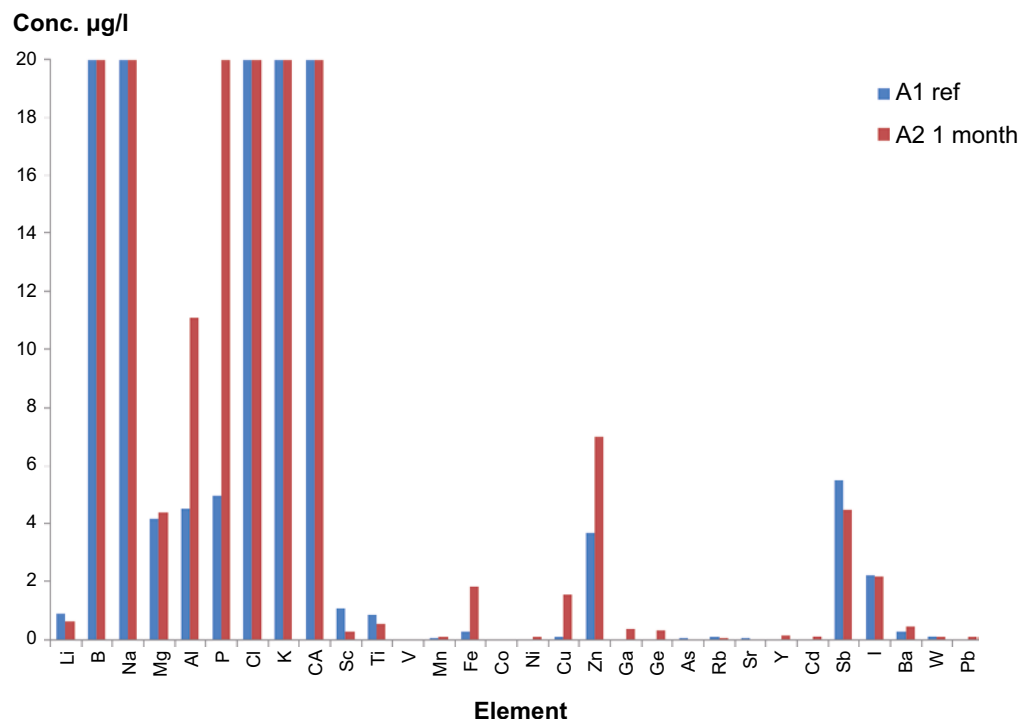
Figure D-5. Assessment of the contents of Li, B, Na, Mg, Al, P, Cl, K, Ca, Sc, Ti, V, Mn, Fe,Co, Ni, Cu, Zn, Ga, Ge, As, Rb, Sr, Y, Cd, Sb, I, Ba, W, and Pb in water samples performed by semi-quantitative analysis. Note that the y axis is cut at 20 mg/L to show elements with low contents more clearly.

Results of measurements on the water phase

The results of the quantitative results did not show any differences between the pure water and the degassed water, as all elements were below the detection limits. It means that the degassing procedure did not introduce any contamination. After 1 month there is a difference between A1 and A2 regarding the contents of Zn, Cu, and Fe (Figure D-6). At 3 months, one can see differences for all analysed elements between top and bottom samples (Figure D-6), but at 6 months the differences have disappeared (Figure D-7). For all samples the resulting Cu content was the same, irrespective of the Cu isotope that was used in the calculations, which indicates that interference from PO_2 is not prevailing. For the 3-month samples, the Fe content was very uncertain as too high Fe contents were used in the calibration standard. The Pd content in the 6-month samples was below the detection limit for all investigated isotopes The contents of certain elements were sometimes higher in samples in which the experiment was interrupted earlier than experiments that continued for a longer period. The differences are probably explained by natural variations in the experimental environment (e.g. different composition of glass beakers, etc.), or, alternatively, by *contamination at some stage of the analysis process*[3]. As all contents are within the same range, there is no indication that the differences are significant for the data interpretation.

D4 Description of XRF measurements on glass

General considerations

Energy dissolved X-ray fluorescence spectroscopy (ED-XRFS) is a method for determination of the element composition in solid (and liquid) substances. The sample is irradiated by X-ray radiation of high energy, and upon absorption of the radiation, electrons in the inner shells are knocked out. When the excited state relaxes, electrons from higher energy levels "fall down". In this relaxation to the base state, X-ray photons are emitted with energies corresponding to the energy level differences of the individual atomic species, that is, element-specific X-ray radiation. By measuring the energy and intensity of the emitted radiation, the composition of solids can be determined quantitatively down to ppm levels. For thorough measurements, standards of known amounts/contents are required.

Measurements were performed on Duran glass to study the copper content, possibly as a coating. The surface concentration is quantified by means of a standard of known amount/thickness. The background in the measurement is corrected for by comparing with a noncoated blank material (e.g. very clean electronics silicon). For copper films thinner than 100 nm the thickness (amount) is proportional to the intensity (from peak area) of the CuKα peak at 8.04 keV, which was utilised in the calibration in our case.

Instrument (Ångström Laboratory)

PANalytical Epsilon 5 for energy-resolved X-ray fluorescence spectroscopy

X-ray tubes:	Gd 25–100 kV, 0.5–24 mA, at most 600W.
Detector:	Ge 0.7–100 keV (cooled with liquid nitrogen).
Resolution:	< 140 eV, maximum count rate 100,000 cps.

## Analysis details for the copper analysis:

Germanium used as secondary radiation source for increased sensitivity to copper.

Settings: 75 kV, 8 mA; measurement time 360 seconds, three measurements per sample.
Sensitivity to copper: $2 \cdot 10^{-10}$ mole/cm^2, which corresponds to a 0.01–0.02 nm thick copper film.

The sensitivity was calculated from a standard (35 nm copper film on electronics silicon) and a blank sample (only electronics silicon). The intensity is correlated to the tube current (in mA).

---

[3] The three-month sample (Figure D-6, right) seems to be contaminated: Samples from the surface systematically give higher analysis values than samples from the bottom. The six-month sample (Figure D-7) does not show such behaviour at all. Due to the very low contents, all analyses are sensitive to systematic errors.
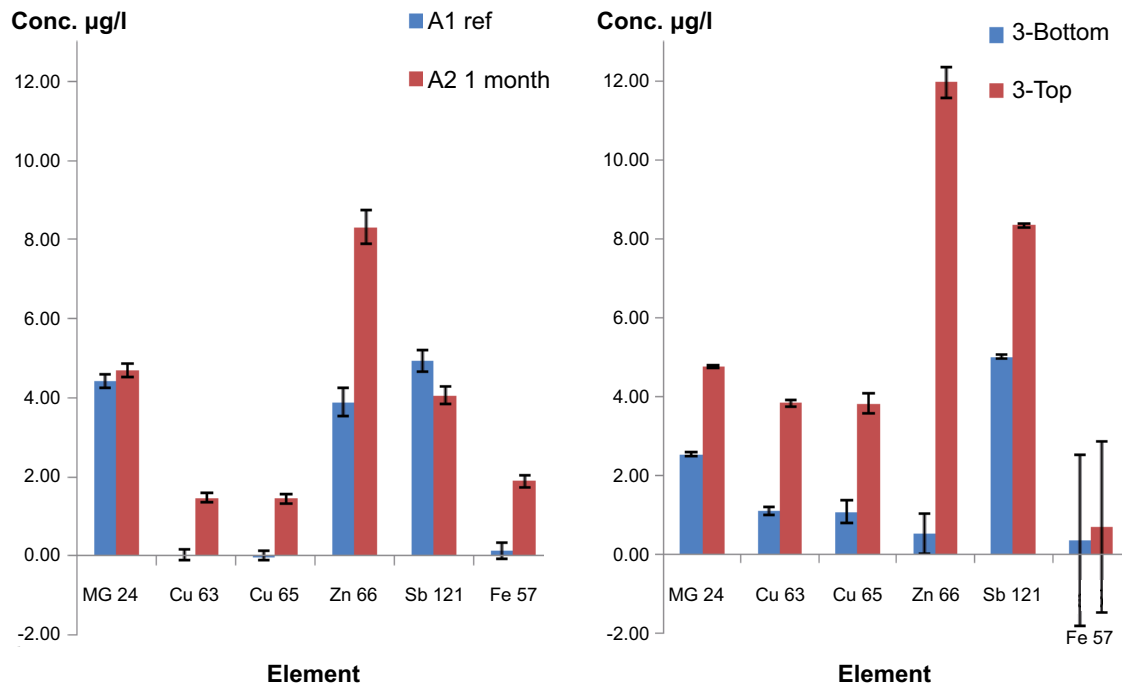
Figure D-6. *Comparison of the concentrations of Mg, Cu, Zn, Sb, and Fe between A1 and A2 (left) and between 3-month top and bottom samples (right). The black bars indicate the uncertainty of the calculated concentrations. (Negative concentrations are artefacts.) For comments on the right part, see the text above.*
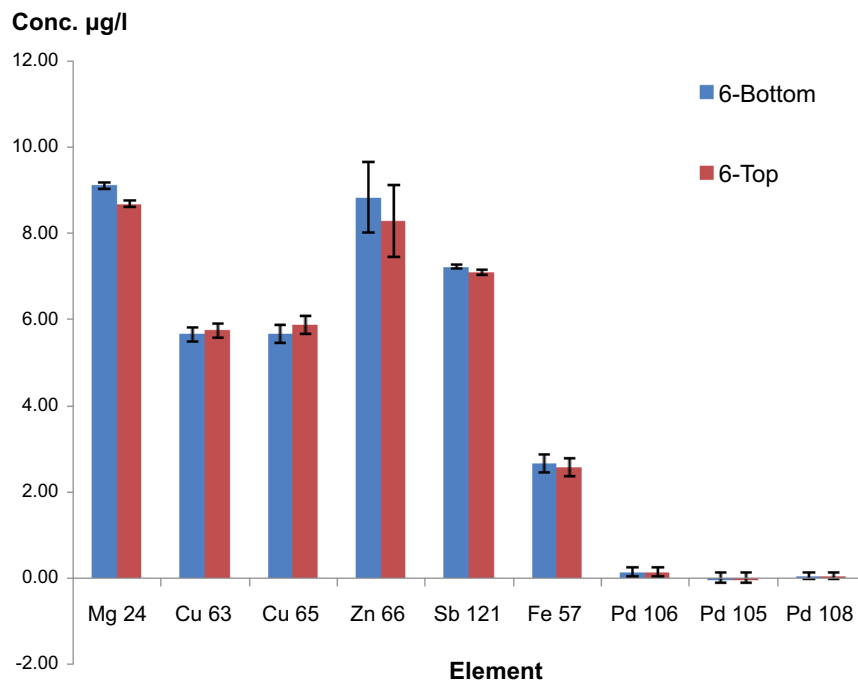
Figure D-7. *Comparison of the concentrations of Mg, Cu, Zn, Sb, Fe, and Pd between 6-month top and bottom samples. The black bars indicate the uncertainty of the calculated concentrations. (Negative concentrations are an artefact.)*

In measurements on the glass, an overlap with the ZnKα peak was observed. Therefore, a profile fit was made to separate the Zn and Cu peaks. A fitted CuKα peak area of 133 cps/mA was obtained for the standard. As the thickness was 35 nm, the sensitivity was 3.80 cps/mA/nm. This value was used in the thickness calculations that are reported in the table below of the glass measurements.

Sample:	Glass – 6 month	Glass – 1 month	Glass blank	Si Blank
CuKa (cps/mA), raw data	1.98; 2.13[a]	1.86	1.86	1.78*
CuKa (cps/mA) corrected data*	0.2; 0.26	0.08	0.08	
Thickness (nm)**	0.05–0.07	0.02	0.02	–
Thickness increase *** (nm)	0.03–0.05	0.00		

[a] Both sides were measured.
* The background level 1.78 is subtracted from the raw data.
** Conversion factor 3.80 cps/mA/Nm.
*** Increase through exposure to water (with copper plate) compared to glass blank.

Calculation of mole/surface area for copper coating.

For 1 Å Cu film (0.1 nm), density 8.92 g/cm^3 and molar mass 63.55 g/mole:

One cm^2 Cu film has a volume of $1 \cdot 10^{-8}$ cm^3 and a mass of $8.92 \cdot 10^{-8}$ g. The amount in 1 cm^2 of this copper film is $8.92 \cdot 10^{-8}/63.55$ moles. This implies $1.40 \cdot 10^{-9}$ mole/Å/cm^2 = $1.40 \cdot 10^{-8}$ mole/nm/cm^2.

Calculations from the glass analyses

0.03–0.05 nm corresponds to the increase of the copper signal in 6 months. At an unchanged growth rate, this is a maximum of 0.1 nm/year = $1.4 \cdot 10^{-9}$ mole/cm^2. As the surface area of the glass is about 100 cm^2, this corresponds to a total amount of $1.4 \cdot 10^{-7}$ moles.

Calculation of penetration and information depth XRF

AbsorbDX V1.1.4

Material
Composition : 40%Si+40%SiO+13%BO+2%AlO+5%KO

Composition: enter a valid formula e.g. Fe3O4 or a mixture using "+" sign e.g. 10%Fe+90%FeO for a mixture, an unspecified percentage defaults to the balance to 100% e.g. 18Cr+10Ni+Fe

Density : 2.23   g/cm3

Beam : radiation and geometry
Radiation : Ge KA1   Wavelength: 1.2541   Ao Energy (kEV) : 9.887

2 Theta: 90   ☑ Bragg condition   Gamma=incidence angle :

Calculated absorption (Photoelectric+Compton+Rayleigh)
Mass (cm2/g) : 25.99   Linear (cm-1) : 57.97

Depth for 90   %   contribution to the diffracted beam (um) : 140.4

Update display   Quit   Quit and save

Press F1 for help

Bruker absorb DX V1.1.4 according to the settings above (example)

The glass is irradiated with GeKα$_1$ radiation and the outgoing CuKα radiation is measured. As the energies are different, the absorption also becomes different. The Duran glass composition according to the field labelled Composition.

Results:

Penetration in Duran glass of incoming GeKα radiation

50% = 42 μm
90% = 140 μm

Penetration in Duran glass of outgoing CuKα radiation

50% = 23 μm
90% = 77 μm

Analysis depth about 30–50 μm, to compare with the highly surface-sensitive electron spectroscopy technique.

Calculations and estimations

E1   Calculation of released amounts of copper

Assuming 10 ppb/years in 100 ml water. (Analysis method: ICP-MS).

10 ppb in 100 grams water = $1 \cdot 10^{-6}$ grams of copper (atomic mass 63.5 g/mole), that is, about $2 \cdot 10^{-8}$ mole Cu released per year.

Assessment of the hydrogen content in the Pd foil at low hydrogen pressures and room temperature

Reference to the relation between hydrogen pressure and hydrogen content in Pd: (Flanagan et al. 1981).

From the graph: 750 mTorr (10 Pa) for $PdH_{0.006}$ at room temperature. Several studies show that the hydrogen content varies between 0.002 and 0.006 depending on the microstructure of the metal (Luo and Flanagan 2002, 2006).

The hydrogen content of the palladium foil (such as atomic hydrogen) is estimated based on the assumption that hydrogen is dissolved in a solid solution where the hydrogen content depends on the hydrogen pressure according to $p(H_2)^{1/2}$.

The dimensions of the palladium foil: Diameter = 20 mm, thickness 0.1 mm; volume = 0.0314 cm^3; Mass = 0.38 grams (Density 12.026 g/cm^3).

0.38 grams Pd therefore corresponds to 0.00357 mole (molar mass 106.42 g/mole).

Hydrogen pressure (mTorr)	Hydrogen content (x) in Pd as PdH$_x$	Amount in Pd as H$_2$ (mole)	ppm (parts by weight)
750	0.006	$21 \cdot 10^{-6}$ mole	56
75	0.0019	$6.8 \cdot 10^{-6}$ mole	18
64 (Main 1)	**0.0017**	**$6.1 \cdot 10^{-6}$ mole**	**16**
7.5	0.0006	$2.1 \cdot 10^{-6}$ mole	6
0.75	0.00019	$0.68 \cdot 10^{-6}$ mole	1.8
0.37**	0.00013	$0.46 \cdot 10^{-6}$ mole	1.2

* From Figure 5-2, 4,000 h. ** Hydrogen gas content in air.

Calculation of the amount of hydrogen gas in the gas phase:

The gas volume in the system is: 186 cm^3.

Formula for the calculation:

$$Amount\ of\ hydrogen\ gas = \frac{0.186(l) \times p(mtorr)}{25.5 \times 760,000}$$

25.5 = Molar volume (l/mole).
760,000 = Pressure conversion factor between mTorr and atm.

Hydrogen pressure (mTorr)	Amount of hydrogen in the gas phase 186 cm³	Amount in Pd as H₂ (mol) RT	Relative amount of hydrogen in the gas phase
750	$7.3 \cdot 10^{-6}$ mol	$21 \cdot 10^{-6}$ mol	26%
75	$7.3 \cdot 10^{-7}$ mol	$6.8 \cdot 10^{-6}$ mol	10%
64 (Main 1)	**$6.4 \cdot 10^{-7}$ mol**	**$6.1 \cdot 10^{-6}$ mol**	**8.7%**
7.5	$7.3 \cdot 10^{-8}$ mol	$2.1 \cdot 10^{-6}$ mol	3.3%
0.75	$7.3 \cdot 10^{-9}$ mol	$0.68 \cdot 10^{-6}$ mol	1.1%
0.37	$3.7 \cdot 10^{-9}$ mol	$0.46 \cdot 10^{-6}$ mol	0.80%

The ERDA analysis result is 4,000 ppm H (atomic ppm).

This implies that there are $1.4 \cdot 10^{-5}$ moles of H (atomic) in 0.38 grams of Pd (= 0.00357 mol) .

Recalculated to molecular hydrogen: $7 \cdot 10^{-6}$ mole H_2

E.2 Calculation of the amount of hydrogen in the copper plates

Total amount of copper is about 6.3 grams.

From melting analysis (Bruker)

The hydrogen concentration was determined at the following values (Appendix D1):

Cu (1 month) = 3.4 ppm (Std.dev. 0.7 ppm).
Cu (at start)[4] = 2.4 ppm.
$3.4 \cdot 10^{-6} \cdot 6.3$ grams H = $2.1 \cdot 10^{-5}$ grams H = $1 \cdot 10^{-5}$ mole H_2.

This value, corrected for hydrogen content in the Cu plates before the corrosion experiment, amounts to $1.0 \cdot 10^{-6} \cdot 6.3$ grams H = $6.3 \cdot 10^{-6}$ grams H = $3 \cdot 10^{-6}$ mole H_2

From the ERDA analyses

Cu (1 month) = 5 ppm
Cu (at start) = 5 ppm

From recalculations, the total hydrogen content for Cu (1 month) amounts to
$5.0 \cdot 10^{-6} \cdot 6.3$ grams = $3.1 \cdot 10^{-5}$ grams = $1.5 \cdot 10^{-5}$ mole H_2

This value corrected for the hydrogen content in the Cu plates before the corrosion experiment:
Cu (1 month) – Cu (at start) = 0

---

[4] Denoted as Cu-HC by Bruker.